

The Galaxy Power Spectrum and Bispectrum in Redshift Space

Vincent Desjacques,^a Donghui Jeong,^b and Fabian Schmidt^c

^a*Physics department, Technion, 3200003 Haifa, Israel*

^b*Department of Astronomy and Astrophysics, and Institute for Gravitation and the Cosmos, The Pennsylvania State University, University Park, PA 16802, USA*

^c*Max-Planck-Institut für Astrophysik, Karl-Schwarzschild-Straße 1, 85748 Garching, Germany*

E-mail: dvince@physics.technion.ac.il, djeong@psu.edu,
fabians@mpa-garching.mpg.de

ABSTRACT: We present the complete expression for the next-to-leading (1-loop) order galaxy power spectrum and the leading-order galaxy bispectrum in redshift space in the general bias expansion, or equivalently the effective field theory of biased tracers. We consistently include all line-of-sight dependent selection effects. These are degenerate with many, but not all, of the redshift-space distortion contributions, and have not been consistently derived before. Moreover, we show that, in the framework of effective field theory, a consistent bias expansion in redshift space must include these selection contributions. Physical arguments about the tracer sample considered and its observational selection have to be used to justify neglecting the selection contributions. In summary, the next-to-leading order galaxy power spectrum and leading-order galaxy bispectrum in the general bias expansion are described by 22 parameters, which reduces to 11 parameters if selection effects can be neglected. All contributions to the power spectrum can be written in terms of 28 independent loop integrals.

Contents

1	Introduction	1
1.1	Summary of key results	3
1.2	Notation	4
2	Galaxy density in redshift space	5
2.1	Bias expansion: no selection effects	5
2.2	Line-of-sight-dependent selection effects	7
2.3	Velocity bias	10
2.4	Mapping from rest frame to redshift space	11
2.5	Summary	12
3	Power spectrum	14
3.1	Linear and higher-derivative bias	15
3.2	2–2	15
3.3	1–3	17
3.3.1	$\Pi^{[1]}\Pi^{[2]}$ -type operators	19
3.3.2	Other contributions	20
3.3.3	$\Pi^{[3]}$ -type operators	20
3.3.4	Projection onto general loop integral	20
3.4	Summary: redshift-space galaxy power spectrum at NLO	22
3.5	IR resummation	23
4	The LO redshift-space galaxy bispectrum	23
5	Connection to previous results	24
5.1	Relation to the “streaming model”	24
5.2	Relation to previous EFT calculations	27
5.2.1	Selection contributions	27
5.2.2	Velocity bias	27
6	Discussion and conclusions	29
A	Counterterms required by redshift-space contributions	32
B	Fourier-space kernels for the redshift-space galaxy density	33
B.1	Second order density contrast	33
B.2	Third order density contrast	35
B.3	NLO power spectrum	36

C	Structure of cubic operators and their contribution to the NLO power spectrum	37
C.1	$(\Pi^{[1]})^3$ type	37
C.2	$\Pi^{[1]}\Pi^{[2]}$ type	38
C.3	$\Pi^{[3]}$ type	39
D	The general 1–3-type loop contribution	41
E	NLO matter and velocity power spectra	43
F	Coefficient matrices for 1–3-type loop contributions	45
G	Multipole decomposition	48
G.1	Linear and higher-derivative	48
G.2	Loop terms	49
H	Configuration space approach	49

1 Introduction

In galaxy redshift surveys, galaxy positions are usually inferred from an observed redshift and position angles on the sky. These “redshift-space” (RS) positions differ from the “rest-frame” positions one would naturally identify on a comoving constant-proper-time slice owing to a number of projection effects. In particular, the line-of-sight component u_{\parallel} of the galaxy peculiar velocities contribute a Doppler shift which changes the observed redshift in a systematic way [1, 2]. In the measured galaxy clustering statistics such as the galaxy two-point correlation function or power spectrum, which depend on the relative position of two galaxies, this relative Doppler shift is proportional to $\partial_{\parallel}u_{\parallel} \propto \mu^2\delta$ in Fourier space, where $\mu^2 = k_{\parallel}^2/k^2$ is the cosine-squared between the wavevector \mathbf{k} and the line of sight and δ is the matter overdensity. Therefore, galaxy peculiar velocities generate coherent, anisotropic patterns in the observed galaxy clustering statistics that can be easily detected even with small surveyed volumes. These patterns are widely referred to as “redshift-space distortions” [or RSD; e.g. 3–9], and can be used to constrain the linear growth rate $f = d \ln D / d \ln a$ of structure as a function of redshift [e.g. 10–19].

In addition to f , the measured galaxy power spectrum encodes important cosmological information ranging from primordial non-Gaussianity on large scales $k \lesssim k_{\text{eq}}$ [20], the physics of the primeval plasma for $k \gtrsim k_{\text{eq}}$ [21] and massive neutrinos on scales $k \gg k_{\text{eq}}$ [22]. In particular, the free-streaming of massive neutrinos and dark matter particles imprints scale-dependencies at wavenumber $k \gtrsim k_{\text{eq}}$ which could be observed with future galaxy surveys. However, extracting unbiased constraints from these small scales requires a detailed account of

all the angle- and scale-dependencies induced by nonlinear gravitational evolution, nonlinear biasing, and selection effects. Therefore, it is essential to go beyond the celebrated Kaiser formula [9, 23] [second line of Eq. (3.1)], which holds only in the linear regime and in the absence of any selection effect. Since the late 1980s, there have been many attempts to extend the validity of theoretical predictions for the RS power spectrum of biased tracers [e.g., 7, 24–36]. However, it has also been realized that the fact that survey galaxy catalogs are selected on observed properties induces additional, line-of-sight-dependent effects, which even exist in the linear regime [29, 33]. Further, biased tracers generally exhibit a velocity bias which can be important on nonlinear scales [32, 37–39].

However, all studies thus far have only included a subset of all these physical effects contributing to redshift-space galaxy statistics. As of today, there is no complete expression for the galaxy RS power spectrum at next-to-leading order (NLO) in perturbation theory that includes all effects. This paper will provide this result which, hopefully, will be useful to the analysis of future galaxy survey data. To achieve this goal, we adopt the effective-field theory (EFT) approach ([40–44]; see [45] for a review), which provides a well-defined perturbative ordering scheme for contributions to galaxy statistics, in addition to consistently removing formally divergent contributions that are sensitive to small-scale fully nonlinear modes. Moreover, we will adopt the approach outlined in [39] to construct the relevant bias and selection contributions, which generalizes early perturbative bias expansions [see, e.g., 46–51] in a consistent and model-independent way. We also introduce a well-defined, gauge-invariant distinction between biasing and selection effects, which can be useful in actual survey analyses, for example if selection effects can be assumed to be small on physical grounds. Furthermore, we will also derive the complete leading-order (LO) expression for the RS galaxy bispectrum using the same approach. While there is abundant literature on the RS power spectrum, there are relatively few theoretical studies of the galaxy bispectrum and 3-point function [52–56], and few joint analyses of the RS galaxy power spectrum and bispectrum [57, 58]. Recently, [59] presented a trispherical harmonic decomposition of the redshift-space bispectrum.

The presence of selection effects leads to degeneracies between the coefficients of these contributions, which are in general unknown a priori, and the growth rate f . However, we show that a certain type of RSD contribution remains free of these degeneracies, and thus allows for a measurement of f even in the presence of selection contributions. This proves and generalizes the arguments made previously in [60].

Since this is a lengthy and technical paper, the remainder of the introduction contains a summary of our key results, and our adopted notation. Sec. 2 provides a detailed derivation of the galaxy density contrast in redshift space up to cubic order, although we also describe how this construction proceeds to higher order. We then continue to galaxy statistics, namely the power spectrum at NLO (Sec. 3) and the bispectrum at LO (Sec. 4). A discussion of the relation of our EFT-based approach to previous results is presented in Sec. 5. We conclude in Sec. 6. The appendices present details on the renormalization and calculation of the various contributions to the NLO power spectrum.

1.1 Summary of key results

- The perturbative expansion of the *observed* galaxy density in the galaxies' rest frame contains two types of contributions: *bias* terms, which involve the local gravitational observables in the galaxy rest frame, and could in principle all be measured by a local observer in the galaxy who knows nothing about the distant observer (us); and *selection* contributions, which quantify the probability that this galaxy is actually detectable from Earth, and which make explicit reference to the line of sight that connects us with the galaxy. The latter have frequently been neglected in the literature, except for the few studies cited above.
- Performing the coordinate transformation of the rest-frame galaxy density to the observed density leads to the well-known redshift-space distortions. Interestingly, in the context of the renormalized bias expansion, or EFT of galaxy clustering, higher-order RSD terms *force* us to introduce the selection contributions mentioned above, since they appear as counterterms which absorb divergent loop contributions. That is, the logical sequence is not to ignore them initially, and add them later if necessary. Rather, one has to argue physically (or astrophysically) why the selection contributions are absent for a given galaxy sample.
- As is well known in case of the leading (Kaiser) RSD contribution, selection effects lead to a perfect degeneracy with RSD, and all cosmological information on the growth rate f from RSD is lost in the leading-order (LO) power spectrum. However, both in the next-to-leading order (NLO) galaxy power spectrum and in the bispectrum there are displacement-type RSD contributions which are protected from selection effects (they involve the galaxy velocity without any derivatives). Thus, at nonlinear order, at least some cosmological information in RSD is preserved even in the presence of selection effects.
- When going to NLO in the galaxy power spectrum, velocity bias becomes important. This includes both a deterministic contribution (galaxy velocities are systematically larger or smaller than those of matter, in a certain specific sense), and a stochastic velocity bias (galaxy velocities scatter around effective matter velocities due to random small-scale motions). One can argue that the latter is strictly the finger-of-god (FoG) contribution in the EFT of galaxy clustering. All other velocity terms are due to long-wavelength modes and thus not strictly FoG.
- In order to completely describe the galaxy power spectrum at NLO, and galaxy bispectrum at LO, we require (i) 5 galaxy bias parameters, and 5 rest-frame stochastic amplitudes; (ii) 9 selection parameters; and (iii) 2 deterministic velocity bias parameters (one of them is due to selection), and 1 stochastic velocity bias amplitude. Thus, this set of statistics in full generality involves 22 parameters, which reduces to 11 parameters if selection effects can be neglected.

The number of operators appearing in the general EFT expansion of the galaxy density grows rapidly in the presence of selection effects, and the resulting expressions quickly become complex. In order to avoid unnecessary complications, we restrict to those operators which appear in the LO+NLO galaxy power spectrum and LO galaxy bispectrum throughout. We stress that if other statistics are considered, e.g. the galaxy trispectrum or cross-correlations of the galaxy density with matter density or velocity, some parameters we have dropped here because of their complete degeneracy with other parameters will in general appear.

1.2 Notation

Our notation largely follows that of [61]. In particular, our Fourier convention and short-hand notation is

$$\begin{aligned} f(\mathbf{k}) &\equiv \int d^3\mathbf{x} f(\mathbf{x}) e^{-i\mathbf{k}\cdot\mathbf{x}} \equiv \int_{\mathbf{x}} f(\mathbf{x}) e^{-i\mathbf{k}\cdot\mathbf{x}} \\ f(\mathbf{x}) &\equiv \int \frac{d^3\mathbf{k}}{(2\pi)^3} f(\mathbf{k}) e^{i\mathbf{k}\cdot\mathbf{x}} \equiv \int_{\mathbf{k}} f(\mathbf{k}) e^{i\mathbf{k}\cdot\mathbf{x}}. \end{aligned} \quad (1.1)$$

Primes on Fourier-space correlators indicate that the momentum conserving Dirac delta $(2\pi)^3\delta_D(\mathbf{k}_1 + \mathbf{k}_2 + \dots)$ is to be dropped. Further, we will use

$$\mathbf{k}_{12\dots n} \equiv \mathbf{k}_1 + \mathbf{k}_2 + \dots + \mathbf{k}_n. \quad (1.2)$$

We will also use the following shorthands for tensor products

$$(MM)_{ij} \equiv M_{ik} M_j^k, \quad (1.3)$$

trace,

$$\text{tr}(M) \equiv M_{ij} \delta^{ij}, \quad (1.4)$$

trace of powers of a tensor,

$$M^n \equiv \text{tr} \left[\underbrace{M \cdots M}_{n \text{ times}} \right], \quad (1.5)$$

and line-of-sight projection:

$$M_{\parallel} \equiv M_{ij} \hat{n}^i \hat{n}^j, \quad (1.6)$$

where \hat{n} denotes the unit vector along the line of sight to a given 3D position. We will also frequently use the nonlocal operator

$$\mathcal{D}_{ij} \equiv \left(\frac{\partial_i \partial_j}{\nabla^2} - \frac{1}{3} \delta_{ij} \right) \quad (1.7)$$

which is defined via its action on fields in the Fourier representation.

The matter and rest-frame galaxy density perturbations are given by

$$\delta(\mathbf{x}, \tau) \equiv \frac{\rho(\mathbf{x}, \tau) - \bar{\rho}_m(\tau)}{\bar{\rho}_m(\tau)} \quad \text{and} \quad \delta_g(\mathbf{x}, \tau) \equiv \frac{n_g(\mathbf{x}, \tau) - \bar{n}_g(\tau)}{\bar{n}_g(\tau)}, \quad (1.8)$$

while the galaxy density in redshift space is $\delta_{g,s}(\mathbf{x}_s, \tau)$. We also employ the scaled matter velocity,

$$\mathbf{u} \equiv \frac{1}{\mathcal{H}} \mathbf{v}, \quad (1.9)$$

and correspondingly \mathbf{u}_g for galaxies. We will frequently use the matter velocity divergence $\theta \equiv \nabla \cdot \mathbf{v}$. Finally, we define the line-of-sight derivative of the scaled line-of-sight velocity

$$\eta \equiv \partial_{\parallel} u_{\parallel}, \quad (1.10)$$

where $\partial_{\parallel} \equiv \hat{n}^i \partial_i$. Note that η is dimensionless.

Since the matter density is related to the potential Φ through the Poisson equation

$$\nabla^2 \Phi = \frac{3}{2} \Omega_m \mathcal{H}^2 \delta, \quad (1.11)$$

this allows us to combine the matter density perturbation and tidal field K_{ij} into a tensor $\Pi^{[1]}$:

$$\Pi_{ij}^{[1]}(\mathbf{x}, \tau) \equiv \frac{2}{3\Omega_m \mathcal{H}^2} \partial_{x,i} \partial_{x,j} \Phi(\mathbf{x}, \tau) = K_{ij}(\mathbf{x}, \tau) + \frac{1}{3} \delta_{ij} \delta(\mathbf{x}, \tau), \quad (1.12)$$

which contains $\delta = \text{tr} \Pi^{[1]}$ and K_{ij} as the trace-free part of $\Pi_{ij}^{[1]}$. All of these quantities denote the evolved, nonlinear quantities.

As for the fiducial cosmology, we use the flat Λ CDM cosmological parameters in the `base_plikHM_TTTEEE_lowTEB_lensing_post_BAO_H080p6_JLA` column from Planck 2015 [62, 63]: $\Omega_{\Lambda} = 0.69179$, $\Omega_{b0} h^2 = 0.022307$, $\Omega_{c0} h^2 = 0.11865$, $\Omega_{\nu 0} h^2 = 0.000638$, $h = 0.6778$, $n_s = 0.9672$. We normalize the linear power spectrum by setting the root-mean-squared value of the smoothed (spherical filter with radius $8 h^{-1} \text{Mpc}$) linear density contrast $\sigma_8 = 0.8166$.

2 Galaxy density in redshift space

We begin by writing down the observed fractional galaxy density perturbation $\delta_{g,s}(\mathbf{x}, \tau)$ in the general perturbative bias expansion. The transformation from the galaxy rest frame into redshift space involves the galaxy velocity \mathbf{v}_g . Hence, we will also describe the relation between galaxy and matter velocity fields.

Throughout, we retain only the leading contributions in the subhorizon limit. That is, we drop terms that are of order $(\mathcal{H}/k)\delta(\mathbf{k})$ and $(\mathcal{H}/k)^2\delta(\mathbf{k})$. These so-called relativistic contributions are known at linear order (see [64–68]).

2.1 Bias expansion: no selection effects

In the general bias expansion (see Sec. 2 of [61] for an introduction), we write the rest-frame galaxy density as

$$\delta_g(\mathbf{x}, \tau) = \sum_O [b_O(\tau) + \epsilon_O(\mathbf{x}, \tau)] [O](\mathbf{x}, \tau) + \epsilon(\mathbf{x}, \tau), \quad (2.1)$$

where the sum runs over a list of operators O (statistical fields) that are successively higher order in perturbations (and spatial derivatives). In the EFT approach, Eq. (2.1) should be thought of as coarse-grained on some scale Λ . The operators are renormalized, as indicated by the brackets $[O]$, which means that they contain counterterms which absorb the dependence on the artificial smoothing scale Λ . Each operator has an associated bias parameter b_O and associated stochastic field ϵ_O ; while the former is a dimensionless parameter, the latter is a field with vanishing mean, so that $\epsilon_O[O]$ is one order in perturbations higher than $b_O[O]$. The stochastic fields take into account that the relation between the galaxy density and any given large-scale field is stochastic due to the small-scale modes that are integrated out when coarse-graining the fields. Note that we will adopt the standard notation $b_1 \equiv b_\delta$, $b_2 \equiv 2b_{\delta^2}$ for the linear and quadratic bias parameters of the density field. All other bias parameters b_O simply multiply the operator O they are associated with.

Ref. [39] provides a convenient way to construct the complete bias expansion in terms of the density and tidal field and their convective time derivatives, which together comprise the complete set of local gravitational observables. First, density and tidal field are combined into the tensor $\Pi^{[1]}$ given in Eq. (1.12), which contains $\delta = \text{tr} \Pi^{[1]}$ and K_{ij} as the trace-free part of $\Pi_{ij}^{[1]}$. Note that the superscript [1], to be distinguished from (1), refers to the fact that $\Pi^{[1]}$ starts at first order in perturbation theory, but contains higher-order terms as well. We then define higher-order tensors $\Pi^{[n]}$ recursively by convective time derivatives:

$$\Pi_{ij}^{[n]} = \frac{1}{(n-1)!} \left[(\mathcal{H}f)^{-1} \frac{D}{D\tau} \Pi_{ij}^{[n-1]} - (n-1) \Pi_{ij}^{[n-1]} \right], \quad (2.2)$$

where

$$\frac{D}{D\tau} \equiv \partial_\tau + v^i \partial_{x,i}. \quad (2.3)$$

For reference,

$$\begin{aligned} \Pi_{ij}^{[2]} \Big|^{(2)} &= \Pi_{ik}^{[1]} \Pi_j^{[1]k} + \frac{10}{21} \frac{\partial_i \partial_j}{\nabla^2} \left(\delta^2 - \frac{3}{2} K^2 \right) \\ &= (KK)_{ij} + \frac{2}{3} \delta K_{ij} + \frac{1}{9} \delta^2 \delta_{ij} + \frac{10}{21} \frac{\partial_i \partial_j}{\nabla^2} \left(\delta^2 - \frac{3}{2} K^2 \right), \end{aligned} \quad (2.4)$$

where all quantities on the r.h.s. are evaluated at linear order. As a convention, δ will always denote the evolved, nonlinear density field unless we explicitly state otherwise, or make use of the notation $\delta^{(1)}$.

The complete set of operators in the galaxy rest frame up to third order in perturbations is then given by

$$\begin{aligned} \text{bias: } 1^{\text{st}} & \quad \text{tr}[\Pi^{[1]}] \\ 2^{\text{nd}} & \quad \text{tr}[\Pi^{[1]} \Pi^{[1]}], (\text{tr}[\Pi^{[1]}])^2 \\ 3^{\text{rd}} & \quad \text{tr}[\Pi^{[1]} \Pi^{[1]} \Pi^{[1]}], \text{tr}[\Pi^{[1]} \Pi^{[1]}] \text{tr}[\Pi^{[1]}], (\text{tr}[\Pi^{[1]}])^3, \text{tr}[\Pi^{[1]} \Pi^{[2]}]. \end{aligned} \quad (2.5)$$

By taking linear combinations of the operators appearing at each order, many different sets of linearly independent operators are possible (in fact, the operators at each order form a vector space); see App. C of [61] for a summary of different conventions used in the literature. Here, we will follow the convention used in [61], and use

$$\begin{aligned} \text{bias: } & 1^{\text{st}} \quad \delta & (2.6) \\ & 2^{\text{nd}} \quad \delta^2, K^2 \equiv \text{tr}[KK] \\ & 3^{\text{rd}} \quad \delta^3, \delta K^2, K^3 \equiv \text{tr}[KKK], O_{\text{td}}, \end{aligned}$$

where

$$O_{\text{td}} \equiv \frac{8}{21} K_{ij} \mathcal{D}^{ij} \left[\delta^2 - \frac{3}{2} K^2 \right] \quad (2.7)$$

is equivalent to $\text{tr}[\Pi^{[1]}\Pi^{[2]}]$ at the order we work in. The subscript td stands for “time derivative”, as this operator corresponds to the first explicit appearance of time derivatives in the bias expansion. Following the discussion above, there are four relevant stochastic fields,

$$\epsilon, \epsilon_\delta, \epsilon_{\delta^2}, \epsilon_{K^2}. \quad (2.8)$$

These are completely described by their statistics which are analytic in k :

$$P_\epsilon(k) \equiv \langle [\epsilon](\mathbf{k})[\epsilon](\mathbf{k}') \rangle' = P_\epsilon^{\{0\}} + k^2 P_\epsilon^{\{2\}} + \mathcal{O}(k^4), \quad (2.9)$$

and analogously for P_{ϵ_δ} , $B_\epsilon \equiv \langle [\epsilon][\epsilon][\epsilon] \rangle$, and so on. In fact, the number of bias operators and stochastic fields at cubic order which appear in the NLO galaxy power spectrum and LO galaxy bispectrum is only a small subset of all these contributions, as we will see.

Finally, we will include the leading higher-derivative operator,

$$b_{\nabla^2\delta}[\nabla^2\delta], \quad (2.10)$$

in the bias expansion. This assumes that the scale associated with the expansion in derivatives is similar to the nonlinear scale where the expansion in perturbations breaks down. We will discuss this in Sec. 6.

2.2 Line-of-sight-dependent selection effects

Now we would like to include line-of-sight dependent selection effects in the galaxy density. These occur for example due to the fact that the probability of escape of a line photon from the source depends on the velocity gradient along the line of sight. *While they can be considered a part of the bias expansion, we refer to these as selection effects, since they are necessarily induced by the fact that we as observers pick out tracers based on their observed properties, which introduces the line of sight as preferred direction.*

These effects are still fully determined by the local gravitational observables at the position of the galaxy, as parametrized conveniently through the basis $\Pi_{ij}^{[n]}$ [Eq. (2.5)]. Now

however, we have to allow for the line of sight $\hat{\mathbf{n}}$ as preferred direction. Denoting, for any tensor Π_{ij} , $\Pi_{\parallel} \equiv \Pi_{ij} \hat{n}^i \hat{n}^j$, this immediately leads to the complete set of selection contributions up to cubic order:

$$\begin{aligned}
\text{selection: } & 1^{\text{st}} \quad \Pi_{\parallel}^{[1]} & (2.11) \\
& 2^{\text{nd}} \quad \text{tr}[\Pi^{[1]}\Pi_{\parallel}^{[1]}], [\Pi^{[1]}\Pi_{\parallel}^{[1]}]_{\parallel}, \left(\Pi_{\parallel}^{[1]}\right)^2, \Pi_{\parallel}^{[2]} \\
& 3^{\text{rd}} \quad \Pi_{\parallel}^{[1]} \text{tr}[\Pi^{[1]}\Pi^{[1]}], \Pi_{\parallel}^{[1]} (\text{tr}[\Pi^{[1]}])^2, [\Pi^{[1]}\Pi^{[1]}]_{\parallel} \text{tr}[\Pi^{[1]}], [\Pi^{[1]}\Pi^{[1]}\Pi^{[1]}]_{\parallel}, \\
& \quad \left(\Pi_{\parallel}^{[1]}\right)^2 \text{tr}[\Pi^{[1]}], \Pi_{\parallel}^{[1]} [\Pi^{[1]}\Pi^{[1]}]_{\parallel}, \left(\Pi_{\parallel}^{[1]}\right)^3, \\
& \quad \text{tr}[\Pi^{[1]}\Pi_{\parallel}^{[2]}], [\Pi^{[1]}\Pi_{\parallel}^{[2]}]_{\parallel}, \Pi_{\parallel}^{[2]}\Pi_{\parallel}^{[1]}, \Pi_{\parallel}^{[3]}. & (2.12)
\end{aligned}$$

As a check, one can perform an angle-average $\int d^2\hat{\mathbf{n}}$ over the line of sight of each operator in Eq. (2.11). Then, all of these operators become degenerate with the operators appearing in the general bias expansion, Eq. (2.5).

Eq. (2.11) shows that, at linear order, these selection effects lead to a single additional term at lowest order in derivatives,

$$\Pi_{\parallel}^{[1]} \equiv \Pi_{ij}^{[1]} \hat{n}^i \hat{n}^j \stackrel{\text{linear order}}{\propto} \eta, \quad (2.13)$$

where η is defined in Eq. (1.10). The proportionality in Eq. (2.13) holds at linear order in perturbations, at which the line-of-sight-projected tidal field and line-of-sight velocity are equivalent. This is the well know term identified by Ref. [33].

Tidal field and velocity gradient are no longer simply proportional beyond linear order, and in general can both enter the selection effects. For example, while the escape probability of line photons considered by [33, 69]¹ naturally depends on the line-of-sight velocity gradient in the vicinity of the galaxy, the tidal field can lead to preferred orientations of the selected galaxies w.r.t. the line of sight, which in turn can impact their detection probability [29, 71]; this effect has recently been detected by [72]. The virtue of the general expansion in Eq. (2.11) however is that it is able to capture both of these effects, and all other large-scale selection effects that could possibly enter in the observed galaxy density (in the absence of primordial non-Gaussianity and relative density and velocity perturbations between baryons and CDM, which we will briefly discuss in Sec. 6).

Using the leading-order relations in Eq. (1.12) and Eq. (2.13), we can equivalently write

¹Recently, Ref. [70] has found smaller selection effect at lower redshifts $2 < z < 6$ from the radiative transfer simulation.

contributions added by selection effects as

$$\begin{aligned}
\text{selection:} \quad & 1^{\text{st}} \quad \eta & (2.14) \\
& 2^{\text{nd}} \quad \delta\eta, (KK)_{\parallel}, \eta^2, \Pi_{\parallel}^{[2]} \\
& 3^{\text{rd}} \Big|_{\text{P}^{\text{NLO}}} \quad \delta\Pi_{\parallel}^{[2]}, (K\Pi^{[2]})_{\parallel}, \eta\Pi_{\parallel}^{[2]}, \Pi_{\parallel}^{[3]}, \\
& 3^{\text{rd}} \Big|_{\text{other}} \quad \eta K^2, \eta\delta^2, \delta(KK)_{\parallel}, (KKK)_{\parallel}, \eta^2\delta, \eta(KK)_{\parallel}, \eta^3.
\end{aligned}$$

The use of η instead of K_{\parallel} is motivated by the fact that the operators involving η appear via the transformation to redshift space. Phrasing the selection effects through these operators allows us to simply combine both contributions. We reiterate that Eq. (2.14) is entirely equivalent to Eq. (2.11); the two are related through an invertible linear map in the vector space of bias operators at each order. The last two lines in Eq. (2.14) contain cubic terms that do not appear in the 1-loop power spectrum, as they are absorbed by counterterms. Specifically, following the result in Appendix C, we only need to include those operators which contain factors of the form $\partial_i\partial_j/\nabla^2(O^{(2)})$, where $O^{(2)}$ is a quadratic operator. This applies to four of the 11 cubic selection operators, namely those involving $\Pi^{[2]}$ and $\Pi^{[3]}$, but only one of the four cubic operators in the rest-frame bias expansion Eq. (2.5) (namely $\text{tr}[\Pi^{[1]}\Pi^{[2]}]$).

Finally, selection effects add additional higher-derivative contributions at leading order as well, namely

$$\partial_{\parallel}^2\delta, \nabla^2\eta, \partial_{\parallel}^2\eta, \quad (2.15)$$

and corresponding stochastic contributions. However, at the order we work in (keeping only the leading higher-derivative terms in the NLO power spectrum), these are degenerate with contributions from velocity bias, as we will show in Sec. 3.1, so we do not need to include them here. Importantly, these contributions might have to be considered separately if one includes cross-correlations of the galaxy density field with other fields, such as matter density or velocity (these are usually observed only as projected fields which no longer contain significant RSD and velocity information however).

Let us now discuss stochastic contributions induced by selection effects. We will argue that, apart from the isotropic terms written in Eq. (2.9) for the power spectrum, there are contributions given by $(k^i\hat{n}_i)^{2n} \times \text{const}$, i.e.

$$P_{\epsilon}(k) \rightarrow P_{\epsilon}(\mathbf{k}) \supset (k^i\hat{n}_i)^2 P_{\epsilon}^{\{2\parallel\}} + (k^i\hat{n}_i)^4 P_{\epsilon}^{\{4\parallel\}} + \dots \quad (2.16)$$

In particular, there are no anisotropic contributions at order k^0 . Eq. (2.16) is the general form of any term that involves the line of sight \hat{n} and is analytic in \mathbf{k} . On the other hand, an anisotropic stochastic contribution at order k^0 would have to scale as $(k^i\hat{n}_i)^2/k^2 \times \text{const}$, and would thus be non-analytic. This means that such a term does not correspond to local processes in configuration space, and hence is unphysical.

Let us consider a concrete example. Ref. [29] showed that the fact that the observed brightness, and hence detection probability, of a galaxy depends on its orientation with respect to the sky plane induces additional selection effects, since galaxy orientations correlate with large-scale tidal fields. These deterministic selection contributions correspond to a subset of the general set of selection operators given above. Now let us consider the corresponding stochastic contributions. Let g_{ij} denote the 3-dimensional moment-of-inertia tensor of the galaxy flux detectable from far outside that galaxy. We assume that the selection probability depends on the area of the galaxy projected onto the sky, which is proportional to

$$A_{\text{sky}}(g_{ij}) \equiv \text{tr}[g_{ij}] - \hat{n}^i \hat{n}^j g_{ij}. \quad (2.17)$$

At linear order in the galaxy shape, $\text{tr}[g_{ij}]$ and $\hat{n}^i \hat{n}^j g_{ij}$ are in fact the only two scalar quantities available. Now, due to the absence of any preferred directions in the galaxy rest frame (at zero'th order), the large-scale, white-noise stochastic shape correlation has to be of the form (this is the three-dimensional analogue of the shape noise in galaxy imaging surveys)

$$\langle g_{ij}(\mathbf{k}) g_{kl}(\mathbf{k}') \rangle' = \frac{1}{3} [\delta_{ij} \delta_{kl} + \delta_{ik} \delta_{jl} + \delta_{il} \delta_{jk}] P_{\epsilon_g} + \mathcal{O}(k^2). \quad (2.18)$$

One immediately sees that contractions with both δ^{ij} and $\hat{n}^i \hat{n}^j$ lead to constant contributions $\propto P_{\epsilon_g}$, and, in particular,

$$\langle A_{\text{sky}}(\mathbf{k}) A_{\text{sky}}(\mathbf{k}') \rangle' = \frac{8}{3} P_{\epsilon_g} + \mathcal{O}(k^2). \quad (2.19)$$

That is, random galaxy orientations together with the orientation-dependent selection lead to a contribution to the constant, isotropic galaxy stochasticity $P_{\epsilon}^{\{0\}}$, but do not yield an anisotropy in the large-scale limit, in agreement with our argument above.

2.3 Velocity bias

In order to transform the rest-frame galaxy density into redshift space, we need a prediction for the galaxy velocity as well. As shown in Sec. 2.7 of [61] (see also [32, 39, 44]), the difference between the galaxy and matter velocity fields has to be higher order in derivatives. This is because the relative velocity between galaxies and matter is in principle locally observable, and hence can only depend on local observables constructed from the tensors $\Pi_{ij}^{[n]}$. Further, in order to obtain a vectorial quantity, we need to take one additional spatial derivative. This also holds for any stochastic component in the galaxy velocity.

Consistently with our higher-derivative expansion for bias and selection contributions, we will thus keep only the leading contribution to velocity bias, which can be written as

$$\mathbf{v}_g = \mathbf{v} + \beta_{\nabla^2 \mathbf{v}} \nabla^2 \mathbf{v} + \beta_{\partial_{\parallel}^2 \mathbf{v}} \partial_{\parallel}^2 \mathbf{v} + \boldsymbol{\varepsilon}_v(\mathbf{x}, \tau). \quad (2.20)$$

Here we have already allowed for selection effects, which depend on the line of sight as preferred direction and lead to the third term in Eq. (2.20). Following the above arguments,

the stochastic field $\varepsilon_v(\mathbf{k})$ in Fourier space is proportional to k in the low- k limit (we denote stochastic fields appearing in the galaxy velocity as ε , while those appearing in the density are denoted as ϵ). For the galaxy velocity divergence, this leads to

$$\eta_g \equiv \mathcal{H}^{-1} \partial_{\parallel} v_{g\parallel} = \left[1 - \beta_{\nabla^2 \mathbf{v}} k^2 - \beta_{\partial^2 \mathbf{v}} k^2 \mu^2 \right] \eta + \varepsilon_{\eta}, \quad (2.21)$$

where, unless otherwise noted, $\mu \equiv \hat{\mathbf{k}} \cdot \hat{\mathbf{n}}$. Note that, since $\varepsilon_v(k) \propto k$ as $k \rightarrow 0$, $\varepsilon_{\eta}(\mathbf{k})$ scales as k^2 in the low- k limit and thus is of the same order in derivatives as the higher-derivative contribution to the galaxy stochasticity. As stated above, given the order we are working in, we can neglect the difference between η_g and η except for the leading linear-order contribution to the galaxy density.

It is worth emphasizing that the deterministic and stochastic velocity bias written in Eq. (2.20) captures both a true, local velocity bias induced for example by baryonic pressure forces, and a statistical velocity bias which arises because biased tracers can occupy special locations of the density field which have statistically biased velocities. A good example of the latter effect are peaks of the initial density field, which show statistically smaller velocities than random locations [32].

2.4 Mapping from rest frame to redshift space

Finally, having described the galaxy bias expansion in the galaxy rest frame, including selection effects, as well as the bias relation for the galaxy velocity field, we can now map the observed galaxy density into redshift space. The coordinate transformation is given by

$$\mathbf{x}_s = \mathbf{x} + u_{\parallel} \hat{\mathbf{n}}. \quad (2.22)$$

Using the fact that the galaxy density transforms as the 0-component of a 4-vector, we can derive the mapping up to third order, to obtain (see e.g. Sec. 9.3.2 of [61]):

$$\begin{aligned} \delta_{g,s} &= \delta_g^{\text{Jac}} + \delta_g^{\text{disp}} \\ \delta_g^{\text{Jac}} &= (1 + \delta_g) (1 - \eta_g + \eta_g^2) - \eta_g^3 - 1 \\ \delta_g^{\text{disp}} &= -u_{g\parallel} \partial_{\parallel} \delta_g^{\text{Jac}} + \frac{1}{2} u_{g\parallel}^2 \partial_{\parallel}^2 \delta_g^{\text{Jac}} + (u_{g\parallel} \partial_{\parallel} u_{g\parallel}) \partial_{\parallel} \delta_g^{\text{Jac}}, \end{aligned} \quad (2.23)$$

where all quantities are evaluated at the same apparent redshift-space spacetime point (\mathbf{x}_s, τ) . δ_g is the rest-frame galaxy density (but evaluated at the redshift-space position) containing the bias and selection contributions listed above.

The contributions in δ_g^{Jac} correspond to the Jacobian of the coordinate mapping, while δ_g^{disp} contains the terms displacing the fields from observed to actual positions. Note that, following the discussion in the previous section, we can set $\eta_g \rightarrow \eta$, $u_{g\parallel} \rightarrow u_{\parallel}$ everywhere except in the linear-order term η_g , since the difference is higher order in derivatives. In the absence of selection contributions inside δ_g , the coefficients of all operators involving η_g and $u_{g,\parallel}$ are fixed by the mapping Eq. (2.23). This has been used to estimate matter velocities and

the linear growth rate f through the contributions from the transformation to redshift space. Note that the operators in δ_g^{disp} do not appear in the list of selection contributions, and are thus unique to the redshift-space mapping. This is because they involve the galaxy velocity directly, which is not locally observable and can only appear through the transformation from rest-frame to observer's frame (in the language of Ref. [73], they are a pure projection effect).

Many of the cubic terms in Eq. (2.23) are absorbed by counterterms to the NLO galaxy power spectrum, and thus do not have to be considered further. However, it is worth noting that several of these, including

$$(b_2/2)\delta^2\eta \subset \delta_g\eta_g \quad \text{and} \quad b_1\delta\eta^2 \subset \delta_g\eta_g^2, \quad (2.24)$$

lead to a counterterm that is proportional to $\sigma^2\eta(\mathbf{x}, \tau)$, as shown in Appendix A. This shows that, in the spirit of the EFT and renormalized bias, *RSD in fact force us to introduce, in general, a free coefficient b_η multiplying η* . That is, it is not strictly consistent in the EFT to set $b_\eta = -1$ for any given tracer. Physical considerations as described in Sec. 1.1 then show that this bias can differ from -1 only through selection effects; that is, effects that are not apparent in the galaxy rest frame.

Correspondingly, other cubic RSD contributions (in particular the displacement terms in the last line of Eq. (2.23)) force us to introduce the line-of-sight-dependent higher-derivative contribution in Eq. (2.15) and Eq. (2.20) (Appendix A).

2.5 Summary

To summarize, we have derived the expression for the galaxy density perturbation in redshift space up to cubic order in perturbations, and including the leading contributions that are higher order in derivatives (here, higher derivatives means that more than two spatial derivatives are acting on each instance of the gravitational potential). We have allowed for all local observables that can affect the rest-frame galaxy density as observed from Earth. For this reason, the expansion is guaranteed to be complete at this order in perturbations and derivatives. That is, when continuing the calculation to higher order and computing loops, any additional terms that are generated are guaranteed to be higher order. Perhaps unsurprisingly, selection effects contribute to all RSD terms coming from the Jacobian, so that these contributions in general have unknown coefficients. On the other hand, the displacement terms are protected by the equivalence principle and do not involve new coefficients. This fact also is robust to loop corrections.

We now list the final expression for the redshift-space galaxy density field *retaining only operators that are relevant for the NLO power spectrum and tree-level bispectrum*. For ease of notation, we define the bias parameters corresponding to the selection effects (e.g., b_η) such that they contain both the selection effects and the contributions from the Jacobian of the coordinate mapping. We drop the brackets around operators, which are all understood to be

renormalized. The result is

$$\begin{aligned} \delta_{g,s} \Big|_{P^{\text{NLO}}} &= \sum_{O \in \mathfrak{D}_{\text{tot}}} b_O O + \epsilon + \epsilon_\delta \delta + \epsilon_\eta \eta \\ &\quad + b_\eta \left[\beta_{\nabla^2 \mathbf{v}} \nabla^2 \eta + \beta_{\partial_\parallel^2 \mathbf{v}} \partial_\parallel^2 \eta + \varepsilon_\eta \right] \\ &\quad - u_\parallel \partial_\parallel \left[b_1 \delta + b_\eta \eta + b_{\Pi_\parallel^{[2]}} \Pi_\parallel^{[2]} \right]. \end{aligned} \quad (2.25)$$

where the last line follows from the ‘‘displacement’’ part of the redshift-space mapping in Eq. (2.23). Here, the sum in the first line runs over all operators that have individual bias coefficients, namely

$$\mathfrak{D}_{\text{tot}} = \mathfrak{D}_1 \cup \mathfrak{D}_{\text{hd}} \cup \mathfrak{D}_2 \cup \mathfrak{D}_3 \quad (2.26)$$

$$\mathfrak{D}_1 = \left\{ \delta, \eta \right\}; \quad \mathfrak{D}_{\text{hd}} = \left\{ \nabla^2 \delta \right\} \quad (2.27)$$

$$\mathfrak{D}_2 = \left\{ \delta^2, K^2, \delta\eta, \eta^2, (KK)_\parallel, \Pi_\parallel^{[2]} \right\} \quad (2.28)$$

$$\mathfrak{D}_3 = \left\{ O_{\text{td}}, \delta\Pi_\parallel^{[2]}, \eta\Pi_\parallel^{[2]}, (\Pi^{[2]}K)_\parallel, \Pi_\parallel^{[3]} \right\}. \quad (2.29)$$

In the first line of Eq. (2.25), we have also allowed for a stochastic field ϵ_η associated with η (or equivalently K_\parallel), which is relevant for the galaxy bispectrum in the presence of selection effects. In Appendix B, we provide the analogous expansion of $\delta_{g,s}(\mathbf{k})$ in Fourier space. Note that we have not included cubic-order stochastic terms, such as $\epsilon_{\delta^2} \delta^2$, in Eq. (2.25). The reason is that these terms do not contribute to the tree-level bispectrum, while their contribution to the one-loop power spectrum is absorbed by the stochastic amplitude $P_\epsilon^{\{0\}}$.

In the absence of selection effects, we have, for the bias parameters and stochastic fields,

$$\begin{aligned} \text{no selection: } \quad &b_\eta = -1, \quad b_{\delta\eta} = -b_1, \quad b_{\eta^2} = 1, \\ &b_{(KK)_\parallel} = b_{\Pi_\parallel^{[2]}} = b_{\delta\Pi_\parallel^{[2]}} = b_{\eta\Pi_\parallel^{[2]}} = b_{(K\Pi^{[2]})_\parallel} = b_{\Pi_\parallel^{[3]}} = 0, \quad \text{and} \\ &\beta_{\partial_\parallel^2 \mathbf{v}} = 0, \quad \epsilon_\eta = 0. \end{aligned} \quad (2.30)$$

The non-vanishing coefficients are now determined by the redshift-space mapping Eq. (2.23).

The second line in Eq. (2.25) contains the higher-derivative velocity bias contributions. We have inserted the matter velocity for the galaxy velocity wherever the distinction is higher order. Finally, the last line contains the relevant displacement terms. Importantly, the displacement terms involve no additional bias parameters, making them robust probes of velocities even when selection effects, which remove the cosmological information in $b_\eta \eta$, for example, are present.

We can now revisit the degeneracies in higher-derivative contributions mentioned in the previous section. In full generality, keeping only the leading higher-derivative contributions

which are linear in perturbations and involve two additional derivatives, three contributions can arise:

$$\nabla^2\delta \sim -k^2\delta, \quad \partial_{\parallel}^2\delta \sim -\mu^2k^2\delta, \quad \partial_{\parallel}^2\eta \sim -\mu^4k^2\delta, \quad (2.31)$$

where we have used the linear relation between density and velocity to express these contributions in Fourier space. The first term is captured by $\nabla^2\delta$ in \mathfrak{D}_1 , while the second and third terms are equivalently parametrized by $\beta_{\nabla^2\mathbf{v}}\nabla^2\eta$ and $\beta_{\partial_{\parallel}^2\mathbf{v}}\partial_{\parallel}^2\eta$ appearing in the velocity bias [second line of Eq. (2.25)]. Thus, at this order there is no need to introduce additional higher-derivative operators such as $\partial_{\parallel}^2\delta$.

Similarly, for the stochastic contributions, we need terms that scale as $k^2 \times \text{const}$ and $\mu^2k^2 \times \text{const}$, which are supplied by $P_{\epsilon}^{\{2\}}$ and $P_{\epsilon\epsilon\eta}^{\{2\}}$, respectively; as argued at the end of Sec. 2.2, there are no $\mu^2 \times \text{const}$ or $\mu^4k^2 \times \text{const}$ stochastic terms, while a term $\mu^4k^4 \times \text{const}$ is higher order in derivatives. This shows that the contribution considered in Eq. (2.16), while in general allowed, is degenerate with other contributions for the observables we consider.

We emphasize again that these degeneracies are only present when considering the NLO galaxy power spectrum and LO galaxy bispectrum. If other statistics are considered, in particular cross-correlations with matter, it is in general necessary to include these individual contributions since they are no longer degenerate.

To summarize, the LO galaxy power spectrum in redshift space involves 2 free bias parameters (b_1, b_η) and 1 stochastic amplitude ($P_{\epsilon}^{\{0\}}$), which reduces to 1 bias parameter and 1 stochastic amplitude in the absence of selection effects. Including the NLO correction to the power spectrum as well as LO bispectrum, we can summarize the number of free parameters as follows: with [without] selection effects, we have

- 14 [5] bias parameters,
- 2 [1] velocity bias parameters, and
- 6 [5] stochastic amplitudes (3 [3] for the NLO power spectrum, 3 [2] for the LO bispectrum),

adding up to 22 [11] free parameters. Note that the stochastic velocity field ϵ_v is present even in the absence of selection effects, and hence $P_{\epsilon\epsilon\eta}^{\{2\}}$ is expected to be always present as well; as we have mentioned, it corresponds to the finger-of-god contribution in the “strict sense.”

3 Power spectrum

We now turn to the computation of the redshift-space galaxy two-point function in Fourier space, the power spectrum, up to next-to-leading order (NLO). The NLO galaxy power spectrum can be broken down into three parts:

1. Linear and higher-derivative bias terms.
2. The 2–2-type bias, selection, and RSD contribution, as well as nonlinear evolution of the matter density and velocity, which involves the coupling of two quadratic operators.

3. The 1–3-type contribution, which contains the coupling of the relevant cubic with linear operators for all of the effects mentioned above.

We consider each of them in turn.

3.1 Linear and higher-derivative bias

It is natural to include all stochastic terms in this contribution as well. Noting that $\eta = \mu^2\theta$ in Fourier space at all orders, and $\eta^{(1)} = -f\mu^2\delta^{(1)}$ at linear order, we straightforwardly obtain

$$\begin{aligned}
P_{gg,s}^{\text{l+hd}}(k, \mu) &= [P_{\delta_g\delta_g}(k) + 2b_\eta P_{\delta_g\eta_g}(k, \mu) + b_\eta^2 P_{\eta_g\eta_g}(k, \mu)]^{\text{l+hd}} \\
&= [b_1 - b_\eta f\mu^2]^2 P_L(k) + P_\epsilon^{\{0\}} \\
&\quad - 2 \left\{ b_1 b_{\nabla^2\delta} - \mu^2 f b_\eta [b_{\nabla^2\delta} + b_1 \beta_{\nabla^2\mathbf{v}} + b_1 \beta_{\partial_{\parallel}^2\mathbf{v}}\mu^2] \right. \\
&\quad \left. + \mu^4 f^2 b_\eta^2 [\beta_{\nabla^2\mathbf{v}} + \beta_{\partial_{\parallel}^2\mathbf{v}}\mu^2] \right\} k^2 P_L(k) \\
&\quad + k^2 P_\epsilon^{\{2\}} + \mu^2 k^2 b_\eta P_{\epsilon\epsilon\eta}^{\{2\}}.
\end{aligned} \tag{3.1}$$

Here, the first line of the second equality contains the tree-level galaxy power spectrum in redshift-space, which is the well-known expression first derived by Kaiser [23], including the leading stochastic term. The following two lines contain the leading (deterministic) higher-derivative contributions, while the last line contains the higher-derivative stochastic terms. Note that we do not include the leading EFT counterterms to the matter density and velocity, as these are degenerate with the higher-derivative galaxy bias (including velocity bias) contributions, following the discussion in Sec. 2.5. The matter counterterms are discussed in Sec. 5.2 and Appendix E.

3.2 2–2

The 2–2 type terms can, as in the case of the rest-frame galaxy or halo power spectrum [74, 75], be succinctly summarized as

$$P_{gg,s}^{2-2}(k, \mu) = \sum_{O, O' \in \mathfrak{D}_{2-2}} b_O b_{O'} \mathcal{I}^{[O, O']}(k, \mu), \tag{3.2}$$

where the list of operators and associated bias parameters is given by

$$\begin{aligned}
\mathfrak{D}_{2-2} &= (\mathfrak{D}_1)^{(2)} \cup \mathfrak{D}_2 \\
&= \left\{ \delta^{(2)}, \eta^{(2)}, \delta^2, K^2, \delta\eta, \eta^2, (KK)_\parallel, \Pi_\parallel^{[2]}, u_\parallel \partial_\parallel \delta, u_\parallel \partial_\parallel \eta \right\}
\end{aligned} \tag{3.3}$$

$$\begin{aligned}
\{b_O\}_{\mathfrak{D}_{2-2}} &= \left\{ b_1, b_\eta, b_{\delta^2} = b_2/2, b_{K^2}, b_{\delta\eta}, b_{\eta^2}, b_{(KK)_\parallel}, b_{\Pi_\parallel^{[2]}}, -b_1, -b_\eta \right\} \\
&\stackrel{\text{no sel.}}{=} \{b_1, -1, b_2/2, b_{K^2}, -b_1, 1, 0, 0, -b_1, 1\}.
\end{aligned} \tag{3.4}$$

Operator	Kernel $S_O(\mathbf{k}_1, \mathbf{k}_2)$
$\delta^{(2)}$	$F_2(\mathbf{k}_1, \mathbf{k}_2)$
$\theta^{(2)}$	$-\mathcal{H}fG_2(\mathbf{k}_1, \mathbf{k}_2)$
δ^2	1
K^2	$\mu_{12}^2 - 1/3$
$s^k \partial_k \delta$	$-\mu_{12}(k_1/k_2 + k_2/k_1)/2$
$\eta^{(2)}$	$-f\mu_{\mathbf{k}_{12}, \hat{\mathbf{n}}}^2 G_2(\mathbf{k}_1, \mathbf{k}_2)$
$\delta\eta$	$-f(\mu_1^2 + \mu_2^2)/2$
η^2	$f^2\mu_1^2\mu_2^2$
$(KK)_{\parallel}$	$\mu_1\mu_2\mu_{12} - (\mu_1^2 + \mu_2^2)/3 + 1/9$
$\Pi_{\parallel}^{[2]}$	$\mu_1\mu_2\mu_{12} + (5/7)\mu_{\mathbf{k}_{12}, \hat{\mathbf{n}}}^2(1 - \mu_{12}^2)$
$u_{\parallel} \partial_{\parallel} \delta$	$-f\mu_1\mu_2(k_1/k_2 + k_2/k_1)/2$
$u_{\parallel} \partial_{\parallel} \eta$	$f^2\mu_1\mu_2(\mu_2^2 k_2/k_1 + \mu_1^2 k_1/k_2)/2$

Table 1. Fourier-space kernels $S_O(\mathbf{k}_1, \mathbf{k}_2)$ corresponding to the quadratic operators appearing in the galaxy power spectrum and bispectrum in redshift space. We have denoted $\mu_{12} \equiv \hat{\mathbf{k}}_1 \cdot \hat{\mathbf{k}}_2$ and $\mu_a \equiv \hat{\mathbf{k}}_a \cdot \hat{\mathbf{n}}$, $a \in \{1, 2\}$, while $\mu_{\mathbf{k}_{12}, \hat{\mathbf{n}}} \equiv \hat{\mathbf{k}}_{12} \cdot \hat{\mathbf{n}}$.

The last line holds in the limit of no selection effects. The loop integral is given by

$$\mathcal{I}^{[O, O']}(k, \mu) = 2 \left[\int_{\mathbf{p}} S_O(\mathbf{k} - \mathbf{p}, \mathbf{p}) S_{O'}(\mathbf{k} - \mathbf{p}, \mathbf{p}) P_L(p) P_L(|\mathbf{k} - \mathbf{p}|) - \int_{\mathbf{p}} S_O(-\mathbf{p}, \mathbf{p}) S_{O'}(-\mathbf{p}, \mathbf{p}) P_L(p) P_L(p) \right], \quad (3.5)$$

where the kernels S_O are summarized in Tab. 1. At first sight, Eq. (3.2) thus consists of 55 distinct contributions, each of which is a function of two arguments k, μ . However, using the fact that all quadratic operators are constructed out of symmetric two-tensors and vectors derived from the density, and using the specific form of Eq. (3.5), this can be reduced significantly, to 23 functions of k only. Specifically, we can write $P_{gg,s}^{2-2}(k, \mu)$ as

$$P_{gg,s}^{2-2}(k, \mu) = \sum_{n=0}^4 \sum_{(m,p)} \mathcal{A}_{n(m,p)}(f, \{b_O\}_{\mathcal{D}_{2-2}}) \mathcal{I}_{mp}(k) \mu^{2n} \quad (3.6)$$

$$= \sum_{\ell=0,2,4,6,8} \sum_{(m,p)} \mathcal{C}_{(m,p)}^{2-2,\ell}(f, \{b_O\}_{\mathcal{D}_{2-2}}) \mathcal{I}_{mp}(k) \mathcal{L}_{\ell}(\mu), \quad (3.7)$$

where \mathcal{L}_n denote the Legendre polynomials, and we have defined

$$\mathcal{I}_{mp}(k) \equiv \left[2 \int_{\mathbf{p}} \frac{p^{p-2} k^{6-p}}{|\mathbf{k} - \mathbf{p}|^4} (\hat{\mathbf{k}} \cdot \hat{\mathbf{p}})^m P_L(p) P_L(|\mathbf{k} - \mathbf{p}|) - \frac{2\delta_{p6}}{m+1} \left(\int_{\mathbf{p}} [P_L(p)]^2 \right) \right]. \quad (3.8)$$

There are 23 distinct loop integrals $\mathcal{I}_{mp}(k)$ corresponding to the (m, p) pairs listed in Tab. 2. The last term in Eq. (3.8) subtracts a constant contribution in the $k \rightarrow 0$ limit for the case

$p = 6$, which would renormalize the stochastic amplitude $P_e^{\{0\}}$. We do not subtract the higher analytic contributions in the $k \rightarrow 0$ limit, which scale as k^2, k^4, \dots (note that m is even if p is even). Since we include the higher-derivative stochastic contributions, this merely amounts to convention. Note that, even though not immediately obvious from Eq. (3.5) and Tab. 1, all 2–2 loop contributions are given as polynomials in μ^2 , up to order μ^8 .

We show the shape of all 23 integrals $\mathcal{I}_{mp}(k)$ for the fiducial cosmology in Fig. 1. While the loop integrals have different slopes in the low- k limit, they are all roughly comparable at wavenumbers where the 1-loop contribution becomes important, $k \gtrsim 0.05 h \text{ Mpc}^{-1}$. Even among the strictly linearly independent terms, many have very similar dependences on k . The coefficients $\mathcal{A}_{n(m,p)}$ and $\mathcal{C}_{2\ell(m,p)}^{2-2}$, which are given by a sum over all quadratic combinations of b_O for $O \in \mathfrak{D}_{2-2}$, are too lengthy to list in this paper (they amount to 15–20 pages of equations) and can be found in the supplementary material [76].

Finally, the 2–2-type contributions can be efficiently evaluated in configuration space. As shown in Appendix H, the 2–2-type contributions to the galaxy correlation function in redshift space can be expressed in terms of only 14 independent integrals. The transformation back to Fourier space requires 5 further integrals over r . This is analogous to the efficient evaluation of perturbation theory loop integrals proposed in [77, 78].

m	0	1	2	3	4	5	6	7	8
p	0, 2, 4, 6	1, 3, 5	0, 2, 4, 6	1, 3, 5	2, 4, 6	3, 5	4, 6	5	6

Table 2. List of all 23 (m, p) combinations that contribute to $P_{gg,s}^{22}(k, \mu)$ in Eq. (3.6).

3.3 1–3

We now turn to the 1–3-type contribution, which consists of individual loop terms of the form

$$\left\langle \delta(\mathbf{k}') O^{(3)}(\mathbf{k}) \right\rangle'. \quad (3.9)$$

As shown in Appendix C, they can be classified into three categories:

1. Operators that are combinations of three powers of $\Pi^{[1]}$, such as $\delta^3, (KKK)_{\parallel}$, and so on. All of these lead to contributions which are absorbed by counterterms, and can be dropped immediately. In fact, we have not included the corresponding cubic operators in Eq. (2.25).
2. Operators that contain, schematically, $\nabla^{-2}[\Pi^{[1]}\Pi^{[1]}]$. This includes all operators involving $\Pi^{[2]}$, as well as several of the quadratic operators in Eq. (2.25) evaluated at next-to-leading, i.e. cubic, order in perturbation theory.
3. Operators that contain, schematically, $\nabla^{-2}\{\Pi^{[1]}\Pi^{[1]}\Pi^{[1]}, \Pi^{[1]}\Pi^{[2]}\}$. This class only consists of $\Pi_{\parallel}^{[3]}$ and $(\Pi_{\parallel}^{[2]})^{(3)}$.

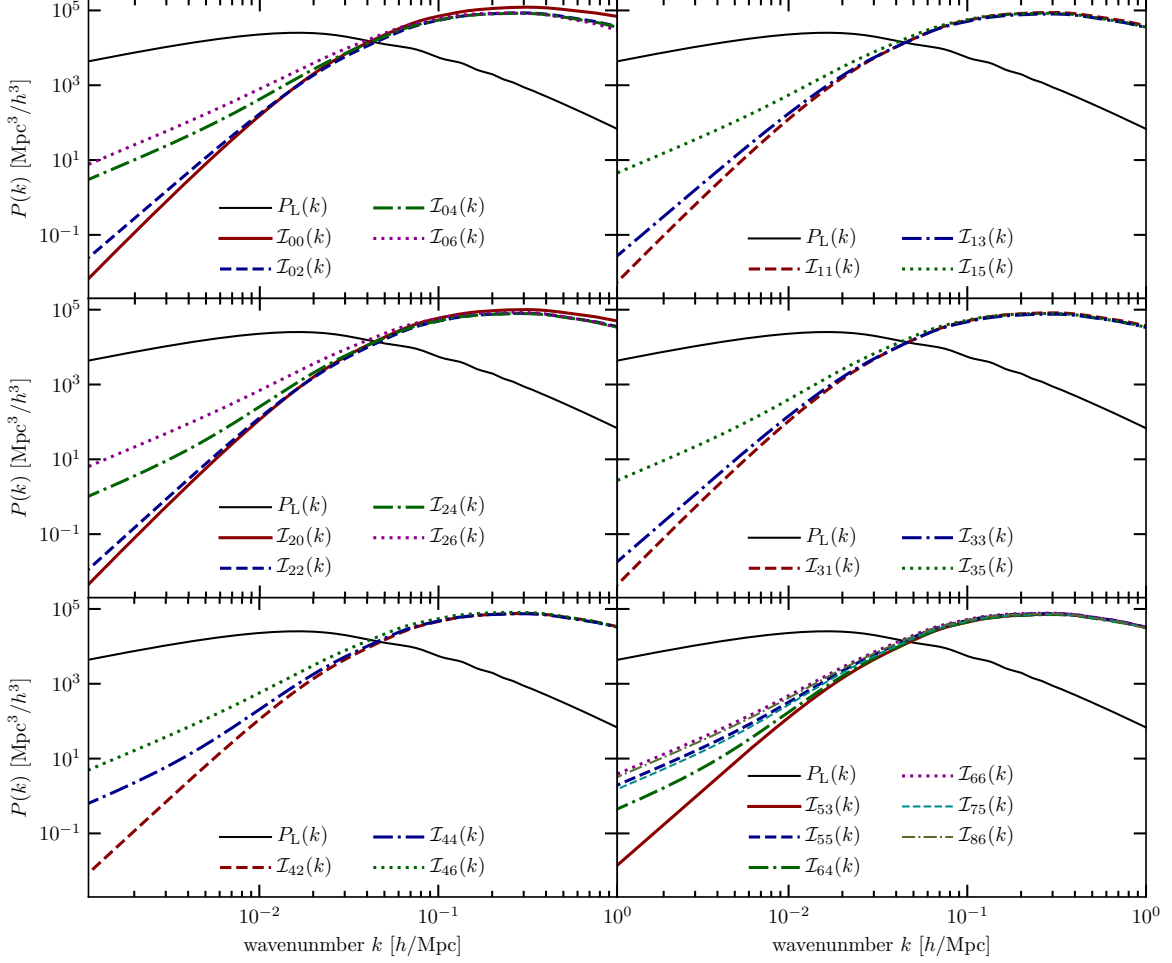


Figure 1. The 23 independent loop integrals $\mathcal{I}_{mp}(k)$ describing the 2–2-type loop contributions to the redshift-space power spectrum, for the index pairs mp listed in Tab. 2.

Thus, we can focus on the second and third class of operators. Specifically, the list to consider is

$$\begin{aligned}
\mathfrak{D}_{1-3} &= (\mathfrak{D}_2)^{(3)} \Big|_{\text{relevant}} \cup \mathfrak{D}_3 \tag{3.10} \\
&= \left\{ 2 \text{tr}[KK^{(2)}], \delta\eta^{(2)}, 2\eta\eta^{(2)}, 2(KK^{(2)})_{\parallel}, O_{\text{td}}, \delta\Pi_{\parallel}^{[2]}, \eta\Pi_{\parallel}^{[2]}, (K\Pi^{[2]})_{\parallel}, \right. \\
&\quad \left. s^k \partial_k \Pi_{\parallel}^{[2]}, s^{(2)k} \partial_k \delta, s^{(2)k} \partial_k \theta, u_{\parallel}^{(2)} \partial_{\parallel} \delta, u_{\parallel}^{(2)} \partial_{\parallel} \eta, u_{\parallel} \partial_{\parallel} \eta^{(2)}, u_{\parallel} \partial_{\parallel} \Pi_{\parallel}^{[2]}, \Pi_{\parallel}^{[3]} \right\}.
\end{aligned}$$

Note that this list includes several operators which appear through lower-order operators evaluated at third order, such as $s^k \partial_k \Pi_{\parallel}^{[2]} \subset \Pi^{[2](3)}$, $s^{(2)k} \partial_k \delta \subset \delta^{(3)}$, and $s^{(2)k} \partial_k \theta \subset \theta^{(3)}$ (see Appendix C.3 and Appendix E, respectively). The first 15 operators belong to the second

class, and we will consider them first. Only the last operator belongs to the third class, which we consider at the end.

Clearly, calculating loop integrals involving 16 individual cubic operators is cumbersome, not very illuminating, and does not allow us to identify how many independent loop integrals in fact exist. Let us thus examine the structure of these contributions. As we will show below, all non-trivial 1–3-type loop contributions that appear in the NLO redshift-space power spectrum can be written as contractions of

$$3P_L(k) \int_{\mathbf{p}} \frac{F_{ijkl}(\mathbf{p}, \mathbf{k})}{p^2 |\mathbf{k} - \mathbf{p}|^2} (1 - \mu_{\mathbf{k}, \mathbf{p}}^2) P_L(p) \quad (3.11)$$

with δ^{ab} and $\hat{n}^a \hat{n}^b$. Here, $F_{ijkl}(\mathbf{p}, \mathbf{k})$ is a fourth-order polynomial in components of \mathbf{p} and \mathbf{k} , which is at least linear in \mathbf{p} . The reason is that all contributions which do not involve the factor $1/|\mathbf{k} - \mathbf{p}|^2$ are analytic in \mathbf{k} , and are absorbed by counterterms. The contraction with δ^{ab} and $\hat{n}^a \hat{n}^b$ simply follows from the fact that $\hat{\mathbf{n}}$ is the only preferred direction involved. The factor $(1 - \mu_{\mathbf{k}, \mathbf{p}}^2)$ is enforced by the requirement that the loop integral go to zero as $k \rightarrow 0$; that is, any other combination of 1 and $\mu_{\mathbf{k}, \mathbf{p}}^2$ leads to a constant counterterm which can be subtracted.

In Appendix D, we show how Eq. (3.11) can be decomposed into linear combinations of only 5 *linearly independent loop integrals*. Expressing each of the operators in Eq. (3.10) as a contraction of Eq. (3.11), and projecting onto the decomposition of the latter, then allows us to express all 1–3-type loop integrals as a linear combination of the 5 loop integrals, weighted by bias parameters and powers of $\mu^2 \equiv (\hat{\mathbf{k}} \cdot \hat{\mathbf{n}})^2$.

3.3.1 $\Pi^{[1]}\Pi^{[2]}$ -type operators

Let us begin with a subset of 8 of the operators in \mathfrak{D}_{1-3} [Eq. (3.10)] which can be written as a projection (using δ_{ab} and $\hat{n}_a \hat{n}_b$) of the following operator:

$$O_{ijkl}^{\Pi_1 - \Pi_2} \equiv \Pi_{ij}^{[1]} \mathcal{D}_{kl} \left(\delta^2 - \frac{3}{2} K^2 \right) = \frac{3}{2} \Pi_{ij}^{[1]} \mathcal{D}_{kl} \left(\delta^2 - \text{tr}[\Pi^{[1]}\Pi^{[1]}] \right), \quad (3.12)$$

where the indices ij, kl are either contracted with each other or with $\hat{\mathbf{n}}$, and \mathcal{D}_{ij} is defined in Eq. (1.7). The correlator Eq. (3.9) in turn immediately becomes (Appendix C)

$$\left\langle \delta(\mathbf{k}') O_{ijkl}^{\Pi_1 - \Pi_2}(\mathbf{k}) \right\rangle' = 3P_L(k) \int_{\mathbf{p}} \frac{p^i p^j}{p^2} \frac{(k-p)^k (k-p)^l}{|\mathbf{k} - \mathbf{p}|^2} (1 - \mu_{\mathbf{k}, \mathbf{p}}^2) P_L(p). \quad (3.13)$$

This is clearly a special case of Eq. (3.11), and can in turn be derived by decomposing it into tensors whose structure is governed by symmetry and which only depend on $\hat{\mathbf{k}}$, multiplied by scalar loop integrals. This is performed in Appendix D.

We then isolate the contribution $\propto O^{\Pi_1 - \Pi_2}$ in each of the operators in \mathfrak{D}_{1-3} to which this applies, which is derived in Appendix F. As expected from symmetry arguments, we obtain four independent contractions of $O_{ijkl}^{\Pi_1 - \Pi_2}$ with $\hat{\mathbf{n}}$ and δ_{ab} . The loop contributions from several operators are simply proportional.

3.3.2 Other contributions

Seven of the remaining eight contributions in Eq. (3.10) have a similar, but not quite identical structure to the contributions involving $O^{\Pi^1-\Pi^2}$. For example, we have

$$\left\langle \delta(\mathbf{k}') \left(s^k \partial_k \Pi_{\parallel}^{[2]} \right) (\mathbf{k}) \right\rangle' = -\frac{10}{7} P_L(k) \int_{\mathbf{p}} \frac{\mathbf{p} \cdot (\mathbf{k} - \mathbf{p}) (k - p)_{\parallel}^2}{p^2 |\mathbf{k} - \mathbf{p}|^2} (1 - \mu_{\mathbf{k}, \mathbf{p}}^2) P_L(p) \quad (3.14)$$

This clearly also corresponds to a specific contraction of Eq. (3.11). The remaining contributions are listed in Appendix F.

3.3.3 $\Pi_{\parallel}^{[3]}$ -type operators

We finally turn to the last operators in the list Eq. (3.10), $\Pi_{\parallel}^{[3]}$, which is also relevant as part of $(\Pi_{\parallel}^{[2]})^{(3)}$. This operator is significantly more complex than the other operators in the list. However, again only a small subset of contributions to this operator leads to nontrivial loop contributions to the power spectrum, and most of these are already among the operators considered above [such as $(K\Pi_{\parallel}^{[2]})_{\parallel}$], so that we do not require full explicit expressions.

As argued in Appendix C.3, the only nontrivial contribution in $\Pi_{\parallel}^{[3]}$ that is not already captured by the remaining operators considered above is

$$\frac{\partial_{\parallel}^2}{\nabla^2} O_{\text{td}}. \quad (3.15)$$

One can easily see that this leads to

$$\left\langle \delta(\mathbf{k}) (\Pi_{\parallel}^{[3]}) (\mathbf{k}') \right\rangle' \propto \mu^2 \left\langle \delta(\mathbf{k}) (O_{\text{td}}) (\mathbf{k}') \right\rangle', \quad (3.16)$$

where the proportionality constant can be determined by comparing to the corresponding loop integral using the full SPT kernel (see Appendix C.3).

3.3.4 Projection onto general loop integral

As we have seen, all 1-3-type contributions can be written as contractions of Eq. (3.11) with δ^{ab} and $\hat{n}^a \hat{n}^b$. In Appendix D, we show how any contraction of Eq. (3.11) can be written as a linear combination of 5 loop integrals $\mathcal{I}_n(k)$. This includes the 1-3-type contributions to the NLO matter and velocity divergence power spectra.

Straightforward linear algebra then leads to

$$\left\langle \delta(\mathbf{k}') [O^{[3]}] (\mathbf{k}) \right\rangle' = f_O(k, \mu) P_L(k), \quad (3.17)$$

where

$$f_O(k, \mu) = (1, \mu^2, \mu^4) \mathbf{M}(O) \begin{pmatrix} \mathcal{I}_1(k) \\ \mathcal{I}_2(k) \\ \mathcal{I}_3(k) \\ \mathcal{I}_4(k) \\ \mathcal{I}_5(k) \end{pmatrix},$$

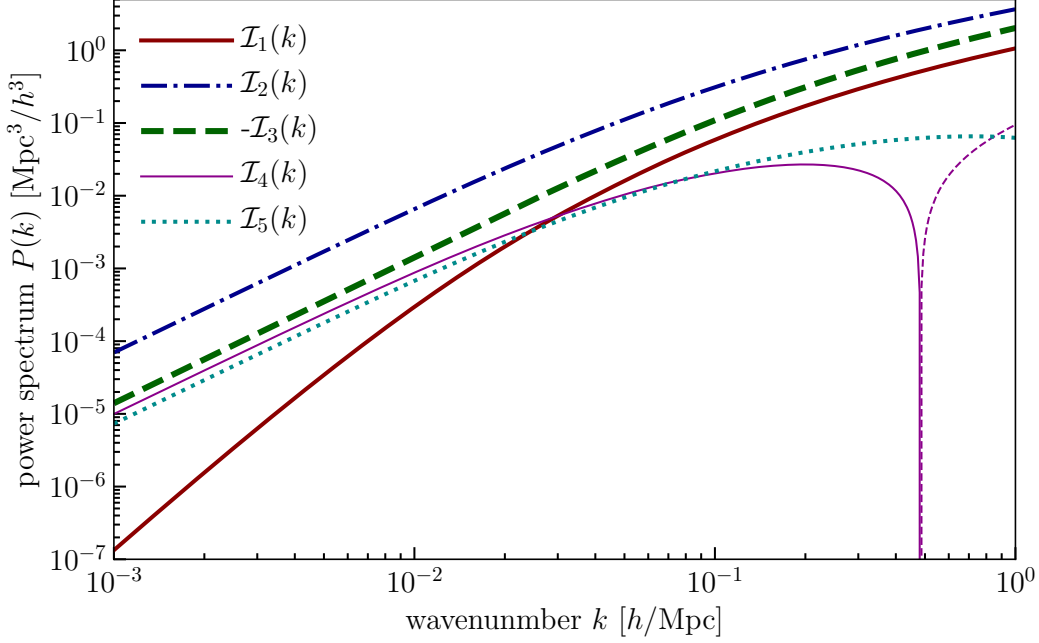


Figure 2. The five independent loop integrals $\mathcal{I}_n(k)$ describing the 1–3-type loop contributions to the redshift-space power spectrum. For the negative contributions, such as $\mathcal{I}_3(k)$ and $\mathcal{I}_4(k)$ at $k > 0.4 h/\text{Mpc}$, we show their absolute value as dashed lines.

and $\mathbf{M}(O)$ is a 3×5 coefficient matrix, listed for each operator in Appendix F, and the dimensionless loop integrals $\mathcal{I}_n(k)$ are defined in Eq. (D.5).

Finally, the 1–3-type contribution to the NLO galaxy power spectrum in redshift space becomes

$$P_{gg,s}^{1-3}(k, \mu) = \sum_{O \in \mathfrak{D}_{1-3}} (b_1 - b_\eta f \mu^2) b_O f^{n_f(O)} f_O(k, \mu) P_L(k), \quad (3.18)$$

where the list of operators, associated bias parameters, and growth-rate powers is given by

$$\mathfrak{D}_{1-3} = \left\{ \delta^{(3)}, \eta^{(3)}, 2 \text{tr}[KK^{(2)}], \delta\eta^{(2)}, 2\eta\eta^{(2)}, 2(KK^{(2)})_{\parallel}, O_{\text{td}}, \delta\Pi_{\parallel}^{[2]}, \eta\Pi_{\parallel}^{[2]}, \right. \\ \left. (K\Pi^{[2]})_{\parallel}, s^k \partial_k \Pi_{\parallel}^{[2]}, u_{\parallel}^{(2)} \partial_{\parallel} \delta, u_{\parallel}^{(2)} \partial_{\parallel} \eta, u_{\parallel} \partial_{\parallel} \eta^{(2)}, u_{\parallel} \partial_{\parallel} \Pi_{\parallel}^{[2]}, \Pi_{\parallel}^{[3]} \right\} \quad (3.19)$$

$$\{b_O\}_{\mathfrak{D}_{1-3}} = \left\{ b_1, b_\eta, b_{K^2}, b_{\delta\eta}, b_{\eta^2}, b_{(KK)_\parallel}, b_{\text{td}}, b_{\delta\Pi_\parallel^{[2]}}, b_{\eta\Pi_\parallel^{[2]}}, \right. \\ \left. b_{(\Pi^{[2]}K)_\parallel}, -b_{\Pi_\parallel^{[2]}}, -b_1, -b_\eta, -b_\eta, -b_{\Pi_\parallel^{[2]}}, b_{\Pi_\parallel^{[3]}} + 2b_{\Pi_\parallel^{[2]}} \right\} \quad (3.20)$$

$$\{n_f(O)\}_{\mathfrak{D}_{1-3}} = \left\{ 0, 1, 0, 1, 2, 0, 0, 0, 1, \right. \\ \left. 0, 0, 1, 2, 2, 1, 0 \right\}. \quad (3.21)$$

Here, we have used Eq. (C.19). One can further reduce the list of operators by making use of the redundancies given in Appendix F. However, from the perspective of numerical evaluation, this does not make a difference, as all contributions are given by linear combinations of the same 5 loop integrals.

The independent loop integrals $\mathcal{I}_n(k)$ are shown in Fig. 2. Interestingly, one finds that $\mathcal{I}_1, \mathcal{I}_2, \mathcal{I}_3$ are somewhat larger than $\mathcal{I}_4, \mathcal{I}_5$. However, precise statements can only be made given knowledge of the various coefficients. A complete decomposition of the 1–3-contributions into multipoles of the form (see Appendix G)

$$P_{gg,s}^{1-3}(k, \mu) = (b_1 - b_\eta f \mu^2) \sum_{m=0}^2 \sum_{n=1}^5 \mathcal{B}_{m,n}(f, \{b_O\}_{\mathfrak{D}_{1-3}}) \mathcal{I}_n(k) P_L(k) \mu^{2m} \\ = \sum_{\ell=0,2,4,6}^5 \sum_{n=1}^5 \mathcal{C}_n^{1-3,\ell}(f, \{b_O\}_{\mathfrak{D}_{1-3}}) \mathcal{I}_n(k) P_L(k) \mathcal{L}_\ell(\mu), \quad (3.22)$$

where the explicit expressions for the coefficients $\mathcal{B}_{m,n}, \mathcal{C}_n^{1-3,\ell}$ can be found in the supplementary material [76].

3.4 Summary: redshift-space galaxy power spectrum at NLO

Compiling the results of this section, we have

$$P_{gg,s}^{\text{LO+NLO}}(k, \mu) = P_{gg,s}^{\text{lb+hd}} + P_{gg,s}^{2-2}(k, \mu) + 2P_{gg,s}^{1-3}(k, \mu), \quad (3.23)$$

where

- $P_{gg,s}^{\text{lb+hd}}(k)$ is given in Eq. (3.1),
- $P_{gg,s}^{2-2}(k, \mu)$ is given in Eqs. (3.6)–(3.8), and
- $P_{gg,s}^{1-3}(k, \mu)$ is given in Eqs. (3.18)–(3.22).

The 2–2 and 1–3 contributions together consist of 28 independent loop integrals. In Appendix G together with the supplementary material [76], we decompose all contributions in multipoles with respect to μ , and provide a complete list of efficient expressions. Appendix H gives some results on the redshift-space galaxy correlation function.

3.5 IR resummation

The NLO galaxy power spectrum contains a subset of quadratic contributions of the form $s^k \partial_k O^{(1)}$ and $u_{\parallel} \partial_{\parallel} O^{(1)}$, where $O^{(1)} \in \{\delta, \eta\}$. These contributions differ from the others in two respects: (i) they involve the linear displacement and velocity without derivatives, which is dominated by large-scale perturbations; (ii) they are not multiplied by free bias parameters, but the coefficients corresponding to $O^{(1)}$. These particular operators correspond to the displacement of the matter and galaxy fields from their Lagrangian to the final Eulerian position, and from the rest frame to redshift space, respectively. In fact, the two properties given above are directly related, since the displacement and velocity are not locally observable, so the galaxy number density cannot depend on them directly, even in the presence of selection effects. In other words, as mentioned above, they are pure projection effects.

The dominant effect of these terms on the power spectrum is to smooth the oscillatory BAO feature in the power spectrum. As shown in Refs. [79–83] (see App. B.4 in [61] for a brief overview), these terms can be resummed. That is, all corresponding higher-order contributions of the form $(s^k \partial_k)^n O^{(1)}$, where n can be arbitrarily large, can be included analytically. This effectively leads to a smoothed BAO component in the power spectrum through

$$P_L^w(k) \longrightarrow P_L^w(k) \exp[-\Sigma^2(\epsilon k)k^2], \quad (3.24)$$

where $P_L^w(k)$ is the oscillatory part of the linear power spectrum, $\Sigma^2(\Lambda)$ is the variance of the displacement field including modes up to a wavenumber Λ , and $\epsilon < 1$ is a parameter. This IR resummation in the rest frame can be extended to include all terms of the form $(u_{\parallel} \partial_{\parallel})^n \{\delta^{(1)}, \eta^{(1)}\}$ by generalizing the damping term to [82, 84–88]

$$\exp[-\Sigma^2(\epsilon k)k^2] \longrightarrow \exp[-(1 + f(f + 2)\mu^2) \Sigma^2(\epsilon k)k^2]. \quad (3.25)$$

Importantly, this resummation is valid even in the presence of selection effects, as these do not affect the displacement terms, as we have argued above. The results obtained by the recent Ref. [88] for biased tracers in redshift space can thus easily be generalized to include selection effects.

4 The LO redshift-space galaxy bispectrum

We now give the result for the LO redshift-space galaxy bispectrum. At this order, we can neglect higher-derivative contributions which includes deterministic and stochastic velocity bias. On the other hand, the deterministic contributions are completely determined by the set of quadratic operators considered for the 2–2 type terms in the NLO power spectrum.

We thus have

$$\begin{aligned}
& B_{ggg,s}^{\text{LO}}(k_1, \mu_1; k_2, \mu_2; k_3, \mu_3) \\
&= \left[2(b_1 - b_\eta f \mu_2^2)(b_1 - b_\eta f \mu_3^2) \sum_{O \in \mathfrak{D}_{2-2}} b_O S_O(\mathbf{k}_2, \mathbf{k}_3) P_L(k_2) P_L(k_3) + 2 \text{ perm.} \right] + B_\epsilon^{\{0\}} \\
&+ \left\{ 2(b_1 - b_\eta f \mu_1^2) P_{\epsilon\epsilon\delta}^{\{0\}} P_L(k_1) + 2 \text{ perm.} \right\} - \left\{ 2(b_1 - b_\eta f \mu_1^2) \mu_1^2 f P_{\epsilon\epsilon\eta}^{\{0\}} P_L(k_1) + 2 \text{ perm.} \right\},
\end{aligned} \tag{4.1}$$

where $\mu_1 \equiv \hat{\mathbf{k}}_1 \cdot \hat{\mathbf{n}}$, and the list of second-order operators and associated bias parameters is given by Eq. (3.3),

$$\begin{aligned}
\mathfrak{D}_{2-2} &= \left\{ \delta^{(2)}, \eta^{(2)}, \delta^2, K^2, \delta\eta, \eta^2, (KK)_\parallel, \Pi_\parallel^{[2]}, u_\parallel \partial_\parallel \delta, u_\parallel \partial_\parallel \eta \right\} \\
\{b_O\}_{\mathfrak{D}_{2-2}} &= \left\{ b_1, b_\eta, b_{\delta^2} = b_2/2, b_{K^2}, b_{\delta\eta}, b_{\eta^2}, b_{(KK)_\parallel}, b_{\Pi_\parallel^{[2]}}, -b_1, -b_\eta \right\} \\
&\stackrel{\text{no sel.}}{=} \{b_1, -1, b_2/2, b_{K^2}, -b_1, 1, 0, 0, -b_1, 1\}.
\end{aligned} \tag{4.2}$$

The kernels S_O in Eq. (4.1) are the same as those appearing in the 2-2-type loop contribution to the power spectrum, and are given in Tab. 1. Unlike the case of the NLO contributions to the galaxy power spectrum, the contributions to the LO galaxy bispectrum all involve distinct shapes with respect to the angles of the vectors \mathbf{k}_i among themselves and with the line of sight. Hence, including the bispectrum information is expected to break many of the parameter degeneracies present in the NLO power spectrum. Note that the list of operators also includes all tidal alignment selection effects considered by [71].

Finally, let us briefly discuss the stochastic contributions in the last two lines of Eq. (4.1). The first, constant term $B_\epsilon^{\{0\}}$ quantifies the bispectrum (essentially skewness) of the leading stochastic field ϵ . There are no line-of-sight dependent corrections for the same reason as for $P_\epsilon^{\{0\}}$. The second term, $\propto P_{\epsilon\epsilon\delta}^{\{0\}}$, quantifies the dependence of the noise variance on the large-scale density. Finally, the last term, $\propto P_{\epsilon\epsilon\eta}^{\{0\}}$, contains the analogous dependence of the stochasticity variance on η . This last term only appears if selection effects are present.

5 Connection to previous results

5.1 Relation to the “streaming model”

Let us now connect our results to previous derivations of large-scale galaxy statistics in redshift space. These are usually referred to as “streaming-model” approaches. The streaming formulation of redshift-space distortions [24, 89, 90] relies on the fact that the number of objects is conserved in the transformation from rest frame to redshift space, so that

$$(1 + \delta_g) d^3 r = (1 + \delta_{g,s}) d^3 r_s. \tag{5.1}$$

As a result, the redshift-space correlation function is related to its rest-frame counterpart through a convolution which, in the notation of [27], is

$$\xi_s(r_{s\parallel}, \mathbf{r}_{s\perp}) = \int_{-\infty}^{+\infty} dr_{\parallel} [1 + \xi(r)] \mathcal{P}(r_{\parallel} - r_{s\parallel}, \mathbf{r}) - 1 + \frac{1}{\bar{n}} \delta_D(\mathbf{r}_s), \quad (5.2)$$

where \mathbf{r}_s is the redshift-space separation vector, $\xi(r)$, $\xi_s(r_{s\parallel}, \mathbf{r}_{s\perp})$ (with $\mathbf{r}_{s\perp} \equiv \mathbf{r}_{\perp}$) are the rest-frame and redshift-space galaxy 2-point correlations, respectively, and $\mathcal{P}(u_g, \mathbf{r})$ is the pairwise velocity PDF, i.e. the probability that a pair separated by a distance \mathbf{r} has a relative line of sight velocity u_g . The pairwise velocity PDF can be expressed as the Fourier transform of the pairwise generating function $\mathcal{M}(\lambda, \mathbf{r})$,

$$\mathcal{P}(u_g, \mathbf{r}) = \int \frac{d\gamma}{2\pi} \mathcal{M}(i\gamma f, \mathbf{r}) e^{-i\gamma u_g}, \quad (5.3)$$

which is defined such that $\mathcal{M}(0, \mathbf{r}) = 1$ for any pair conserving map. At large separations $r_{s\parallel} \gg f\sigma_{12}$, where σ_{12}^2 is the pairwise velocity variance derived below, the convolution is sharply peaked around $r_{\parallel} = r_{s\parallel}$ and one can expand the rest-frame position around the redshift-space position as in [27], i.e.

$$\mathcal{P}(u_g, r_{\parallel}) \approx \mathcal{P}(u_g, r_{s\parallel}) + (r_{\parallel} - r_{s\parallel}) \mathcal{P}'(u_g, r_{s\parallel}) + \frac{1}{2} (r_{\parallel} - r_{s\parallel})^2 \mathcal{P}''(u_g, r_{s\parallel}) + \dots \quad (5.4)$$

$$\xi(r) \approx \xi(s) + (r_{\parallel} - r_{s\parallel}) \xi'(s) + \frac{1}{2} (r_{\parallel} - r_{s\parallel})^2 \xi''(s) + \dots \quad (5.5)$$

Here, a prime denotes a derivative w.r.t. $r_{s\parallel}$. Substituting these expressions into Eq. (5.2), integrating over $u_g = r_{\parallel} - r_{s\parallel}$ and taking the Fourier transform, one eventually obtains [27]

$$P_{gg,s}^{\text{LO}}(k, \mu) = \left(1 - f^2 k^2 \mu^2 \sigma_{-1}^2\right) P_L(k) + i f k \mu u_{g12}(\mathbf{k}) - \frac{1}{2} f^2 k^2 \mu^2 \sigma_{12}^2(\mathbf{k}). \quad (5.6)$$

at leading order, where u_{g12} and σ_{12}^2 are the mean and variance of the pairwise velocity PDF,

$$u_{g12}(\mathbf{r}) \equiv \int du_g u_g \mathcal{P}(u_g, \mathbf{r}) \quad (5.7)$$

$$\sigma_{12}^2(\mathbf{r}) \equiv \int du_g u_g^2 \mathcal{P}(u_g, \mathbf{r}),$$

and σ_{-1} is the 1-dimensional rms velocity dispersion [Eq. (A.2)]. Comparing this result with Eq. (3.1) shows that, at this order,

$$\begin{aligned} i k u_{g12}(\mathbf{k}) &= -2\mu b_{\eta} \left[b_1 - (b_{\nabla^2 \delta} + b_1 \beta_{\nabla^2 \mathbf{v}}) k^2 \right] P_L(k) \\ k^2 \sigma_{12}^2(\mathbf{k}) &= -2\mu^2 \left[b_{\eta} + 2(f^{-1} b_1 \beta_{\partial_{\parallel}^2 \mathbf{v}} - b_{\eta} \beta_{\nabla^2 \mathbf{v}}) k^2 \right] P_L(k) - 2f^{-2} b_{\eta} k^2 P_{\epsilon\epsilon\eta}^{\{2\}}, \end{aligned} \quad (5.8)$$

while the term σ_{-1}^2 , which includes the contributions from the bulk velocity dispersion and from fingers-of-god, can be absorbed into the term proportional to $\mu^2 k^2 b_{\eta} b_{\nabla^2 \delta}$. These expressions generalize the results of [32] [who used the streaming model to derive their Eqs.(34) and (35)] as they include also b_{η} along with the line-of-sight velocity bias $\beta_{\partial_{\parallel}^2 \mathbf{v}}$.

Higher-order moments of the pairwise velocity PDF can be matched analogously, which is guaranteed by the EFT expansion. That is, in the EFT approach we are using the fact that in the regime of validity of the perturbative expansion of the displacements due to RSD, we can expand the pairwise velocity PDF in moments. Thus, while the streaming model in general requires a full pairwise velocity PDF, in the EFT approach everything is reduced to a finite number of free parameters (stochastic and deterministic) at a fixed order in perturbation theory.

The streaming formulation of redshift-space distortions is also useful to understand why there is no line-of-sight dependence in the shot noise, even in the presence of nontrivial selection effects. As we shall see below, the fundamental reason is conservation of pairs in the mapping from rest frame to redshift space, which implies $\int d^3r \xi(\mathbf{r}) = \int d^3r_s \xi_s(\mathbf{r}_s)$ and, therefore, anisotropies in shot noise can be at best of order $\mu^2 k^2$.

To see this, we take advantage of the fact that, upon Fourier transforming Eq. (5.2), the term $-(2\pi)^3 \delta_D(\mathbf{k})$ obtained from the “-1” is cancelled by

$$\begin{aligned} \int d^3\mathbf{r}_s \int dr_{\parallel} \mathcal{P}(r_{\parallel} - r_{s\parallel}, \mathbf{r}) e^{-i\mathbf{k}\cdot\mathbf{r}_s} &= \int d^3\mathbf{r}_s \left(\int du_g \mathcal{P}(u_g, \mathbf{r}) \right) e^{-i\mathbf{k}\cdot\mathbf{r}_s} \\ &= \int d^3\mathbf{r}_s \left(\int du_g \left[\mathcal{P}(u_g, \mathbf{r}_s) - u_g \mathcal{P}'(u_g, \mathbf{r}_s) + \dots \right] \right) e^{-i\mathbf{k}\cdot\mathbf{r}_s} \\ &\approx (2\pi)^3 \delta_D(\mathbf{k}) , \end{aligned} \quad (5.9)$$

The second equality arises from the rest frame to redshift space mapping. The last equality is the leading order contribution, which follows from the normalization of the pairwise velocity PDF. Therefore, the redshift-space power spectrum is given by

$$P_s(k_{\parallel}, \mathbf{k}_{\perp}) = \int d^2\mathbf{r}_{s\perp} \int dr_{\parallel} \xi(r) \int dr_{s\parallel} \mathcal{P}(r_{\parallel} - r_{s\parallel}, \mathbf{r}) e^{-i\mathbf{k}\cdot\mathbf{r}_s} + \frac{1}{\bar{n}} . \quad (5.10)$$

The Fourier transform of \mathcal{P} along the line of sight is

$$\begin{aligned} \int dr_{s\parallel} \mathcal{P}(r_{\parallel} - r_{s\parallel}, \mathbf{r}) e^{-ik_{\parallel}r_{s\parallel}} &= \int dr_{s\parallel} \int \frac{d\gamma}{2\pi} e^{-i\gamma(r_{\parallel} - r_{s\parallel})} \mathcal{M}(i\gamma f, \mathbf{r}) e^{-ik_{\parallel}r_{s\parallel}} \\ &= \int \frac{d\gamma}{2\pi} e^{-i\gamma r_{\parallel}} \left(\int dr_{s\parallel} e^{-i(k_{\parallel} - \gamma)r_{s\parallel}} \right) \mathcal{M}(i\gamma f, \mathbf{r}) \\ &= \int d\gamma e^{-i\gamma r_{\parallel}} \delta_D(k_{\parallel} - \gamma) \mathcal{M}(i\gamma f, \mathbf{r}) \\ &= e^{-ik_{\parallel}r_{\parallel}} \mathcal{M}(ik_{\parallel} f, \mathbf{r}) . \end{aligned} \quad (5.11)$$

Hence, the redshift-space power spectrum reads

$$P_s(k_{\parallel}, \mathbf{k}_{\perp}) = \int d^2\mathbf{r}_{s\perp} e^{-i\mathbf{k}_{\perp}\cdot\mathbf{r}_{s\perp}} \int dr_{\parallel} e^{-ik_{\parallel}r_{\parallel}} \xi(r) \mathcal{M}(ik_{\parallel} f, \mathbf{r}) + \frac{1}{\bar{n}} . \quad (5.12)$$

This implies

$$P_s(k_{\parallel}, \mathbf{k}_{\perp}) \stackrel{k \rightarrow 0}{\equiv} \int d^3r \xi(r) + \frac{1}{\bar{n}} \equiv P_{\epsilon} \quad (5.13)$$

independently of whether the limit is taken along k_{\parallel} or \mathbf{k}_{\perp} . This proves that P_{ϵ} cannot depend on μ (at order k^0) so long as the number of pairs is conserved, in agreement with the argument presented in Sec. 2.2.

5.2 Relation to previous EFT calculations

We now discuss the relation of our results to those of previous references who have considered biased tracers in redshift space using the EFT approach, in particular [82, 91]. The EFT of LSS is equivalent to the general bias expansion described in Sec. 2, hence we expect to find agreement. Indeed, for the bias expansion as well as stochastic contributions, we essentially find agreement with these references. There are differences however, which we will describe in detail below, in the treatment of selection contributions, and the velocity-bias expansion.

5.2.1 Selection contributions

Refs. [82, 91] did not consider the contributions from line-of-sight dependent selection effects, and restricted the redshift-space galaxy density to the result of the coordinate transformation Eq. (2.23). Hence, all selection contributions do not appear in their final results.

We have argued above that the counterterms required by higher-order terms in the coordinate transformation force us to introduce free coefficients that correspond to the selection bias contributions. The reason that [82, 91] came to a different conclusion is that they assumed that they are equal to the corresponding counterterms for matter in redshift space. As we will discuss below, this assumption does not hold in general, as galaxy and matter velocities differ at higher order in derivatives.

All this notwithstanding, selection effects can of course justly be set to zero if they are irrelevant for a given galaxy sample.

5.2.2 Velocity bias

Let us now consider velocity bias. Eq. (3.9) in [82] contains exactly our deterministic velocity bias contributions: $b_{\nabla^2\delta}, \beta_v, \beta_{v_{\parallel}}$. However, the authors argue that $\beta_{v_{\parallel}}$ should be replaced with the corresponding counterterm for matter, since one obtains the same term when looking at matter in redshift space. We will return to this below. Similarly, their Eq. (3.20) contains our $P_{\epsilon}^{\{0\}}, P_{\epsilon}^{\{2\}}$, and $P_{\epsilon\epsilon_{\eta}}^{\{2\}}$ contributions. The corresponding relation in [91] is their Eq. (2.22). They do not assume a relation between the galaxy and matter counterterms.

In order to understand the number of additional free parameters in the galaxy 1-loop power spectrum in redshift space, let us consider the auto- and cross-correlation of matter as well. We are dealing exclusively with higher-derivative terms (which renormalize the cutoff-dependent terms of the 1 – 3-type), so it is sufficient to work at linear order. To recap, for galaxies we have [Eq. (2.20)]

$$\begin{aligned}\delta_g &= b_1\delta + b_{\nabla^2\delta}\nabla^2\delta + \epsilon^{\{0\}} + \nabla^2\epsilon^{\{2\}} + \mathcal{O}(\delta^2) \\ \mathbf{v}_g &= \mathbf{v} + \beta_v\nabla^2\mathbf{v} + \beta_{v_{\parallel}}\nabla_{\parallel}^2\mathbf{v} + \boldsymbol{\varepsilon}_v.\end{aligned}\tag{5.14}$$

The stochastic velocity has to be derived from local observables, and thus ε_v involves at leads three derivatives of the potential. It is thus of the same order in derivatives as the other higher-derivative terms. As discussed in Sec. 2.5, we drop the term $\partial_{\parallel}^2 \delta$, since at this order it is completely degenerate with the term $\propto \beta_v$ coming from the Jacobian $\partial_{\parallel} v_{g\parallel}$. Since the bias coefficients are physical (they do not make reference to the perturbative order we work in), δ and \mathbf{v} stand for the matter density and velocity including counterterms. That is, at the same order, including leading higher-derivative contributions, δ and \mathbf{v} are related to the SPT predictions by

$$\begin{aligned}\delta &= \delta_{\text{SPT}} + C_{s,\text{eff}}^2 \nabla^2 \delta_{\text{SPT}} + (\text{higher-order counterterms}) \\ \mathbf{v} &= \mathbf{v}_{\text{SPT}} + \beta_v^m \nabla^2 \mathbf{v}_{\text{SPT}} + \beta_{v_{\parallel}}^m \nabla_{\parallel}^2 \mathbf{v}_{\text{SPT}} + \varepsilon_v^m + (\prime\prime).\end{aligned}\quad (5.15)$$

Here, $C_{s,\text{eff}}$ is the scaled effective sound speed, which corresponds to the leading counterterm for the matter density in the EFT description [42]. On the other hand, $\beta_v^m, \beta_{v_{\parallel}}^m$ capture the effect of small-scale motions of matter that are not described correctly by SPT, which through the equivalence principle are of course constrained to involve two additional spatial derivatives. Note that at this order in derivatives, at which matter no longer is a perfect fluid, the precise definition of the velocity field matters; i.e. how one goes from the well-defined momentum density T_i^0 to v^i . When applying different definitions to N-body simulation results (e.g. using grid-based velocity, or Delaunay tessellation), for example, one expects the measured coefficients $\beta_v^m, \beta_{v_{\parallel}}^m$ to differ as well. Furthermore, it is clear that these are physically different parameters than those describing the galaxy velocity field Eq. (2.20). The reason that Ref. [82] come to a different conclusion regarding these counterterms appears to be that they argue that the operators $v_{g,\parallel}^2$ and $v_{m,\parallel}^2$ should receive the same counterterms due to Galilei invariance. However, since these are contact operators which are sensitive to small-scale modes, this does not have to hold. We will now show that the distinction between β_O and β_O^m becomes relevant when considering the galaxy and matter auto and cross power spectra in redshift space beyond the large-scale limit.

In the following, let us focus on the deterministic higher-derivative terms. At linear order, the galaxy and matter densities in redshift space are simply

$$\delta_{g,s} = \delta_g - \eta_g \quad \text{and} \quad \delta_m^s = \delta_m - \eta. \quad (5.16)$$

The deterministic higher-derivative contributions to the matter and galaxy auto and cross power spectra in redshift space are then

$$\begin{aligned}P_{mm}^s(k, \mu) \Big|_{\text{det. hd.}} &= -k^2 P_L(k) 2(1 + f\mu^2) \left[C_{s,\text{eff}}^2 + \beta_v^m f\mu^2 + \beta_{v_{\parallel}}^m f\mu^4 \right] \\ P_{gg}^s(k, \mu) \Big|_{\text{det. hd.}} &= -k^2 P_L(k) 2(b_1 + f\mu^2) \left[b_{\nabla^2 \delta} + \beta_v f\mu^2 + \beta_{v_{\parallel}} f\mu^4 \right] \\ P_{gm}^s(k, \mu) \Big|_{\text{det. hd.}} &= -k^2 P_L(k) \left\{ (b_1 + f\mu^2) \left[C_{s,\text{eff}}^2 + \beta_v^m f\mu^2 + \beta_{v_{\parallel}}^m f\mu^4 \right] \right. \\ &\quad \left. + (1 + f\mu^2) \left[b_{\nabla^2 \delta} + \beta_v f\mu^2 + \beta_{v_{\parallel}} f\mu^4 \right] \right\}.\end{aligned}\quad (5.17)$$

We see that the statistics of the two fluids at first higher-derivative order can be described by the six parameters $\{C_{s,\text{eff}}^2, \beta_v^m, \beta_{v_{\parallel}}^m, b_{\nabla^2\delta}, \beta_v, \beta_{v_{\parallel}}\}$. On the other hand, it does make a difference in the cross- and auto power spectra between galaxies and matter whether $\beta_v^m = \beta_v, \beta_{v_{\parallel}}^m = \beta_{v_{\parallel}}$ or not; that is, unlike argued in [82], one cannot fix them to be the same. On the other hand, the number of free counterterms in the redshift-space galaxy power spectrum at this order agrees with the corresponding Eqs. (2.24)–(2.25) in [91]. However, it is not apparent whether the consistency relation between the counter-terms presented in their Eq. (2.26) is consistent with our Eq. (5.17).

6 Discussion and conclusions

In this paper, we have derived the NLO expression for the observed galaxy power spectrum in redshift space, along with the LO three-point function or bispectrum. We have included all observational selection effects which can affect realistic galaxy samples. These contributions can, for example, be induced by radiative transfer effects which modulate the observed emission line strength depending on the local line-of-sight velocity gradient. We have shown that these selection contributions are in fact required in order to obtain a consistent renormalization in the context of the EFT approach.

Including selection contributions, the description of the galaxy power spectrum at NLO, and galaxy bispectrum at LO, requires *(i)* 5 galaxy bias parameters, and 5 rest-frame stochastic amplitudes; *(ii)* 9 selection parameters; and *(iii)* 2 deterministic velocity bias parameters (one of them is due to selection), and 1 stochastic velocity bias amplitude. Thus, this set of statistics in full generality involves 22 parameters. Still, there are certain contributions from the redshift-space mapping which remain free of selection contributions and can thus be used to constrain the growth rate f . These are what we refer to as displacement contributions. Given the similar shape of, and corresponding degeneracy between, the various NLO contributions to the galaxy power spectrum, these displacement terms can most likely only be robustly isolated in the galaxy bispectrum.

If one can physically argue that selection effects can be neglected for a given galaxy sample, the number of free parameters reduces significantly: from 22 to 11. Of course, an intermediate regime is also possible, where selection effects are not entirely absent but suppressed by an additional small parameter. Then, it could be sufficient to keep only the leading selection contribution, $b_{\eta}\eta$, which would still reduce the number of parameters significantly (from 22 to 12). In terms of physical galaxy samples, we expect that the radiative transfer effect is stronger for galaxy samples selected from narrow spectral features and will be most significant for the emission-line selected galaxy samples from future galaxy surveys such as HETDEX ($\text{Ly}\alpha$), WFIRST, Euclid, and SPHEREx ($\text{H}\alpha$). It might be possible to mitigate this effect for surveys which also have broad-band imaging data (Euclid and WFIRST). As for the tidal alignment effect, Ref. [72] has reported a measurement of the tidal alignment effect from early-type (BOSS CMASS) galaxies, but there is no reported measurement for late-type galaxies to date.

Throughout, we have assumed that the scale that controls higher-derivative bias, including velocity bias, is of the same order as the nonlinear scale. If this scale is significantly larger, i.e. controlled by a smaller wavenumber in Fourier space, it might be necessary to keep operators that are higher order in derivatives [92]. The same scale is expected to control the higher-derivative contributions to the deterministic velocity bias. However, the stochasticity in the galaxy velocity field due to small-scale motions, which we refer to as “Fingers-of-God in the strict sense,” could involve a new scale. For example, as an extreme case, if the redshifts of galaxies were inferred from single objects in their dense cores, one would expect large random velocities, which would lead to large higher-derivative corrections to the redshift-space galaxy power spectrum of the form

$$\mu^{2n}(L_v^2 k^2)^n \times \text{const}, \quad \mu^{2n}(L_v^2 k^2)^n P_{gg}(k). \quad (6.1)$$

Here, $L_v^2 = \sigma_v^2/\mathcal{H}^2$ is the length scale associated with the small-scale velocity dispersion σ_v^2 , which adds another cutoff to the perturbative description, in addition to the nonlinear scale and the length scale associated with the rest-frame higher-derivative contributions. However, for most realistic galaxy samples, L_v is not expected to be much larger than the nonlinear scale. Moreover, as is apparent from Eq. (6.1), the actual cutoff in Fourier space is μ/L_v , so that transverse modes with $\mu \ll 1$ are not contaminated.

There are further potentially important contributions neglected in this paper: in particular, baryon-CDM perturbations and massive neutrinos. The latter are not expected to have a strong effect on redshift-space contributions. For the former, there are velocity-bias contributions both due to the decaying initial relative velocity between photons and baryons [75, 93–95], and due to Compton drag [96]:

$$\mathbf{v}_g \Big|_{\text{baryon-CDM}} = \beta_{bc}(\mathbf{v}_b - \mathbf{v}_c) + \beta_{\text{drag}}\mathbf{v}, \quad (6.2)$$

where β_{bc} is expected to be of order one, while β_{drag} is several orders of magnitude smaller. Note that Compton drag leads to a velocity bias without derivatives (the apparent violation of the equivalence principle is explained by the existence of a preferred frame provided by the CMB). The corresponding contribution to η_g can be absorbed by b_η , and a nontrivial contribution only appears at second order through $b_{\text{drag}}\mathbf{v}^2$ and $\beta_{\text{drag}}u_{\parallel}\partial_{\parallel}\delta$. Roughly, these contributions are at most percent-level corrections to the power spectrum, although they are most likely only partially degenerate with the other contributions considered here. Finally, since large-scale galaxy velocities are protected by the equivalence principle, primordial non-Gaussianity does not have an effect on velocities of biased tracers [97], and the impact of non-Gaussianity on redshift-space statistics is the same as that on the rest-frame statistics (note however that the displacement terms in Eq. (2.25) also contain the non-Gaussian contributions). This however assumes that the only relevant part of the initial conditions is the adiabatic growing mode.

In upcoming work, we will perform a Fisher forecast to estimate information gained by including the NLO power spectrum and LO bispectrum, over the LO power spectrum. We will

also perform a principle-component analysis to determine how many independent parameters are in fact necessary to describe redshift-space galaxy statistics to a given accuracy level.

Acknowledgments

We would like to thank Mikhail Ivanov, Eiichiro Komatsu, Shun Saito, Marko Simonović, and Zvonimir Vlah for helpful discussions, and Joseph Kuruvilla for pointing out the subtlety of the normalization of the pairwise velocity PDF in eq. (5.9).

DJ acknowledges support from National Science Foundation grant (AST-1517363) and Astrophysics Theory Program (80NSSC18K1103) of National Aeronautics and Space Administration. FS acknowledges support from the Starting Grant (ERC-2015-STG 678652) “GrInflaGal” from the European Research Council. VD acknowledges support from the Israel Science Foundation (grant no. 1395/16).

We are grateful to the Lewiner Institute for Theoretical Physics (LITP), Technion, for bringing us together at various stages of this project.

A Counterterms required by redshift-space contributions

In this appendix, we show how selection contributions arise as counterterms to nonlinear contributions to the galaxy density from the mapping to redshift space. For this, we introduce a momentum cutoff Λ in the loop integrals. All contributions which depend on this artificial cutoff need to be absorbed by counterterms.

I. $\delta\eta^2$ requires counterterm η : The cubic operator $\delta\eta^2$ which appears in the mapping from rest frame to redshift space (Sec. 2.4) adds the following contribution to the 1-loop galaxy power spectrum:

$$\begin{aligned}
P_{gg,s}^{\text{NLO}}(k) &\supset \langle \delta(\mathbf{k})(\delta\eta^2)(\mathbf{k}') \rangle' \\
&= \int_{\mathbf{p}_1}^{\Lambda} \int_{\mathbf{p}_2}^{\Lambda} \int_{\mathbf{p}_3}^{\Lambda} (2\pi)^3 \delta_D(\mathbf{k}' - \mathbf{p}_{123}) f^2 \mu_{\mathbf{p}_2}^2 \mu_{\mathbf{p}_3}^2 \langle \delta(\mathbf{k}) \delta(\mathbf{p}_1) \delta(\mathbf{p}_2) \delta(\mathbf{p}_3) \rangle' \\
&= f^2 P_L(k) \left\{ \int_{\mathbf{p}}^{\Lambda} \mu_{\mathbf{p}}^4 P_L(p) + 2\mu^2 \int_{\mathbf{p}}^{\Lambda} \mu_{\mathbf{p}}^2 P_L(p) \right\} \\
&= f^2 P_L(k) \left\{ \frac{1}{5} \sigma_0^2(\Lambda) + \frac{2}{3} \mu^2 \sigma_0^2(\Lambda) \right\}, \tag{A.1}
\end{aligned}$$

where

$$\sigma_n^2(\Lambda) \equiv \frac{1}{2\pi^2} \int_0^{\Lambda} p^{2+2n} dp P_L(p). \tag{A.2}$$

In the renormalized bias expansion, the first contribution in Eq. (A.1) can be absorbed by adding a correction to the bare linear bias $c_1 \rightarrow c_1 - f^2 \sigma_0^2(\Lambda)/10$. On the other hand, in order to absorb the second contribution in Eq. (A.1), which scales as $\mu^2 P_L(k)$, we need to correct the coefficient of η in the redshift-space galaxy density, which naively is simply -1 [Eq. (2.23)]. This shows that, in the context of the renormalized bias expansion, we have to allow for a free renormalized coefficient of η in the redshift-space galaxy density. Several other cubic RSD contributions require similar counterterms.

II. $(u_{\parallel} \partial_{\parallel})^2 \delta$ requires velocity bias $\beta_{\nabla^2 \mathbf{v}}$: in analogy to Eq. (A.1), we obtain

$$\begin{aligned}
P_{gg,s}^{\text{NLO}}(k) &\supset \langle \delta(\mathbf{k}) [(u_{\parallel} \partial_{\parallel})^2 \delta](\mathbf{k}') \rangle' \\
&= f^2 \mu^2 k^2 P_L(k) \frac{1}{3} \sigma_{-1}^2(\Lambda). \tag{A.3}
\end{aligned}$$

In order to absorb this contribution, we need to either add the velocity-bias term $\beta_{\nabla^2 \mathbf{v}} \nabla^2 \mathbf{v}$, or a line-of-sight-dependent higher-derivative contribution $b_{\partial_{\parallel}^2 \delta} \partial_{\parallel}^2 \delta$ to the galaxy bias expansion. At the order we work in, these two contributions are degenerate, and we have included the former here.

III. $(u_{\parallel} \partial_{\parallel})^2 \eta$ requires velocity bias $\beta_{\partial_{\parallel}^2 \mathbf{v}}$: for this term, we obtain

$$\begin{aligned}
P_{gg,s}^{\text{NLO}}(k) &\supset \langle \delta(\mathbf{k}) [(u_{\parallel} \partial_{\parallel})^2 \eta](\mathbf{k}') \rangle' \\
&= -f^3 \mu^4 k^2 P_L(k) \frac{1}{3} \sigma_{-1}^2(\Lambda). \tag{A.4}
\end{aligned}$$

In our expansion, the operator available to absorb this contribution is the velocity-bias term $\beta_{\partial_{\parallel}^2 \mathbf{v}} \partial_{\parallel}^2 \mathbf{v}$. Thus, the transformation to redshift space requires us to introduce a line-of-sight dependent higher-derivative velocity bias. Alternatively, one can introduce a higher-derivative selection bias contribution given by $\partial_{\parallel}^2 \Pi_{\parallel}^{[1]}$ in the bias expansion, which again is degenerate with the velocity bias at the order we are working in.

IV. (22)-type contributions leading to stochastic velocity term: finally, consider the following contribution of (22)-type:

$$\begin{aligned} P_{gg,s}^{\text{NLO}}(k) &\supset b_{\eta} b_{\delta^2} \left\langle \eta^{(2)}(\mathbf{k})(\delta^2)(\mathbf{k}') \right\rangle' \\ &= -2f\mu^2 b_{\eta} b_{\delta^2} \int_{\mathbf{p}}^{\Lambda} G_2(\mathbf{k} - \mathbf{p}, \mathbf{p}) P_L(p) P_L(|\mathbf{k} - \mathbf{p}|). \end{aligned} \quad (\text{A.5})$$

We now consider the low- k limit of this loop integral, specifically the regime where $k \ll p$. In this regime, the perturbation theory kernel scales as $G_2(\mathbf{k} - \mathbf{p}, \mathbf{p}) \propto k^2/p^2$, where the term $\propto \mathbf{k} \cdot \mathbf{p}/p^2$ vanishes after the angular integral. We then obtain

$$\left\langle \eta^{(2)}(\mathbf{k})(\delta^2)(\mathbf{k}') \right\rangle' \stackrel{k \rightarrow 0}{\simeq} -2f\mu^2 k^2 \times \text{const}(\Lambda), \quad (\text{A.6})$$

which involves a Λ -dependent constant. This contribution is absorbed by the stochastic velocity contribution ε_{η} through the term $\mu^2 k^2 P_{\varepsilon\varepsilon_{\eta}}^{\{2\}}$.

We see that the various types of selection and velocity-bias contributions introduced in this paper are in fact required as counterterms in a consistent renormalized expansion.

B Fourier-space kernels for the redshift-space galaxy density

In the main text of the paper, we have discussed the nonlinear contributions to the galaxy density contrast in terms of configuration-space operators. The same calculation can of course also be done with the usual perturbation theory kernels, as we show in this appendix.

B.1 Second order density contrast

Combining Eqs. (3.3)–(3.4), we calculate the second order galaxy density contrast in redshift space as

$$\begin{aligned} \delta_{g,s}^{(2)} &= [b_1 \delta + b_{\eta} \eta]^{(2)} + \frac{1}{2} b_2 \delta^2 + b_{K^2} K^2 + b_{\eta^2} \eta^2 + b_{\delta\eta} \delta\eta + b_{(KK)_{\parallel}} (KK)_{\parallel} + b_{\Pi_{\parallel}^{[2]} \Pi_{\parallel}^{[2]}} \\ &\quad - b_1 u_{\parallel} \partial_{\parallel} \delta - b_{\eta} u_{\parallel} \partial_{\parallel} \eta. \end{aligned} \quad (\text{B.1})$$

Note that, as in rest of main text, linear fields are denoted without superscript (1). Following the usual practice in cosmological perturbation theory, we may write the Fourier space expression for the second order density contrast in a form of

$$\delta_{g,s}^{(2)}(\mathbf{k}) = \int_{\mathbf{k}_1} \int_{\mathbf{k}_2} \delta^D(\mathbf{k} - \mathbf{k}_{12}) \delta^{(1)}(\mathbf{k}_1) \delta^{(1)}(\mathbf{k}_2) K_{g,s}^{(2)}(\mathbf{k}_1, \mathbf{k}_2), \quad (\text{B.2})$$

with the linear density contrast field $\delta^{(1)}(\mathbf{k})$. Here, we use the shorthand notation of $\mathbf{k}_{1\dots n} \equiv \mathbf{k}_1 + \dots + \mathbf{k}_n$. The second order density kernel $K_{g,s}^{(2)}(\mathbf{k}_1, \mathbf{k}_2)$ is given as the summation over the kernels in Tab. 1, and we use the second order density and velocity fields of perturbation theory [61, 98],

$$\begin{aligned}\delta^{(2)}(\mathbf{k}) &= \int_{\mathbf{k}_1} \int_{\mathbf{k}_2} \delta^D(\mathbf{k} - \mathbf{k}_{12}) \delta^{(1)}(\mathbf{k}_1) \delta^{(1)}(\mathbf{k}_2) F_2(\mathbf{k}_1, \mathbf{k}_2), \\ \theta^{(2)}(\mathbf{k}) &= \frac{\mathcal{H}}{\mu_{\mathbf{k}, \hat{n}}^2} \eta(\mathbf{k}) = -f\mathcal{H} \int_{\mathbf{k}_1} \int_{\mathbf{k}_2} \delta^D(\mathbf{k} - \mathbf{k}_{12}) \delta^{(1)}(\mathbf{k}_1) \delta^{(1)}(\mathbf{k}_2) G_2(\mathbf{k}_1, \mathbf{k}_2),\end{aligned}\quad (\text{B.3})$$

with corresponding kernels

$$F_2(\mathbf{k}_1, \mathbf{k}_2) = \frac{5}{7} + \frac{2}{7} \frac{(\mathbf{k}_1 \cdot \mathbf{k}_2)^2}{k_1^2 k_2^2} + \frac{1}{2} \frac{\mathbf{k}_1 \cdot \mathbf{k}_2}{k_1 k_2} \left(\frac{k_1}{k_2} + \frac{k_2}{k_1} \right) = \frac{5}{7} \left[1 - \frac{(\mathbf{k}_1 \cdot \mathbf{k}_2)^2}{k_1^2 k_2^2} \right] + \frac{1}{2} \frac{\mathbf{k}_1 \cdot \mathbf{k}_2 |\mathbf{k}_{12}|^2}{k_1^2 k_2^2}, \quad (\text{B.4})$$

$$G_2(\mathbf{k}_1, \mathbf{k}_2) = \frac{3}{7} + \frac{4}{7} \frac{(\mathbf{k}_1 \cdot \mathbf{k}_2)^2}{k_1^2 k_2^2} + \frac{1}{2} \frac{\mathbf{k}_1 \cdot \mathbf{k}_2}{k_1 k_2} \left(\frac{k_1}{k_2} + \frac{k_2}{k_1} \right) = \frac{3}{7} \left[1 - \frac{(\mathbf{k}_1 \cdot \mathbf{k}_2)^2}{k_1^2 k_2^2} \right] + \frac{1}{2} \frac{\mathbf{k}_1 \cdot \mathbf{k}_2 |\mathbf{k}_{12}|^2}{k_1^2 k_2^2}. \quad (\text{B.5})$$

Combining all, we find that the second order kernel is

$$\begin{aligned}K_{g,s}^{(2)}(\mathbf{k}_1, \mathbf{k}_2) &= \frac{1}{2} b_2 + \frac{1}{9} b_{(KK)\parallel} - \frac{1}{3} b_{K^2} + \frac{5}{7} \left(b_1 + b_{\Pi\parallel^{[2]}} \mu^2 \right) - \frac{3}{7} f b_\eta \mu_{\mathbf{k}_{12}, \hat{n}}^2 \\ &\quad + \frac{1}{2} (b_1 - f b_\eta \mu_{\mathbf{k}_{12}, \hat{n}}^2) \frac{k^2 \mathbf{k}_1 \cdot \mathbf{k}_2}{k_1^2 k_2^2} + \left[b_{K^2} - \frac{5}{7} b_1 + \left(\frac{3}{7} f b_\eta - \frac{5}{7} b_{\Pi\parallel^{[2]}} \right) \mu^2 \right] \frac{(\mathbf{k}_1 \cdot \mathbf{k}_2)^2}{k_1^2 k_2^2} \\ &\quad + \left(b_{\Pi\parallel^{[2]}} + b_{(KK)\parallel} \right) \frac{\mathbf{k}_1 \cdot \mathbf{k}_2 k_{1\parallel} k_{2\parallel}}{k_1^2 k_2^2} - \frac{1}{6} \left(3f(b_{\delta\eta} + b_1) + 2b_{(KK)\parallel} \right) \frac{k_{1\parallel}^2 k_2^2 + k_1^2 k_{2\parallel}^2}{k_1^2 k_2^2} \\ &\quad + f^2 (b_{\eta^2} + b_\eta) \frac{k_{1\parallel}^2 k_{2\parallel}^2}{k_1^2 k_2^2} + \frac{(fk\mu)^2}{2} \frac{k_{1\parallel} k_{2\parallel}}{k_1^2 k_2^2} \\ &\quad + \frac{fk\mu}{2} \left[\frac{k_{1\parallel}}{k_1^2} \left(b_1 - f(b_\eta + 1) \frac{k_{2\parallel}^2}{k_2^2} \right) + \frac{k_{2\parallel}}{k_2^2} \left(b_1 - f(b_\eta + 1) \frac{k_{1\parallel}^2}{k_1^2} \right) \right].\end{aligned}\quad (\text{B.6})$$

To facilitate the implementation, we further simplify the kernel by using the identity $k_{1\parallel} k_{2\parallel} = \frac{1}{2} (k_{\parallel}^2 - k_{1\parallel}^2 - k_{2\parallel}^2)$, following from $k_{\parallel} = k_{1\parallel} + k_{2\parallel}$, so that the second order kernel only contains

even power of $k_{1\parallel}$ and $k_{2\parallel}$. The final form of the kernel that we use for the computation is

$$\begin{aligned}
& K_{g,s}^{(2)}(\mathbf{k}_1, \mathbf{k}_2) \\
&= \frac{1}{2}b_2 + \frac{1}{9}b_{(KK)\parallel} - \frac{1}{3}b_{K^2} + \frac{5}{7}\left(b_1 + b_{\Pi\parallel^{[2]}\mu^2}\right) - \frac{3}{7}fb_\eta\mu^2 \\
&+ \frac{1}{2}\left(b_1 - fb_\eta\mu^2\right)\frac{k^2\mathbf{k}_1\cdot\mathbf{k}_2}{k_1^2k_2^2} + \left[b_{K^2} - \frac{5}{7}b_1 + \left(\frac{3}{7}fb_\eta - \frac{5}{7}b_{\Pi\parallel^{[2]}}\right)\mu^2\right]\frac{(\mathbf{k}_1\cdot\mathbf{k}_2)^2}{k_1^2k_2^2} \\
&- \frac{1}{6}\left(3fb_{\delta\eta} + 2b_{(KK)\parallel}\right)\left(\frac{k_{1\parallel}^2}{k_1^2} + \frac{k_{2\parallel}^2}{k_2^2}\right) + f^2(b_{\eta^2} + b_\eta)\frac{k_{1\parallel}^2k_{2\parallel}^2}{k_1^2k_2^2} \\
&+ \left[\left(b_{\Pi\parallel^{[2]}} + b_{(KK)\parallel}\right)\frac{\mathbf{k}_1\cdot\mathbf{k}_2}{k_1^2k_2^2} - \frac{(fk\mu)^2}{2}\frac{b_\eta}{k_1^2k_2^2} - \frac{f}{2}b_1\left(\frac{1}{k_1^2} + \frac{1}{k_2^2}\right)\right]\left(\frac{k_{\parallel}^2 - k_{1\parallel}^2 - k_{2\parallel}^2}{2}\right).
\end{aligned} \tag{B.7}$$

B.2 Third order density contrast

Adding all cubic contributions from Eq. (2.25), we find that the third-order density contrast which contributes nontrivially to $P_{gg,2}^{(1-3)}(k, \mu)$ [via $\mathcal{I}_n(k)$ in Eq. (D.5)] becomes

$$\begin{aligned}
\delta_{g,s}^{(3),\text{NLO}} &= b_1\delta^{(3)} + b_\eta\eta^{(3)} + b_{K^2}[K^2]^{(3)} + b_{\text{td}}\mathcal{O}_{\text{td}}^{(3)} \\
&+ b_{\delta\eta}[\delta\eta]^{(3)} + b_{\eta^2}[\eta^2]^{(3)} + b_{(KK)\parallel}[(KK)\parallel]^{(3)} + b_{\Pi\parallel^{[2]}}[\Pi\parallel^{[2]}]^{(3)} \\
&+ b_{\delta\Pi\parallel^{[2]}}\delta\Pi\parallel^{[2]} + b_{\eta\Pi\parallel^{[2]}}\eta\Pi\parallel^{[2]} + b_{(K\Pi\parallel^{[2]})\parallel}(K\Pi\parallel^{[2]})\parallel + b_{\Pi\parallel^{[3]}}\Pi\parallel^{[3]} \\
&- \left[u_{\parallel}\partial_{\parallel}\left(b_1\delta + b_\eta\eta + b_{\Pi\parallel^{[2]}}\Pi\parallel^{[2]}\right)\right]^{(3)}.
\end{aligned} \tag{B.8}$$

In Fourier space, we may write the third-order density contrast as

$$\delta_{g,s}^{(3),\text{NLO}}(\mathbf{k}) = \int_{\mathbf{k}_1} \int_{\mathbf{k}_2} \int_{\mathbf{k}_3} \delta^D(\mathbf{k} - \mathbf{k}_{123})\delta^{(1)}(\mathbf{k}_1)\delta^{(1)}(\mathbf{k}_2)\delta^{(1)}(\mathbf{k}_3)K_{g,s}^{(3),\text{NLO}}(\mathbf{k}_1, \mathbf{k}_2, \mathbf{k}_3), \tag{B.9}$$

with the third order kernel $K_{g,s}^{(3),\text{NLO}}$. As explained in Sec. 3.3, we only need to retain the second-order terms that are proportional to $1 - (\hat{k}_i \cdot \hat{k}_j)^2$, as the others are absorbed by counterterms. Combining all, we find the following expression for the cubic kernel in the kinematic configuration that is relevant for the NLO galaxy power spectrum [see Eq. (B.12)]

below]:

$$\begin{aligned}
& \int_{\mathbf{q}} K_{g,s}^{(3),\text{NLO}}(\mathbf{k}, \mathbf{q}, -\mathbf{q}) P_L(q) \\
= & \left[b_1 + \mu^2 \left(2b_{\Pi_{\parallel}^{[2]}} + b_{\Pi_{\parallel}^{[3]}} \right) \right] \int_{\mathbf{q}} F_3(\mathbf{k}, \mathbf{q}, -\mathbf{q}) P_L(q) - fb_{\eta} \mu^2 \int_{\mathbf{q}} G_3(\mathbf{q}, -\mathbf{q}, \mathbf{k}) P_L(q) \\
& + \int_{\mathbf{q}} \left[1 - (\hat{\mathbf{k}} \cdot \hat{\mathbf{q}})^2 \right] P_L(q) \\
& \times \left\{ \frac{4}{21} (5b_{K^2} + 2b_{\text{td}}) \left[\left(\frac{(\mathbf{k} - \mathbf{q}) \cdot \mathbf{q}}{|\mathbf{k} - \mathbf{q}|q} \right)^2 - \frac{1}{3} \right] - \frac{2}{21} fb_{\delta\eta} \left[\frac{3(k_{\parallel} - q_{\parallel})^2}{|\mathbf{k} - \mathbf{q}|^2} + \frac{5q_{\parallel}^2}{q^2} \right] \right. \\
& + \frac{4}{7} f^2 b_{\eta^2} \frac{q_{\parallel}^2 (k_{\parallel} - q_{\parallel})^2}{q^2 |\mathbf{k} - \mathbf{q}|^2} + \frac{20}{21} b_{(KK)_{\parallel}} \left[\frac{(\mathbf{k} \cdot \mathbf{q} - q^2)(k_{\parallel} - q_{\parallel})q_{\parallel}}{|\mathbf{k} - \mathbf{q}|^2 q^2} - \frac{1}{3} \frac{(k_{\parallel} - q_{\parallel})^2}{|\mathbf{k} - \mathbf{q}|^2} - \frac{1}{3} \frac{q_{\parallel}^2}{q^2} + \frac{1}{9} \right] \\
& - \frac{2}{21} b_{\Pi_{\parallel}^{[2]}} \frac{(\mathbf{k} \cdot \mathbf{q} - q^2)}{|\mathbf{k} - \mathbf{q}|^2} \left[\frac{3q_{\parallel}^2}{q^2} + \frac{5(k_{\parallel} - q_{\parallel})^2}{q^2} \right] + \frac{10}{21} \left[b_{\delta\Pi_{\parallel}^{[2]}} - \frac{1}{3} b_{(K\Pi^{[2]})_{\parallel}} - fb_{\eta\Pi_{\parallel}^{[2]}} \frac{q_{\parallel}^2}{q^2} \right] \frac{(k_{\parallel} - q_{\parallel})^2}{|\mathbf{k} - \mathbf{q}|^2} \\
& + \frac{10}{21} b_{(K\Pi^{[2]})_{\parallel}} \frac{(\mathbf{q} \cdot \mathbf{k} - q^2)}{q|\mathbf{k} - \mathbf{q}|} \frac{q_{\parallel}(k_{\parallel} - q_{\parallel})}{q|\mathbf{k} - \mathbf{q}|} - b_{\Pi_{\parallel}^{[3]}} \left[\frac{1}{7} \frac{q_{\parallel}^2 \mathbf{k} \cdot \mathbf{q} - q^2}{q^2 |\mathbf{k} - \mathbf{q}|^2} + \frac{10}{21} \frac{(k_{\parallel} - q_{\parallel})^2 \mathbf{k} \cdot \mathbf{q} - q^2}{|\mathbf{k} - \mathbf{q}|^2 q^2} \right] \\
& + \frac{2}{21} fb_1 \left[5 \frac{q_{\parallel}(k_{\parallel} - q_{\parallel})}{q^2} + 3 \frac{q_{\parallel}(k_{\parallel} - q_{\parallel})}{|\mathbf{k} - \mathbf{q}|^2} \right] - \frac{2}{7} f^2 b_{\eta} \frac{q_{\parallel}(k_{\parallel} - q_{\parallel})}{q^2 |\mathbf{k} - \mathbf{q}|^2} \left[(k_{\parallel} - q_{\parallel})^2 + q_{\parallel}^2 \right] \\
& \left. + \frac{10}{21} fb_{\Pi_{\parallel}^{[2]}} \frac{q_{\parallel}(k_{\parallel} - q_{\parallel})^3}{q^2 |\mathbf{k} - \mathbf{q}|^2} \right\}. \tag{B.10}
\end{aligned}$$

B.3 NLO power spectrum

We then calculate the NLO contribution to the power spectrum through

$$P_{gg,s}^{2-2}(k, \mu) = 2 \left\{ \int_{\mathbf{q}} \left[K_{g,s}^{(2)}(\mathbf{k} - \mathbf{q}, \mathbf{q}) \right]^2 P_L(q) P_L(|\mathbf{k} - \mathbf{q}|) - \int_{\mathbf{q}} \left[K_{g,s}^{(2)}(-\mathbf{q}, \mathbf{q}) \right]^2 P_L(q)^2 \right\}, \tag{B.11}$$

$$P_{gg,s}^{1-3}(k, \mu) = 3(b_1 - b_{\eta} f \mu^2) P_L(k) \int_{\mathbf{q}} K_{g,s}^{(3),\text{NLO}}(\mathbf{k}, \mathbf{q}, -\mathbf{q}) P_L(q). \tag{B.12}$$

For the angular integration, we introduce the azimuthal angle φ_{kq} so that one can write the line-of-sight component of the \mathbf{q} vector as

$$q_{\parallel} = q \left(\mu_{kq} \mu - \sqrt{1 - \mu^2} \sqrt{1 - \mu_{kq}^2} \cos \varphi_{kq} \right), \tag{B.13}$$

with $\mu_{kq} \equiv \mathbf{q} \cdot \mathbf{k} / (kq)$. We then compute the azimuthal integration as

$$\int \frac{d\varphi_{kq}}{2\pi} q_{\parallel}^n = q^n \sum_{m=0}^{\lfloor n/2 \rfloor} \frac{n!}{(n-2m)!((2m)!!)^2} \left[\mu^{n-2m} (1 - \mu^2)^m \right] \left[\mu_{kq}^{n-2m} (1 - \mu_{kq}^2)^m \right], \tag{B.14}$$

where $0 \leq n \leq 8$, from which, and using the binomial expansion, we also find that

$$\int \frac{d\varphi_{kq}}{2\pi} q_{\parallel}^n (k_{\parallel} - q_{\parallel})^m = \sum_{p=0}^m \sum_{q=0}^{\lfloor (n+p)/2 \rfloor} \frac{(-1)^p m!}{p!(m-p)!} \frac{(n+p)!}{(n+p-2q)! [(2q)!!]^2} \\ \times k^{m-p} q^{n+p} [\mu^{n+m-2q} (1-\mu^2)^q] \left[\mu_{kq}^{n+p-2q} (1-\mu_{kq}^2)^q \right]. \quad (\text{B.15})$$

Here, $\lfloor x \rfloor$ is the floor function, the largest integer smaller than x , and $x!! \equiv x(x-2)(x-4) \cdots (1 \text{ or } 2)$.

C Structure of cubic operators and their contribution to the NLO power spectrum

Cubic operators $O^{(3)}$ contribute to NLO power spectra via their cross-correlation with linear operators. Since, in Fourier space, η is trivially related to δ , it is sufficient to consider the correlators

$$\left\langle \delta(\mathbf{k}') O^{(3)}(\mathbf{k}) \right\rangle', \quad (\text{C.1})$$

where here and throughout this appendix, δ without superscript denotes the linear density field. Moreover, for any cubic operator we can write

$$O^{(3)}(\mathbf{k}) = \int_{\mathbf{p}_1} \int_{\mathbf{p}_2} \int_{\mathbf{p}_3} (2\pi)^3 \delta_D(\mathbf{k} - \mathbf{p}_{123}) F_O(\mathbf{p}_1, \mathbf{p}_2, \mathbf{p}_3) \delta(\mathbf{p}_1) \delta(\mathbf{p}_2) \delta(\mathbf{p}_3). \quad (\text{C.2})$$

With this, Eq. (C.1) becomes

$$\left\langle \delta(\mathbf{k}') O^{(3)}(\mathbf{k}) \right\rangle' = \int_{\mathbf{p}_1} \int_{\mathbf{p}_2} \int_{\mathbf{p}_3} (2\pi)^3 \delta_D(\mathbf{k} - \mathbf{p}_{123}) F_O(\mathbf{p}_1, \mathbf{p}_2, \mathbf{p}_3) \left\langle \delta(\mathbf{k}') \delta(\mathbf{p}_1) \delta(\mathbf{p}_2) \delta(\mathbf{p}_3) \right\rangle'. \quad (\text{C.3})$$

Importantly, if this correlator is of the form

$$\left\langle \delta(\mathbf{k}') O^{(3)}(\mathbf{k}) \right\rangle' = \mu_{\mathbf{k}}^{2l} k^{2m} P_L(k) \sigma_n^2, \quad (\text{C.4})$$

where $l, m, n \geq 0$ are non-negative integers, then this operator's contribution to NLO power spectra is completely absorbed by a counterterm involving a lower-order operator (e.g., δ , if $l = m = 0$, or η , if $l = 1, m = 0$). Equivalently, this contribution is absorbed in a lower-order renormalized bias parameter (b_1 and b_η , respectively).

In this section, we show how operators can be classified according to their structure, and which structures lead to pure counterterms.

C.1 $(\Pi^{[1]})^3$ type

The first class of operators involves three powers of $\Pi^{[1]}$. This includes

$$\delta^3, \delta K^2, K^3, \eta^3, \delta\eta^2, \eta K^2, \quad (\text{C.5})$$

and others. The kernel corresponding to any operator of this type can always be written as

$$F_O(\mathbf{p}_1, \mathbf{p}_2, \mathbf{p}_3) = \mathcal{P}_{ijklmn}^O \frac{p_1^i p_1^j}{p^2} \frac{p_2^k p_2^l}{p^2} \frac{p_3^m p_3^n}{p^2}, \quad (\text{C.6})$$

where \mathcal{P}^O is a projection operator constructed from δ_{kl} and even powers of \hat{n}^i . Without loss of generality, Eq. (C.3) becomes

$$\begin{aligned} \left\langle \delta(\mathbf{k}') O^{(3)}(\mathbf{k}) \right\rangle' &\stackrel{(\Pi^{[1]})^3}{=} \mathcal{P}_{ijklmn}^O \frac{k^i k^j}{k^2} P_L(k) \int_{\mathbf{p}} \frac{p^k p^l p^m p^n}{p^4} P_L(p) \\ &= \mathcal{P}_{ijklmn}^O \frac{k^i k^j}{k^2} P_L(k) \sigma^2 \left[\delta^{kl} \delta^{mn} + \text{perm.} \right]. \end{aligned} \quad (\text{C.7})$$

We see that all of these operators lead to pure counterterms, and can be dropped. Correspondingly, we have not included this type of operator in our list of bias operators in Eqs. (2.26)–(2.29). As described in Appendix A, these operators do however force us to allow for a (in general) free bias coefficient b_η of the linear operator η .

This class of operators can be slightly expanded to also include cubic operators involving $u_{\parallel} \partial_{\parallel}$ or $s^k \partial_k$. First, by use of the product rule, the derivative can always be made to act on only a single instance of $\Pi^{[1]}$. Then, the structure of the kernels is the same as that given in Eq. (C.6), apart from an additional factor of (say) p_1/p_2 . Inserting this into the correlator above, one immediately sees that these contributions either vanish or lead to pure counterterms.

C.2 $\Pi^{[1]}\Pi^{[2]}$ type

The second class of cubic operators has the following general structure:

$$\left(\frac{\partial \dots}{\nabla^2} \delta \right) \frac{\partial \dots}{\nabla^2} \left(\delta^2 - \frac{3}{2} K^2 \right), \quad (\text{C.8})$$

where each numerator involves one to three spatial derivatives, with the sum of both adding to four spatial derivatives (so that there are always two net spatial derivatives acting on each instance of the gravitational potential). Let us consider a specific example, which describes about two thirds of the relevant contributions:

$$\mathcal{P}_{ijkl}^O \left(\frac{\partial^i \partial^j}{\nabla^2} \delta \right) \frac{\partial^k \partial^l}{\nabla^2} \left(\delta^2 - \frac{3}{2} K^2 \right), \quad (\text{C.9})$$

where \mathcal{P}_{ijkl}^O is a projection operator (different from the one considered in the last section) constructed from Kronecker delta and even powers of $\hat{\mathbf{n}}$. Further, we can assume $\mathcal{P}_{ijkl}^O \delta^{kl} = 0$, since the operator reduces to the $(\Pi^{[1]})^3$ category otherwise.

Without loss of generality, the loop contribution in Eq. (C.3) can be written as

$$\begin{aligned}
\langle \delta(\mathbf{k}') O^{(3)}(\mathbf{k}) \rangle' &\stackrel{\Pi^{[1]}\Pi^{[2]}}{=} \mathcal{P}_{ijkl}^O \frac{3}{2} \int_{\mathbf{p}_1} \int_{\mathbf{p}_2} \int_{\mathbf{p}_3} (2\pi)^3 \delta_D(\mathbf{k} - \mathbf{p}_{123}) \frac{p_1^i p_1^j}{p_1^2} \frac{p_{23}^k p_{23}^l}{p_{23}^2} (1 - \mu_{2,3}^2) \\
&\quad \times \langle \delta(\mathbf{k}') \delta(\mathbf{p}_1) \delta(\mathbf{p}_2) \delta(\mathbf{p}_3) \rangle' \\
&= \mathcal{P}_{ijkl}^O 3P_L(k) \int_{\mathbf{p}} \frac{p^i p^j}{p^2} \frac{(k-p)^k (k-p)^l}{|\mathbf{k}-\mathbf{p}|^2} (1 - \mu_{\mathbf{k},-\mathbf{p}}^2) P_L(p). \quad (\text{C.10})
\end{aligned}$$

We see that, apart from any contribution $\propto \delta^{kl}$ in \mathcal{P}_{ijkl}^O which we have excluded above, this does not reduce to a counterterm and must be included. The general operator corresponding to these nontrivial contributions is $O_{ijkl}^{\Pi^1-\Pi^2}$ defined in Eq. (3.12),

$$O_{ijkl}^{\Pi^1-\Pi^2} \equiv \left(\frac{\partial_i \partial_j}{\nabla^2} \delta \right) \mathcal{D}_{kl} \left(\delta^2 - \frac{3}{2} K^2 \right). \quad (\text{C.11})$$

The remaining contributions of this type correspond to moving one of the spatial derivatives in Eq. (C.9) from one numerator to another. It is easy to see that Eq. (C.10) is then modified by swapping one of the powers of $\mathbf{k} - \mathbf{p}$ in the numerator with \mathbf{p} , or vice-versa, e.g.

$$p^i p^j (k-p)^k (k-p)^l \rightarrow p^i p^j p^k (k-p)^l \quad \text{or} \quad p^i p^j (k-p)^k (k-p)^l \rightarrow p^i (k-p)^j (k-p)^k (k-p)^l.$$

The result is clearly of the form given in Eq. (3.11). We will evaluate all of these correlators in Appendix D.

C.3 $\Pi^{[3]}$ type

There are only two contributions of this type, which are purely selection effects, namely

$$\Pi_{\parallel}^{[3]} \quad \text{and} \quad \Pi_{\parallel}^{[2]} \Big|^{(3)}. \quad (\text{C.12})$$

Recall the definition of $\Pi^{[3]}$ from Eq. (2.2):

$$\Pi_{ij}^{[3]} = \frac{1}{2} \left[(\mathcal{H}f)^{-1} \frac{D}{D\tau} \Pi_{ij}^{[2]} - 2\Pi_{ij}^{[2]} \right], \quad (\text{C.13})$$

where the leading, second-order contribution to $\Pi^{[2]}$ cancels. At third order, we can write

$$\Pi_{ij}^{[2]} \Big|^{(3)} = \Pi_{ij}^{[2](3\text{bi})} - s^k \partial_k \Pi_{ij}^{2}, \quad (\text{C.14})$$

where the first ‘‘boost-invariant’’ (bi) contribution does not involve a displacement, and the second contribution is the leading displacement term. Now, the spatial part of the convective time derivative in Eq. (C.13) precisely cancels this displacement term, and, noting that $\Pi_{ij}^{[2]} \Big|^{(3)} \propto D^3(\tau)$, we obtain

$$\Pi_{ij}^{[3]} \Big|^{(3)} = \frac{1}{2} \Pi_{ij}^{[2](3\text{bi})}. \quad (\text{C.15})$$

The derivation of the full kernel of $\Pi^{[3]}$ is quite lengthy, however we in fact do not need it. As shown above, $\Pi^{[3]}$ evaluated at third order does not contain displacement terms. This means that it has to be of the form

$$\begin{aligned} \Pi_{ij}^{[3]} \Big|^{(3)} &= \mathcal{O} \left([\Pi^{[1]} \Pi^{[2]}]_{ij}, \text{tr}[\Pi^{[1]} \Pi_{ij}^{[2]}], [\Pi^{[1]}]_{ij}^3, \dots \right) + \frac{\partial_i \partial_j}{\nabla^2} \left(\sum_{O \in \mathfrak{D}_3^r} c_O O \right), \quad \text{where} \\ \mathfrak{D}_3^r &= \left\{ [\text{tr}(\Pi^{[1]})]^3, [\text{tr}(\Pi^{[1]})] \text{tr}[\Pi^{[1]} \Pi^{[1]}], \text{tr}[\Pi^{[1]} \Pi^{[1]} \Pi^{[1]}], \text{tr}[\Pi^{[1]} \Pi^{[2]}] \right\} \end{aligned} \quad (\text{C.16})$$

is the set of cubic bias operators (i.e. without selection effects). For example, the boost-invariant parts of $\delta^{(3)}$ and $\theta^{(3)}$ can be written as a linear combination of these operators. Further, the $\mathcal{O}(\dots)$ denotes operators of the two types discussed above. In particular, the only terms that are not absorbed by counterterms are $[\Pi^{[1]} \Pi^{[2]}]_{ij}$ and $\text{tr}[\Pi^{[1]} \Pi_{ij}^{[2]}]$; equivalently, for the contraction $\Pi_{\parallel}^{[3]}$ relevant here, these correspond to $\delta \Pi_{\parallel}^{[2]}$ and $(K \Pi^{[2]})_{\parallel}$. Since we have considered these above, we can focus on the last term here.

Considering only this contribution, the loop integral Eq. (C.3) becomes

$$\begin{aligned} \left\langle \delta(\mathbf{k}') \Pi_{ij}^{[3]}(\mathbf{k}) \right\rangle' &= \int_{\mathbf{p}_1} \int_{\mathbf{p}_2} \int_{\mathbf{p}_3} (2\pi)^3 \delta_D(\mathbf{k} - \mathbf{p}_{123}) \frac{p_{123}^i p_{123}^j}{p_{123}^2} \left(\sum_{O \in \mathfrak{D}_3^r} c_O F_O(\mathbf{p}_1, \mathbf{p}_2, \mathbf{p}_3) \right) \\ &\quad \times \left\langle \delta(\mathbf{k}') \delta(\mathbf{p}_1) \delta(\mathbf{p}_2) \delta(\mathbf{p}_3) \right\rangle' \\ &= \frac{k^i k^j}{k^2} \sum_{O \in \mathfrak{D}_3^r} c_O \left\langle \delta(\mathbf{k}') O(\mathbf{k}) \right\rangle'. \end{aligned} \quad (\text{C.17})$$

Now, as we have seen in the previous two subsections, all operators in \mathfrak{D}_3^r but one lead to counterterms. Dropping these, we thus have

$$\left\langle \delta(\mathbf{k}') \Pi_{\parallel}^{[3]}(\mathbf{k}) \right\rangle' = \mu_{\mathbf{k}}^2 c \left\langle \delta(\mathbf{k}') (\Pi^{[1]} \Pi^{[2]})(\mathbf{k}) \right\rangle' = \mu_{\mathbf{k}}^2 c' \left\langle \delta(\mathbf{k}') O_{\text{td}}(\mathbf{k}) \right\rangle', \quad (\text{C.18})$$

where c, c' are constants which follow from the perturbative expression for $\Pi^{[3]}$. We see that only one particular contribution inside $\Pi^{[3]}$ needs to be considered, and it is of the same form as one of the previously derived 1-loop contributions. *Magic!*

Finally, by matching the full SPT kernel for $\Pi_{\parallel}^{[3]}$ with the kernels appearing in the 1–3-type loop integrals derived above, we can derive the full contribution of the two operators of this type to the one-loop power spectrum:

$$\begin{aligned} \Pi_{\parallel}^{[3]} &= \frac{13}{30} \delta \Pi_{\parallel}^{[2]} + \frac{13}{10} (K \Pi^{[2]})_{\parallel} - \frac{35}{24} \frac{\partial_{\parallel}^2}{\nabla^2} O_{\text{td}} + \mathcal{O} \left([\Pi^{[1]}]^3, \frac{\partial_{\parallel}^2}{\nabla^2} [\Pi^{[1]}]^3 \right) \\ \Pi_{\parallel}^{[2]} \Big|^{(3)} &= 2 \Pi_{\parallel}^{[3]} - s^k \partial_k \Pi_{\parallel}^{[2]}. \end{aligned} \quad (\text{C.19})$$

D The general 1–3-type loop contribution

As we have seen, all non-trivial 1–3-type loop contributions that appear in the NLO redshift-space power spectrum can be written as contractions with δ^{ab} and $\hat{n}^c \hat{n}^d$ of

$$3P_L(k) \int_{\mathbf{p}} \frac{F_{ijkl}(\mathbf{p}, \mathbf{k})}{p^2 |\mathbf{k} - \mathbf{p}|^2} (1 - \mu_{\mathbf{k}, \mathbf{p}}^2) P_L(p), \quad (\text{D.1})$$

where $F_{ijkl}(\mathbf{p}, \mathbf{k})$ is a fourth-order polynomial in components of \mathbf{p} and \mathbf{k} , which is at least linear in \mathbf{p} . Clearly, we can pull out the components of \mathbf{k} , and it suffices to parametrize the four tensor correlators involving p^i , $p^i p^j$, $p^i p^j p^k$, and $p^i p^j p^k p^l$. Since these cannot involve any preferred direction apart from \mathbf{k} , we can use the symmetry to decompose each of them as follows:

$$\begin{aligned} f_i(k) &\equiv k^3 \int_{\mathbf{p}} \frac{p_i}{p^2 |\mathbf{k} - \mathbf{p}|^2} (1 - \mu_{\mathbf{k}, \mathbf{p}}^2) P_L(p) = \hat{k}_i f_1(k) \\ f_{ij}(k) &\equiv k^2 \int_{\mathbf{p}} \frac{p_i p_j}{p^2 |\mathbf{k} - \mathbf{p}|^2} (1 - \mu_{\mathbf{k}, \mathbf{p}}^2) P_L(p) = \delta_{ij} f_2^{\text{D}}(k) + \hat{k}_i \hat{k}_j f_2^{\text{K}}(k) \\ f_{ijk}(k) &\equiv k \int_{\mathbf{p}} \frac{p_i p_j p_k}{p^2 |\mathbf{k} - \mathbf{p}|^2} (1 - \mu_{\mathbf{k}, \mathbf{p}}^2) P_L(p) = [\hat{k}_i \delta_{jk} + 2 \text{ perm.}] f_3^{\text{D}}(k) + \hat{k}_i \hat{k}_j \hat{k}_k f_3^{\text{K}}(k) \\ f_{ijkl}(k) &\equiv \int_{\mathbf{p}} \frac{p_i p_j p_k p_l}{p^2 |\mathbf{k} - \mathbf{p}|^2} (1 - \mu_{\mathbf{k}, \mathbf{p}}^2) P_L(p) = [\delta_{ij} \delta_{kl} + 2 \text{ perm.}] f_4^{\text{DD}}(k) \\ &\quad + [\delta_{ij} \hat{k}_k \hat{k}_l + 5 \text{ perm.}] f_4^{\text{DK}}(k) + \hat{k}_i \hat{k}_j \hat{k}_k \hat{k}_l f_4^{\text{KK}}(k). \end{aligned} \quad (\text{D.2})$$

By contracting these relations with δ^{ab} and $\hat{k}^c \hat{k}^d$, we can solve for the f_n^{X} . Moreover, we know that if $F_{ijkl}(\mathbf{p}, \mathbf{k}) \propto |\mathbf{k} - \mathbf{p}|^2$, then the loop integral becomes trivial (i.e., it becomes proportional to σ^2). This further reduces the number of independent functions.

We are thus looking for contractions of F_{ijkl} that are (i) proportional to $|\mathbf{k} - \mathbf{p}|^2$, and (ii) at least first and at most fourth order in p ; any contraction involving lower or higher powers of p would contain other loop integrals than those written in Eq. (D.2), and hence not yield interesting constraints. Three possible contractions of F_{ijkl} of this form remain:

$$p^2 |\mathbf{k} - \mathbf{p}|^2; \quad (\mathbf{k} \cdot \mathbf{p}) |\mathbf{k} - \mathbf{p}|^2; \quad (\hat{\mathbf{k}} \cdot \mathbf{p})^2 |\mathbf{k} - \mathbf{p}|^2. \quad (\text{D.3})$$

These translate to the following three conditions:

$$\begin{aligned} p^2 |\mathbf{k} - \mathbf{p}|^2 : \quad & \delta^{ij} f_{ij}(k) - 2 \hat{k}^i \delta^{jk} f_{ijk}(k) + \delta^{ij} \delta^{kl} f_{ijkl}(k) = \text{trivial} \\ (\mathbf{k} \cdot \mathbf{p}) |\mathbf{k} - \mathbf{p}|^2 : \quad & \hat{k}^i f_i(k) - 2 \hat{k}^i \hat{k}^j f_{ij}(k) + \hat{k}^i \delta^{jk} f_{ijk}(k) = \text{trivial} \\ (\hat{\mathbf{k}} \cdot \mathbf{p})^2 |\mathbf{k} - \mathbf{p}|^2 : \quad & \hat{k}^i \hat{k}^j f_{ij}(k) - 2 \hat{k}^i \hat{k}^j \hat{k}^k f_{ijk}(k) + \hat{k}^i \hat{k}^j \delta^{kl} f_{ijkl}(k) = \text{trivial}. \end{aligned} \quad (\text{D.4})$$

This reduces the independent functions appearing in Eq. (D.2) by 3. *Thus, all 1–3-type loop integrals can be parametrized through 5 independent functions.* Any further degeneracies can only appear due to a special simple shape of $P_L(p)$. The evaluation of all 1–3-type loop contributions now proceeds in four steps.

1. We first solve for the coefficients $f_n^X(k)$ in terms of loop integrals, by contracting Eq. (D.2) with δ^{ab} and $\hat{k}^c \hat{k}^d$:

$$\begin{aligned}
f_1(k) &= \mathcal{I}_1(k) \equiv k^2 \int_{\mathbf{p}} \frac{\mathbf{k} \cdot \mathbf{p}}{p^2 |\mathbf{k} - \mathbf{p}|^2} (1 - \mu_{\mathbf{k},\mathbf{p}}^2) P_L(p) \\
3f_2^D(k) + f_2^K(k) &= \mathcal{I}_2(k) \equiv k^2 \int_{\mathbf{p}} \frac{p^2}{p^2 |\mathbf{k} - \mathbf{p}|^2} (1 - \mu_{\mathbf{k},\mathbf{p}}^2) P_L(p) \\
f_2^D(k) + f_2^K(k) &= \tilde{\mathcal{I}}_2^K(k) \equiv \int_{\mathbf{p}} \frac{(\mathbf{k} \cdot \mathbf{p})^2}{p^2 |\mathbf{k} - \mathbf{p}|^2} (1 - \mu_{\mathbf{k},\mathbf{p}}^2) P_L(p) \\
5f_3^D(k) + f_3^K(k) &= \tilde{\mathcal{I}}_3^D(k) \equiv \int_{\mathbf{p}} \frac{p^2 (\mathbf{k} \cdot \mathbf{p})}{p^2 |\mathbf{k} - \mathbf{p}|^2} (1 - \mu_{\mathbf{k},\mathbf{p}}^2) P_L(p) \\
3f_3^D(k) + f_3^K(k) &= \tilde{\mathcal{I}}_3^K(k) \equiv k \int_{\mathbf{p}} \frac{(\hat{\mathbf{k}} \cdot \mathbf{p})^3}{p^2 |\mathbf{k} - \mathbf{p}|^2} (1 - \mu_{\mathbf{k},\mathbf{p}}^2) P_L(p) \\
15f_4^{DD}(k) + 10f_4^{DK}(k) + f_4^{KK}(k) &= \mathcal{I}_3(k) \equiv \int_{\mathbf{p}} \frac{p^4}{p^2 |\mathbf{k} - \mathbf{p}|^2} (1 - \mu_{\mathbf{k},\mathbf{p}}^2) P_L(p) - \frac{2}{3} \sigma^2 \\
&= \int_{\mathbf{p}} \left[\frac{p^2}{|\mathbf{k} - \mathbf{p}|^2} (1 - \mu_{\mathbf{k},\mathbf{p}}^2) - \frac{2}{3} \right] P_L(p) \\
5f_4^{DD}(k) + 8f_4^{DK}(k) + f_4^{KK}(k) &= \mathcal{I}_4(k) \equiv \int_{\mathbf{p}} \frac{p^2 (\hat{\mathbf{k}} \cdot \mathbf{p})^2}{p^2 |\mathbf{k} - \mathbf{p}|^2} (1 - \mu_{\mathbf{k},\mathbf{p}}^2) P_L(p) - \frac{2}{15} \sigma^2 \\
&= \int_{\mathbf{p}} \left[\frac{(\hat{\mathbf{k}} \cdot \mathbf{p})^2}{|\mathbf{k} - \mathbf{p}|^2} (1 - \mu_{\mathbf{k},\mathbf{p}}^2) - \frac{2}{15} \right] P_L(p) \\
3f_4^{DD}(k) + 6f_4^{DK}(k) + f_4^{KK}(k) &= \mathcal{I}_5(k) \equiv \int_{\mathbf{p}} \frac{(\hat{\mathbf{k}} \cdot \mathbf{p})^4}{p^2 |\mathbf{k} - \mathbf{p}|^2} (1 - \mu_{\mathbf{k},\mathbf{p}}^2) P_L(p) - \frac{2}{35} \sigma^2 \\
&= \int_{\mathbf{p}} \left[\frac{(\hat{\mathbf{k}} \cdot \mathbf{p})^4}{p^2 |\mathbf{k} - \mathbf{p}|^2} (1 - \mu_{\mathbf{k},\mathbf{p}}^2) - \frac{2}{35} \right] P_L(p). \quad (\text{D.5})
\end{aligned}$$

In $\mathcal{I}_3, \mathcal{I}_4, \mathcal{I}_5$, we have subtracted the constant in the $k \rightarrow 0$ limit, which corresponds to the counterterm to any cubic operator $[O^{(3)}]$ that is proportional to $\sigma_n^2(\Lambda)\delta$. All other loop integrals already scale as k^2 in this limit, and do not involve this leading counterterm.

2. One can then solve for $f_n^X(k)$ in terms of $\mathcal{I}_m^Y(k)$, an exercise in linear algebra which we do not reproduce here. Eq. (D.4) can be used to eliminate

$$\begin{aligned}
\tilde{\mathcal{I}}_2^K(k) &= \frac{1}{4} (2\mathcal{I}_1(k) + \mathcal{I}_2(k) + \mathcal{I}_3(k)) ; \quad \tilde{\mathcal{I}}_3^D(k) = \frac{1}{2} (\mathcal{I}_2(k) + \mathcal{I}_3(k)) \\
\tilde{\mathcal{I}}_3^K(k) &= \frac{1}{8} (2\mathcal{I}_1(k) + \mathcal{I}_2(k) + \mathcal{I}_3(k) + 4\mathcal{I}_4(k)) . \quad (\text{D.6})
\end{aligned}$$

3. We now construct the desired correlators which involve powers of $(k-p)^a$ in terms of

$f_i, f_{ij}, f_{ijk}, f_{ijkl}$:

$$\int_{\mathbf{p}} \frac{p^i p^j p^k (k-p)^l}{p^2 |\mathbf{k}-\mathbf{p}|^2} (1 - \mu_{\mathbf{k},\mathbf{p}}^2) P_L(p) = k_l f_{ijk}(k) - f_{ijkl}(k) \quad (\text{D.7})$$

$$= \left[\hat{k}_l \hat{k}_i \delta_{jk} + 2 \text{ perm.} \right] f_3^{\text{D}}(k) + \hat{k}_i \hat{k}_j \hat{k}_k \hat{k}_l f_3^{\text{K}}(k) - f_{ijkl}(k)$$

$$\int_{\mathbf{p}} \frac{p^i p^j (k-p)^k (k-p)^l}{p^2 |\mathbf{k}-\mathbf{p}|^2} (1 - \mu_{\mathbf{k},\mathbf{p}}^2) P_L(p) = k_k k_l f_{ij}(k) - 2k_{(k} f_{ij)l}(k) + f_{ijkl}(k)$$

$$= \hat{k}_k \hat{k}_l \left[\delta_{ij} f_2^{\text{D}}(k) + \hat{k}_i \hat{k}_j f_2^{\text{K}}(k) \right] - \left[\hat{k}_k \hat{k}_i \delta_{jl} + \hat{k}_k \hat{k}_j \delta_{li} + \hat{k}_l \hat{k}_i \delta_{jk} + \hat{k}_l \hat{k}_j \delta_{ki} + 2 \hat{k}_k \hat{k}_l \delta_{ij} \right] f_3^{\text{D}}(k)$$

$$- 2 \hat{k}_i \hat{k}_j \hat{k}_k \hat{k}_l f_3^{\text{K}}(k) + f_{ijkl}(k) \quad (\text{D.8})$$

$$\int_{\mathbf{p}} \frac{p^i (k-p)^j (k-p)^k (k-p)^l}{p^2 |\mathbf{k}-\mathbf{p}|^2} (1 - \mu_{\mathbf{k},\mathbf{p}}^2) P_L(p)$$

$$= k_j \int_{\mathbf{p}} \frac{p_i (k-p)_k (k-p)_l}{p^2 |\mathbf{k}-\mathbf{p}|^2} (1 - \mu_{\mathbf{k},\mathbf{p}}^2) P_L(p) - \{pp(k-p)(k-p)\}$$

$$= \hat{k}_i \hat{k}_j \hat{k}_k \hat{k}_l f_1(k) - \left[\left(\hat{k}_j \hat{k}_k \delta_{il} + \hat{k}_j \hat{k}_l \delta_{ik} \right) f_2^{\text{D}}(k) + 2 \hat{k}_i \hat{k}_j \hat{k}_k \hat{k}_l f_2^{\text{K}}(k) \right]$$

$$+ \left[\hat{k}_j \hat{k}_i \delta_{kl} + \hat{k}_j \hat{k}_k \delta_{li} + \hat{k}_j \hat{k}_l \delta_{ik} \right] f_3^{\text{D}}(k) + \hat{k}_i \hat{k}_j \hat{k}_k \hat{k}_l f_3^{\text{K}}(k) - \{pp(k-p)(k-p)\}. \quad (\text{D.9})$$

Here, “ $\{pp(k-p)(k-p)\}$ ” stands for the loop integral given in Eq. (D.8).

4. By contracting these relations with $\delta^{ab}, \hat{n}^c \hat{n}^d$, we can finally express the correlators of all desired cubic operators in terms of the $f_n^{\text{X}}(k)$, and then the $\mathcal{I}_m(k)$. This is again simple linear algebra, and we do not reproduce it here. The result is given in Eq. (3.18) together with Appendix F.

E NLO matter and velocity power spectra

The NLO matter density and velocity divergence power spectra can be written as

$$P_{mm}^{\text{NLO}}(k) = P_{mm}^{(22)}(k) + 2P_{mm}^{(13)}(k) \quad (\text{E.1})$$

$$P_{m\theta}^{\text{NLO}}(k) = P_{m\theta}^{(22)}(k) + 2P_{m\theta}^{(13)}(k) \quad (\text{E.2})$$

$$P_{\theta\theta}^{\text{NLO}}(k) = P_{\theta\theta}^{(22)}(k) + 2P_{\theta\theta}^{(13)}(k). \quad (\text{E.3})$$

Note that we include both 2–2 and 1–3 contributions in our decomposition of the redshift-space galaxy power spectrum. We have, through Eq. (3.5) together with the definitions in Tab. 1,

$$P_{mm}^{(22)}(k) \equiv \left\langle \delta^{(2)}(\mathbf{k}) \delta^{(2)}(\mathbf{k}') \right\rangle' = \mathcal{I}^{[\delta^{(2)}, \delta^{(2)}]}(k)$$

$$P_{\theta\theta}^{(22)}(k) \equiv \left\langle \theta^{(2)}(\mathbf{k}) \theta^{(2)}(\mathbf{k}') \right\rangle' = \mathcal{I}^{[\theta^{(2)}, \theta^{(2)}]}(k)$$

$$P_{m\theta}^{(22)}(k) \equiv \left\langle \delta^{(2)}(\mathbf{k}) \theta^{(2)}(\mathbf{k}') \right\rangle' = \mathcal{I}^{[\delta^{(2)}, \theta^{(2)}]}(k). \quad (\text{E.4})$$

The 1–3-type loop contributions $P_{mm}^{(13)}$ and $P_{\theta\theta}^{(13)}$ are usually written as

$$\begin{aligned} P_{mm}^{(13)}(k) &\equiv \left\langle \delta^{(1)}(\mathbf{k})\delta^{(3)}(\mathbf{k}') \right\rangle' = 3P_L(k) \int_{\mathbf{p}} F_3(\mathbf{p}, -\mathbf{p}, \mathbf{k}) P_L(p) \\ P_{\theta\theta}^{(13)}(k) &\equiv \left\langle \theta^{(1)}(\mathbf{k})\theta^{(3)}(\mathbf{k}') \right\rangle' = 3(\mathcal{H}f)^2 P_L(k) \int_{\mathbf{p}} G_3(\mathbf{p}, -\mathbf{p}, \mathbf{k}) P_L(p). \end{aligned} \quad (\text{E.5})$$

However, they can also be expressed in terms of our general loop integral decomposition. Keeping only the terms that are not absorbed by counterterms, the relevant contributions to the configuration-space expressions of $\delta^{(3)}$ and $\theta^{(3)}$ are (see [39] and App. B of [61])

$$\begin{aligned} \delta^{(3)} \Big|_{\text{NLO}} &= \frac{1}{6} O_{\text{td}} - s^{(2)k} \partial_k \delta \\ (-f\mathcal{H})^{-1} \theta^{(3)} \Big|_{\text{NLO}} &= \frac{1}{2} O_{\text{td}} - s^{(2)k} \partial_k \delta. \end{aligned} \quad (\text{E.6})$$

where

$$s^{(2)k} = \frac{1}{2} \frac{\partial^k}{\nabla^2} \left[-\frac{2}{7} \delta^2 + \frac{3}{7} K^2 \right] = \frac{1}{2} \frac{3}{7} \frac{\partial^k}{\nabla^2} \left(\text{tr}[\Pi^{[1]}\Pi^{[1]}] - \delta^2 \right) \quad (\text{E.7})$$

is the second-order displacement.² This leads to

$$\begin{aligned} \left\langle \delta(\mathbf{k}') \left(-s_k^{(2)} \partial^k \delta \right) (\mathbf{k}) \right\rangle' &= \frac{3}{7} P_L(k) \int_{\mathbf{p}} \frac{p^2 \mathbf{p} \cdot (\mathbf{k} - \mathbf{p})}{p^2 |\mathbf{k} - \mathbf{p}|^2} (1 - \mu_{\mathbf{k},\mathbf{p}}^2) P_L(p) \\ &= \frac{3}{14} [\mathcal{I}_2(k) - \mathcal{I}_3(k)] P_L(k), \end{aligned} \quad (\text{E.8})$$

where we have used the results of Appendix D in the last line. Together with our previously derived expression for $\langle \delta(\mathbf{k}') O_{\text{td}}(\mathbf{k}) \rangle'$, this yields

$$\begin{aligned} P_{mm}^{(13)}(k) &= \left[\frac{2}{21} \mathcal{I}_1(k) + \frac{1}{14} \mathcal{I}_2(k) - \frac{1}{6} \mathcal{I}_3(k) - \frac{1}{6} \sigma_{-1}^2 k^2 \right] P_L(k) \\ P_{\theta\theta}^{(13)}(k) &= (\mathcal{H}f)^2 \left[\frac{2}{7} \mathcal{I}_1(k) - \frac{3}{14} \mathcal{I}_2(k) - \frac{1}{14} \mathcal{I}_3(k) - \frac{1}{6} \sigma_{-1}^2 k^2 \right] P_L(k), \end{aligned} \quad (\text{E.9})$$

and Eq. (F.7). Here, the “bare” counterterms $\propto \sigma_{-1}^2 k^2$ absorb the leading cutoff dependence of the 1–3 contributions. In the EFT description, we should also add counterterms with free coefficients [see Eq. (5.15) and Eq. (5.17)], which can absorb these bare counterterms. Finally, the 1–3-type contribution to the cross-correlation is given by the linear combination

$$P_{m\theta}^{(13)}(k) = -\frac{1}{2} \left[(\mathcal{H}f) P_{mm}^{(13)}(k) + (\mathcal{H}f)^{-1} P_{\theta\theta}^{(13)}(k) \right]. \quad (\text{E.10})$$

²Note that $D\mathbf{s}/D\tau = \mathbf{v}$, so that $\mathbf{s}^{(2)}(\mathbf{q}, \tau) = \mathbf{v}^{(2)}(\mathbf{x}[\mathbf{q}], \tau)/2f\mathcal{H}$.

F Coefficient matrices for 1–3-type loop contributions

In this appendix, we derive the projection of the 1–3-type loop contributions onto the general decomposition derived in Appendix D. First, we isolate the contribution $\propto O^{\Pi_1-\Pi_2}$ in each of the operators in \mathfrak{D}_{1-3} to which this applies:

$$\begin{aligned}
O_{\text{td}} &= \frac{8}{21} \delta^{ik} \delta^{jl} O_{ijkl}^{\Pi_1-\Pi_2} \\
\delta\Pi_{\parallel}^{[2]} &= \frac{10}{21} \delta^{ij} \hat{n}^k \hat{n}^l O_{ijkl}^{\Pi_1-\Pi_2} \\
f^{-1}\eta\Pi_{\parallel}^{[2]} &= -\frac{10}{21} \hat{n}^i \hat{n}^j \hat{n}^k \hat{n}^l O_{ijkl}^{\Pi_1-\Pi_2} \\
(\Pi^{[2]}\Pi^{[1]})_{\parallel} &= (\Pi^{[2]}K)_{\parallel} + \frac{1}{3}\delta\Pi_{\parallel}^{[2]} = \frac{5}{21} \left[\delta^{jk} \hat{n}^i \hat{n}^l + \delta^{il} \hat{n}^j \hat{n}^k \right] O_{ijkl}^{\Pi_1-\Pi_2}. \tag{F.1}
\end{aligned}$$

The following operators involve the same contractions, and their loop contributions are thus linearly proportional:

$$\begin{aligned}
2KK^{(2)} &= \frac{20}{21} \delta^{ik} \delta^{jl} O_{ijkl}^{\Pi_1-\Pi_2} = \frac{5}{2} O_{\text{td}} \\
f^{-1}\delta\eta^{(2)} &= -\frac{2}{7} \delta^{ij} \hat{n}^k \hat{n}^l O_{ijkl}^{\Pi_1-\Pi_2} = -\frac{3}{5} \delta\Pi_{\parallel}^{[2]} \\
2f^{-2}\eta\eta^{(2)} &= \frac{4}{7} \hat{n}^i \hat{n}^j \hat{n}^k \hat{n}^l O_{ijkl}^{\Pi_1-\Pi_2} = -\frac{6}{5} f^{-1}\eta\Pi_{\parallel}^{[2]} \\
2K_{ij}^{(2)} K^j_k \hat{n}^i \hat{n}^k &= 2\Pi_{ij}^{[2]} K^j_k \hat{n}^i \hat{n}^k, \tag{F.2}
\end{aligned}$$

where we have used Eq. (2.4) and the following configuration-space expressions of operators at second order:

$$\begin{aligned}
K_{ij}^{(2)} &= \frac{10}{21} \mathcal{D}_{ij} \left[\delta^2 - \frac{3}{2} K^2 \right] + [KK]_{ij} - \frac{1}{3} \delta_{ij} K^2 + \frac{2}{3} \delta K_{ij} - s^k \partial_k K_{ij} \\
-(f\mathcal{H})^{-1}\theta^{(2)} &= \frac{13}{21} \delta^2 + \frac{4}{7} K^2 - s^k \partial_k \delta \\
f^{-1}u_{\parallel}^{(2)} &= \frac{\partial_{\parallel}}{\nabla^2} (f\mathcal{H})^{-1}\theta^{(2)} = -\frac{2}{7} \frac{\partial_{\parallel}}{\nabla^2} \left[\delta^2 - \frac{3}{2} K^2 \right] + s^k \Pi_{ki}^{[1]} \hat{n}^i \\
f^{-1}\eta^{(2)} &= -\frac{2}{7} \frac{\partial_{\parallel}^2}{\nabla^2} \left[\delta^2 - \frac{3}{2} K^2 \right] - [\Pi^{[1]}\Pi^{[1]}]_{\parallel} + s^k \partial_{\parallel} \Pi_{ki}^{[1]} \hat{n}^i. \tag{F.3}
\end{aligned}$$

Seven of the remaining eight contributions in Eq. (3.10) have a similar, but not quite identical structure to the contributions involving $O^{\Pi_1-\Pi_2}$. They are:

$$\begin{aligned}
\langle \delta(\mathbf{k}') \left(f^{-1} u_{\parallel} \partial_{\parallel} \Pi_{\parallel}^{[2]} \right) (\mathbf{k}) \rangle' &= -\frac{5}{3} \langle \delta(\mathbf{k}') \left(f^{-2} u_{\parallel} \partial_{\parallel} \eta^{(2)} \right) (\mathbf{k}) \rangle' \\
&= -\frac{10}{7} P_L(k) \int_{\mathbf{p}} \frac{p_{\parallel} (k-p)_{\parallel}^3}{p^2 |\mathbf{k}-\mathbf{p}|^2} (1 - \mu_{\mathbf{k},\mathbf{p}}^2) P_L(p) \\
\langle \delta(\mathbf{k}') \left(s^k \partial_k \Pi_{\parallel}^{[2]} \right) (\mathbf{k}) \rangle' &= -\frac{10}{7} P_L(k) \int_{\mathbf{p}} \frac{\mathbf{p} \cdot (\mathbf{k}-\mathbf{p}) (k-p)_{\parallel}^2}{p^2 |\mathbf{k}-\mathbf{p}|^2} (1 - \mu_{\mathbf{k},\mathbf{p}}^2) P_L(p) \\
\langle \delta(\mathbf{k}') \left(f^{-1} u_{\parallel}^{(2)} \partial_{\parallel} \delta \right) (\mathbf{k}) \rangle' &= -\frac{6}{7} P_L(k) \int_{\mathbf{p}} \frac{p^2 p_{\parallel} (k-p)_{\parallel}}{p^2 |\mathbf{k}-\mathbf{p}|^2} (1 - \mu_{\mathbf{k},\mathbf{p}}^2) P_L(p) \\
\langle \delta(\mathbf{k}') \left(f^{-2} u_{\parallel}^{(2)} \partial_{\parallel} \eta \right) (\mathbf{k}) \rangle' &= \frac{6}{7} P_L(k) \int_{\mathbf{p}} \frac{p_{\parallel}^3 (k-p)_{\parallel}}{p^2 |\mathbf{k}-\mathbf{p}|^2} (1 - \mu_{\mathbf{k},\mathbf{p}}^2) P_L(p) \\
\langle \delta(\mathbf{k}') \left(-s_k^{(2)} \partial^k \delta \right) (\mathbf{k}) \rangle' &= -f^{-1} \langle \delta(\mathbf{k}') \left(-s_k^{(2)} \partial^k \theta \right) (\mathbf{k}) \rangle' \\
&= \frac{3}{7} P_L(k) \int_{\mathbf{p}} \frac{p^2 \mathbf{p} \cdot (\mathbf{k}-\mathbf{p})}{p^2 |\mathbf{k}-\mathbf{p}|^2} (1 - \mu_{\mathbf{k},\mathbf{p}}^2) P_L(p). \tag{F.4}
\end{aligned}$$

Clearly, they also correspond to specific contractions of Eq. (3.11).

We now list the coefficient matrices corresponding to each of the relevant cubic operators:

$$\begin{aligned}
\mathbf{M}[O_{\text{td}}] &= \frac{1}{7} \begin{pmatrix} 4 & -6 & 2 & 0 & 0 \\ 0 & 0 & 0 & 0 & 0 \\ 0 & 0 & 0 & 0 & 0 \end{pmatrix} \\
\mathbf{M}[\delta\Pi_{\parallel}^{[2]}] &= \frac{1}{7} \begin{pmatrix} 0 & 0 & 5 & -5 & 0 \\ 0 & 0 & -15 & 15 & 0 \\ 0 & 0 & 0 & 0 & 0 \end{pmatrix} \\
\mathbf{M}[f^{-1}\eta\Pi_{\parallel}^{[2]}] &= \frac{1}{7} \begin{pmatrix} 0 & 0 & -\frac{15}{4} & \frac{15}{2} & -\frac{15}{4} \\ -5 & \frac{15}{2} & 20 & -60 & \frac{75}{2} \\ 5 & -\frac{15}{2} & -\frac{65}{4} & \frac{125}{2} & -\frac{175}{4} \end{pmatrix} \\
\mathbf{M}[(\Pi^{[2]}K)_{\parallel}] &= \frac{1}{7} \begin{pmatrix} \frac{5}{4} & -\frac{15}{8} & \frac{35}{24} & -\frac{5}{6} & 0 \\ \frac{5}{4} & -\frac{15}{8} & -\frac{15}{8} & \frac{5}{2} & 0 \\ 0 & 0 & 0 & 0 & 0 \end{pmatrix} \\
\mathbf{M}[f^{-1}u_{\parallel}^{(2)}\partial_{\parallel}\delta] &= \frac{1}{7} \begin{pmatrix} 0 & 0 & 3 & -3 & 0 \\ 0 & -3 & -6 & 9 & 0 \\ 0 & 0 & 0 & 0 & 0 \end{pmatrix} \\
\mathbf{M}[f^{-2}u_{\parallel}^{(2)}\partial_{\parallel}\eta] &= \frac{1}{7} \begin{pmatrix} 0 & 0 & -\frac{9}{4} & \frac{9}{2} & -\frac{9}{4} \\ -\frac{9}{4} & \frac{27}{8} & \frac{63}{8} & -\frac{63}{2} & \frac{45}{2} \\ \frac{15}{4} & -\frac{21}{8} & -\frac{39}{8} & 30 & -\frac{105}{4} \end{pmatrix} \\
\mathbf{M}[s^k\partial_k\Pi_{\parallel}^{[2]}] &= \frac{1}{7} \begin{pmatrix} \frac{5}{4} & -\frac{15}{8} & \frac{25}{8} & -\frac{5}{2} & 0 \\ -\frac{15}{4} & \frac{45}{8} & -\frac{75}{8} & \frac{15}{2} & 0 \\ 0 & 0 & 0 & 0 & 0 \end{pmatrix} \\
\mathbf{M}[f^{-1}u_{\parallel}\partial_{\parallel}\Pi_{\parallel}^{[2]}] &= \frac{1}{7} \begin{pmatrix} 0 & 0 & \frac{15}{4} & -\frac{15}{2} & \frac{15}{4} \\ \frac{15}{4} & -\frac{45}{8} & -\frac{225}{8} & \frac{135}{2} & -\frac{75}{2} \\ -\frac{25}{4} & \frac{75}{8} & \frac{225}{8} & -75 & \frac{175}{4} \end{pmatrix} \\
\mathbf{M}[\Pi_{\parallel}^{[3]}] &= \frac{1}{7} \begin{pmatrix} \frac{13}{8} & -\frac{39}{16} & \frac{65}{16} & -\frac{13}{4} & 0 \\ -\frac{101}{24} & \frac{101}{16} & -\frac{569}{48} & \frac{39}{4} & 0 \\ 0 & 0 & 0 & 0 & 0 \end{pmatrix}. \tag{F.5}
\end{aligned}$$

In the last line, we have used Eq. (C.19). Further, we have

$$\begin{aligned}
\mathbf{M}\left[2KK^{(2)}\right] &= \frac{5}{2}\mathbf{M}\left[O_{\text{td}}\right] \\
\mathbf{M}\left[f^{-1}\delta\eta^{(2)}\right] &= -\frac{3}{5}\mathbf{M}\left[\delta\Pi_{\parallel}^{[2]}\right] \\
\mathbf{M}\left[f^{-1}u_{\parallel}\partial_{\parallel}\eta^{(2)}\right] &= -\frac{3}{5}\mathbf{M}\left[u_{\parallel}\partial_{\parallel}\Pi_{\parallel}^{[2]}\right] \\
\mathbf{M}\left[2f^{-2}\eta\eta^{(2)}\right] &= -\frac{6}{5}\mathbf{M}\left[\eta\Pi_{\parallel}^{[2]}\right] \\
\mathbf{M}\left[2(KK^{(2)})_{\parallel}\right] &= 2\mathbf{M}\left[(\Pi^{[2]}K)_{\parallel}\right].
\end{aligned} \tag{F.6}$$

Finally, as shown in Appendix E, we have

$$\begin{aligned}
\mathbf{M}\left[\delta^{(3)}\right] &= \frac{1}{7}\begin{pmatrix} \frac{2}{3} & \frac{1}{2} & -\frac{7}{6} & 0 & 0 \\ 0 & 0 & 0 & 0 & 0 \\ 0 & 0 & 0 & 0 & 0 \end{pmatrix} \\
\mathbf{M}\left[f^{-1}\eta^{(3)}\right] &= \frac{1}{7}\begin{pmatrix} 0 & 0 & 0 & 0 & 0 \\ 2 & \frac{3}{2} & -\frac{1}{2} & 0 & 0 \\ 0 & 0 & 0 & 0 & 0 \end{pmatrix}.
\end{aligned} \tag{F.7}$$

G Multipole decomposition

In this appendix, together with the supplementary material [76], we give explicit expressions for the Legendre multipoles of the redshift-space galaxy power spectrum at NLO. We write

$$P_{gg,s}^{\text{LO+NLO}}(k, \mu) = \sum_{\ell=0,2,4,6,8} \left[P_{gg,s}^{\text{lb+hd},\ell}(k) + P_{gg,s}^{2-2,\ell}(k) + 2P_{gg,s}^{1-3,\ell}(k) \right] \mathcal{L}_{\ell}(\mu), \tag{G.1}$$

where $\mathcal{L}_{\ell}(\mu)$ are the Legendre polynomials. For clarity, we give the three components—LO and higher-derivative contributions, 2–2-, and 1–3-type—separately below. Note that

$$P_{gg,s}^{X,\ell}(k) = \frac{2\ell+1}{2} \int_{-1}^1 d\mu \mathcal{L}_{\ell}(\mu) P_{gg,s}^X(k, \mu). \tag{G.2}$$

G.1 Linear and higher-derivative

The multipoles of the linear and higher-derivative contributions from Eq. (3.1) are given by

$$\begin{aligned}
P_{gg,s}^{\text{1+hd},\ell=0}(k) &= b_1^2 P_L(k) - \frac{2}{15} b_1 P_L(k) \left(f b_{\eta} \left(-5\beta_{\nabla^2 \mathbf{v}} k^2 - 3\beta_{\partial_{\parallel}^2 \mathbf{v}} k^2 + 5 \right) + 15b_{\nabla^2 \delta} k^2 \right) \\
&\quad - \frac{1}{35} f^2 P_L(k) b_{\eta}^2 \left(14\beta_{\nabla^2 \mathbf{v}} k^2 + 10\beta_{\partial_{\parallel}^2 \mathbf{v}} k^2 - 7 \right) + \frac{1}{3} k^2 b_{\eta} (2b_{\nabla^2 \delta} f P_L(k) + P_{\epsilon\epsilon\eta}^{\{2\}}) \\
&\quad + k^2 P_{\epsilon}^{\{2\}} + P_{\epsilon}^{\{0\}}
\end{aligned} \tag{G.3}$$

$$\begin{aligned}
P_{gg,s}^{\text{1+hd},\ell=2}(k) &= \frac{2}{21} b_\eta \left\{ 2f P_L(k) \left[f b_\eta \left(3 - k^2 (6\beta_{\nabla^2 \mathbf{v}} + 5\beta_{\partial_{\parallel}^2 \mathbf{v}}) \right) + b_1 \left(k^2 (7\beta_{\nabla^2 \mathbf{v}} + 6\beta_{\partial_{\parallel}^2 \mathbf{v}}) - 7 \right) \right] \right. \\
&\quad \left. + 7k^2 (2b_{\nabla^2 \delta} f P_L(k) + P_{\epsilon\epsilon_\eta}^{\{2\}}) \right\} \\
P_{gg,s}^{\text{1+hd},\ell=4}(k) &= -\frac{8}{385} f P_L(k) b_\eta \left(f b_\eta \left(22\beta_{\nabla^2 \mathbf{v}} k^2 + 30\beta_{\partial_{\parallel}^2 \mathbf{v}} k^2 - 11 \right) - 22b_1 \beta_{\partial_{\parallel}^2 \mathbf{v}} k^2 \right) \\
P_{gg,s}^{\text{1+hd},\ell=6}(k) &= -\frac{32}{231} \beta_{\partial_{\parallel}^2 \mathbf{v}} f^2 k^2 P_L(k) b_\eta^2. \tag{G.4}
\end{aligned}$$

G.2 Loop terms

Decomposing the 2–2-contribution and the 1–3-contribution to the NLO galaxy redshift-space power spectrum in multipoles, we write, first,

$$P_{gg,s}^{2-2,\ell}(k, \mu) = \sum_{(m,p)} \mathcal{C}_{(m,p)}^{2-2,\ell}(f, \{b_O\}_{\mathfrak{D}_{2-2}}) \mathcal{I}_{mp}(k), \tag{G.5}$$

where $\mathcal{I}_{mp}(k)$ are defined in Eq. (3.8), and mp runs over the 23 pairs listed in Tab. 2. The coefficients can be written as

$$\mathcal{C}_{(m,p)}^{2-2,\ell}(f, \{b_O\}) = \sum_{O,O' \in \mathfrak{D}_{2-2}} b_O b_{O'} \mathcal{C}_{\ell,(m,p)}^{OO'}(f). \tag{G.6}$$

For each ℓ and mp , $\mathcal{C}_{\ell,(m,p)}^{OO'}$ is an 8×8 symmetric matrix which only depends on the growth rate f . The complete set of the $23 \times 5 = 115$ such matrices, out of which 98 are non-vanishing, can be found in the supplementary material [76]. Similarly we can write

$$P_{gg,s}^{1-3,\ell}(k) = \sum_{n=1}^5 \mathcal{C}_n^{1-3,\ell}(f, \{b_O\}_{\mathfrak{D}_{1-3}}) \mathcal{I}_n(k) P_L(k), \tag{G.7}$$

where the coefficient vectors for each multipole can be found in the supplementary material [76].

Note that Eqs. (G.5)–(G.7) also include the complete contributions to the nonlinear matter density and velocity statistics.

H Configuration space approach

In this Appendix, we outline how the Fourier-space results presented in this paper can be easily converted into predictions in configuration space, that is, galaxy 2-point and 3-point correlation functions. We will focus on the NLO P_{22} term for illustration. This is closely related to the fast evaluation of perturbation-theory integrals proposed in [77, 78], and could be used to speed up the computation of the galaxy power spectrum in redshift space as well.

There are two types of quadratic operators, which we denote as tensor (T) and vector (V):

$$\begin{aligned}
\text{T :} \quad O^{(2)} &= C_{ijkl}^{O,\text{T}} \Pi^{ij} \Pi^{kl} \\
\text{V :} \quad O^{(2)} &= C_{ijkl}^{O,\text{V}} \left(\frac{\partial^i}{\nabla^2} \delta \right) \partial^j \Pi^{kl}. \tag{H.1}
\end{aligned}$$

Here, $C^{O,T}$ and $C^{O,V}$ are tensors constructed out of δ^{ab} , $\hat{n}^a\hat{n}^b$, while all the fields δ, Π are evaluated at linear order. The vector type precisely corresponds to what we refer to as displacement terms. Furthermore, $\Pi_{\parallel}^{[2]}$ can be written as $\mu^2 \equiv (\hat{\mathbf{k}} \cdot \hat{\mathbf{n}})^2$ times a linear combination of δ^2 and K^2 and, thus, is effectively of the tensor type. Given these two different structures of quadratic operators, we can divide the correlator in Eq. (3.5) into three classes, comprising tensor- and vector-type auto- and cross-correlations, which we consider separately in the following.

Expressing the momentum conservation in Fourier space, the T-T 2-2 contribution include integrals of the form

$$\int d^3r \int_{\mathbf{k}_1} \int_{\mathbf{k}_2} k_1^{-4} k_2^{-4} k_1^i k_1^j k_1^k k_1^l k_2^m k_2^n k_2^o k_2^p P_L(k_1) P_L(k_2) e^{i(\mathbf{k}_1 + \mathbf{k}_2 - \mathbf{k}) \cdot \mathbf{r}} . \quad (\text{H.2})$$

The T-V and V-V contributions can be recast in a similar form, except that their integrand can include up to 6 factors of k_1^i (or k_2^i). Therefore, we are led to evaluate integrals of the form

$$\mathcal{I}_{i_1 \dots i_n}(kr) \equiv \frac{1}{4\pi} \int d\Omega_{\hat{\mathbf{k}}} \hat{k}_{i_1} \dots \hat{k}_{i_n} e^{i\mathbf{k} \cdot \mathbf{r}} , \quad (\text{H.3})$$

where $0 \leq n \leq 6$. While the cases $n = 0, 1$ are trivial, we shall discuss $n \geq 2$ in some detail for sake of completeness. Beginning with $n = 2$, we have

$$\begin{aligned} \mathcal{I}_{ij}(kr) &\equiv \frac{1}{4\pi} \int d\Omega_{\hat{\mathbf{k}}} \hat{k}_i \hat{k}_j e^{i\mathbf{k} \cdot \mathbf{r}} \\ &= \alpha_0^{(2)}(kr) \delta_{ij} + \alpha_2^{(2)}(kr) \hat{r}_i \hat{r}_j . \end{aligned} \quad (\text{H.4})$$

The functions $\alpha_i^{(n)}(kr)$, with $0 \leq i \leq n$, can be systematically computed by contracting $\mathcal{I}_{i_1 \dots i_n}$ with products of Kronecker symbols δ^{ij} and unit vector components \hat{r}^i . In the case $n = 2$, the two possible contractions $\delta^{ij} \mathcal{I}_{ij}$ and $\hat{r}^i \hat{r}^j \mathcal{I}_{ij}$ immediately lead to

$$\begin{aligned} \alpha_0^{(2)}(kr) &= \frac{1}{3} (j_0(kr) + j_2(kr)) \\ \alpha_2^{(2)}(kr) &= -j_2(kr) . \end{aligned} \quad (\text{H.5})$$

For the computation of the higher-order $\mathcal{I}_{i_1\dots i_n}$, we need the following integrals:

$$\begin{aligned}
\frac{1}{2} \int_{-1}^{+1} d\mu \mu e^{i\mathbf{k}\cdot\mathbf{r}} &= i j_1(kr) \\
\frac{1}{2} \int_{-1}^{+1} d\mu \mu^2 e^{i\mathbf{k}\cdot\mathbf{r}} &= \frac{1}{3} j_0(kr) - \frac{2}{3} j_2(kr) \\
\frac{1}{2} \int_{-1}^{+1} d\mu \mu^3 e^{i\mathbf{k}\cdot\mathbf{r}} &= \frac{3i}{5} j_1(kr) - \frac{2i}{5} j_3(kr) \\
\frac{1}{2} \int_{-1}^{+1} d\mu \mu^4 e^{i\mathbf{k}\cdot\mathbf{r}} &= \frac{1}{5} j_0(kr) - \frac{4}{7} j_2(kr) + \frac{8}{35} j_4(kr) \\
\frac{1}{2} \int_{-1}^{+1} d\mu \mu^5 e^{i\mathbf{k}\cdot\mathbf{r}} &= \frac{3i}{7} j_1(kr) - \frac{4i}{9} j_3(kr) + \frac{8i}{63} j_5(kr) \\
\frac{1}{2} \int_{-1}^{+1} d\mu \mu^6 e^{i\mathbf{k}\cdot\mathbf{r}} &= \frac{1}{7} j_0(kr) - \frac{10}{21} j_2(kr) + \frac{24}{77} j_4(kr) - \frac{16}{231} j_6(kr),
\end{aligned} \tag{H.6}$$

along with the following results, which follow from symmetry considerations:

$$\begin{aligned}
\mathcal{I}_{ijl}(kr) &= \alpha_1^{(3)}(kr) \left(\delta_{ij} \hat{r}_l + 2 \text{ perms.} \right) + \alpha_3^{(3)}(kr) \hat{r}_i \hat{r}_j \hat{r}_l \\
\mathcal{I}_{ijlm}(kr) &= \alpha_0^{(4)}(kr) \left(\delta_{ij} \delta_{lm} + 2 \text{ perms.} \right) + \alpha_2^{(4)}(kr) \left(\hat{r}_i \hat{r}_j \delta_{lm} + 5 \text{ perms.} \right) + \alpha_4^{(4)}(kr) \hat{r}_i \hat{r}_j \hat{r}_l \hat{r}_m \\
\mathcal{I}_{ijklm}(kr) &= \alpha_1^{(5)}(kr) \left(\delta_{ij} \delta_{kl} \hat{r}_m + 14 \text{ perms.} \right) + \alpha_3^{(5)}(kr) \left(\delta_{ij} \hat{r}_k \hat{r}_l \hat{r}_m + 9 \text{ perms.} \right) \\
&\quad + \alpha_5^{(5)}(kr) \hat{r}_i \hat{r}_j \hat{r}_k \hat{r}_l \hat{r}_m \\
\mathcal{I}_{ijklmnl}(kr) &= \alpha_0^{(6)}(kr) \left(\delta_{ij} \delta_{kl} \delta_{mn} + 14 \text{ perms.} \right) + \alpha_2^{(6)}(kr) \left(\delta_{ij} \delta_{kl} \hat{r}_m \hat{r}_n + 44 \text{ perms.} \right) \\
&\quad + \alpha_4^{(6)}(kr) \left(\delta_{ij} \hat{r}_k \hat{r}_l \hat{r}_m \hat{r}_n + 14 \text{ perms.} \right) + \alpha_6^{(6)}(kr) \hat{r}_i \hat{r}_j \hat{r}_k \hat{r}_l \hat{r}_m \hat{r}_n.
\end{aligned} \tag{H.7}$$

The higher-order functions $\alpha_i^{(n)}(kr)$ with $n \geq 3$ can now be computed analogously to the case

$n = 2$. After some algebra, we find

$$\begin{aligned}
\alpha_1^{(3)}(kr) &= \frac{i}{5} \left(j_1(kr) + j_3(kr) \right) \\
\alpha_3^{(3)}(kr) &= -i j_3(kr) \\
\alpha_0^{(4)}(kr) &= \frac{1}{15} j_0(kr) + \frac{2}{21} j_2(kr) + \frac{1}{35} j_4(kr) \\
\alpha_2^{(4)}(kr) &= -\frac{1}{7} \left(j_2(kr) + j_4(kr) \right) \\
\alpha_4^{(4)}(kr) &= j_4(kr) \\
\alpha_1^{(5)}(kr) &= \frac{i}{35} j_1(kr) + \frac{2i}{45} j_3(kr) + \frac{i}{63} j_5(kr) \\
\alpha_3^{(5)}(kr) &= -\frac{i}{9} \left(j_3(kr) + j_5(kr) \right) \\
\alpha_5^{(5)}(kr) &= i j_5(kr) \\
\alpha_0^{(6)}(kr) &= \frac{1}{105} j_0(kr) + \frac{1}{63} j_2(kr) + \frac{3}{385} j_4(kr) + \frac{1}{693} j_6(kr) \\
\alpha_2^{(6)}(kr) &= -\frac{1}{63} j_2(kr) - \frac{2}{77} j_4(kr) - \frac{1}{99} j_6(kr) \\
\alpha_4^{(6)}(kr) &= \frac{1}{11} \left(j_4(kr) + j_6(kr) \right) \\
\alpha_6^{(6)}(kr) &= -j_6(kr) .
\end{aligned} \tag{H.8}$$

It is obvious that $\alpha_n^{(n)}(kr) = i^n j_n(kr)$ (no summation). General expressions for the other functions $\alpha_i^{(n)}(kr)$ could also be conjectured from these explicit relations.

The T-T, T-V and V-V 2-2 contributions involve the angular average $\mathcal{I}_{i_1 \dots i_n}(kr)$ with $0 \leq n \leq 6$. In order to perform the integral over the wavenumber k , we must evaluate integrals of the form

$$\frac{1}{2\pi^2} \int_0^\infty dk k^{m+2} \alpha_j^{(i)}(kr) P_L(k) \tag{H.9}$$

in order to predict the configuration space 2-2 contribution. Here, the exponent m is restricted to vary in the range $-2 \leq m \leq 2$, whereas $0 \leq j \leq i \leq 6$. Since all the functions $\alpha_i^{(j)}(kr)$ can be expressed as a linear superposition of spherical Bessel functions $j_n(kr)$ with $0 \leq n \leq 6$, the structure of the T-T, T-V and V-V terms implies that relevant combinations are:

$$\begin{aligned}
m = -2 : & \quad j_0(kr) , j_2(kr) \\
m = -1 : & \quad j_1(kr) , j_3(kr) \\
m = 0 : & \quad j_0(kr) , j_2(kr) , j_4(kr) \\
m = +1 : & \quad j_1(kr) , j_3(kr) , j_5(kr) \\
m = +2 : & \quad j_0(kr) , j_2(kr) , j_4(kr) , j_6(kr) .
\end{aligned} \tag{H.10}$$

This shows that 14 independent integrals

$$\xi_n^{(m)}(r) \equiv \frac{1}{2\pi^2} \int_0^\infty dk k^{m+2} j_n(kr) P_L(k) \tag{H.11}$$

must be evaluated in the calculation of the configuration space 2-2 contribution. The latter takes the form

$$\xi_{gg,s}^{2-2}(r, \mu) = \sum_{O, O' \in \mathcal{D}_{2-2}} b_O b_{O'} \int_{\mathbf{k}_1} \int_{\mathbf{k}_2} S_O(\mathbf{k}_1, \mathbf{k}_2) S_{O'}(\mathbf{k}_1, \mathbf{k}_2) P_L(k_1) P_L(k_2) e^{i(\mathbf{k}_1 + \mathbf{k}_2) \cdot \mathbf{r}} \quad (\text{H.12})$$

where the kernels S_O are summarized in Tab. 1.

For illustration, consider the contribution $(\delta^{(2)})^2$, which corresponds to $S_O(\mathbf{k}_1, \mathbf{k}_2) = S_{O'}(\mathbf{k}_1, \mathbf{k}_2) = F_2(\mathbf{k}_1, \mathbf{k}_2)$. Beginning with the angular average of $S_O S_{O'}$ yields

$$\frac{1}{(4\pi)^2} \int d\Omega_{\hat{\mathbf{k}}_1} \int d\Omega_{\hat{\mathbf{k}}_2} [F_2(\mathbf{k}_1, \mathbf{k}_2)]^2 = \sum_{n=0}^4 \beta_{i_1 \dots i_n}^{j_1 \dots j_n}(k_1, k_2) \mathcal{I}_{i_1 \dots i_n}(k_1 r) \mathcal{I}_{j_1 \dots j_n}(k_2 r). \quad (\text{H.13})$$

The functions $\beta_{i_1 \dots i_n}^{j_1 \dots j_n}(k_1, k_2)$ are symmetric under the exchange $k_1 \leftrightarrow k_2$ and, in this particular case, only involve Kronecker symbols (they generally encode also a dependence on the line-of-sight direction). On performing the integral over the wavenumbers k_1 and k_2 , we eventually obtain

$$b_1^2 \left\{ \frac{1}{10290} \left[8533 \xi_0^{(0)}(r) \xi_0^{(0)}(r) + 3910 \xi_2^{(0)}(r) \xi_2^{(0)}(r) + 11200 \xi_4^{(0)}(r) \xi_4^{(0)}(r) \right] \right. \\ \left. + \frac{1}{6} \left[\xi_0^{(-2)}(r) \xi_0^{(2)}(r) + 2 \xi_2^{(-2)}(r) \xi_2^{(2)}(r) \right] - \frac{1}{35} \left[62 \xi_1^{(-1)}(r) \xi_1^{(1)}(r) + 8 \xi_3^{(-1)}(r) \xi_3^{(1)}(r) \right] \right\}. \quad (\text{H.14})$$

The calculation of the other 2-2 terms proceeds analogously.

The configuration space expression can be Fourier transformed to obtain the 2-2 power spectrum. This requires evaluating integrals of the generic form ($0 \leq n \leq 4$)

$$\int d^3 r \hat{r}^{2n} \xi_{n_1}^{(m_1)}(r) \xi_{n_2}^{(m_2)}(r) e^{-i\mathbf{k} \cdot \mathbf{r}}, \quad (\text{H.15})$$

the angular part of which can be performed analytically using the explicit expressions for $\mathcal{I}_{i_1 \dots i_n}$ given above. Therefore, one is left with line-of-sight integrals of the form

$$\int dr r^2 j_q(kr) \xi_{n_1}^{(m_1)}(r) \xi_{n_2}^{(m_2)}(r), \quad (\text{H.16})$$

which can be easily performed numerically.

References

- [1] J. C. Jackson, *A critique of Rees's theory of primordial gravitational radiation*, *Mon. Not. R. Astron. Soc.* **156** (1972) 1P, [[arXiv:0810.3908](https://arxiv.org/abs/0810.3908)].
- [2] W. L. W. Sargent and E. L. Turner, *A statistical method for determining the cosmological density parameter from the redshifts of a complete sample of galaxies*, *Astrophys. J. Lett.* **212** (Feb., 1977) L3–L7.

- [3] M. Davis and P. J. E. Peebles, *A survey of galaxy redshifts. V - The two-point position and velocity correlations*, *Astrophys. J.* **267** (Apr., 1983) 465–482.
- [4] P. B. Lilje and G. Efstathiou, *Gravitationally induced velocity fields in the universe. I - Correlation functions*, *Mon. Not. R. Astron. Soc.* **236** (Feb., 1989) 851–864.
- [5] J. A. Peacock and S. J. Dodds, *Reconstructing the Linear Power Spectrum of Cosmological Mass Fluctuations*, *Mon. Not. R. Astron. Soc.* **267** (Apr., 1994) 1020, [[astro-ph/9311057](#)].
- [6] K. B. Fisher, C. A. Scharf, and O. Lahav, *A spherical harmonic approach to redshift distortion and a measurement of $\Omega(0)$ from the 1.2-Jy IRAS Redshift Survey*, *Mon. Not. R. Astron. Soc.* **266** (Jan., 1994) 219, [[astro-ph/9309027](#)].
- [7] A. F. Heavens, S. Matarrese, and L. Verde, *The non-linear redshift-space power spectrum of galaxies*, *Mon. Not. R. Astron. Soc.* **301** (Dec., 1998) 797–808, [[astro-ph/9808016](#)].
- [8] H. Magira, Y. P. Jing, and Y. Suto, *Cosmological Redshift-Space Distortion on Clustering of High-Redshift Objects: Correction for Nonlinear Effects in the Power Spectrum and Tests with N-Body Simulations*, *Astrophys. J.* **528** (Jan., 2000) 30–50, [[astro-ph/9907438](#)].
- [9] A. J. S. Hamilton, *Linear Redshift Distortions: a Review*, in *The Evolving Universe* (D. Hamilton, ed.), vol. 231 of *Astrophysics and Space Science Library*, p. 185, 1998. [[astro-ph/9708102](#)].
- [10] J. Loveday, G. Efstathiou, S. J. Maddox, and B. A. Peterson, *The Stromlo-APM Redshift Survey. III. Redshift Space Distortions, Omega, and Bias*, *Astrophys. J.* **468** (Sept., 1996) 1, [[astro-ph/9505099](#)].
- [11] J. A. Peacock, S. Cole, P. Norberg, C. M. Baugh, J. Bland-Hawthorn, T. Bridges, R. D. Cannon, M. Colless, C. Collins, W. Couch, G. Dalton, K. Deeley, R. De Propris, S. P. Driver, G. Efstathiou, R. S. Ellis, C. S. Frenk, K. Glazebrook, C. Jackson, O. Lahav, I. Lewis, S. Lumsden, S. Maddox, W. J. Percival, B. A. Peterson, I. Price, W. Sutherland, and K. Taylor, *A measurement of the cosmological mass density from clustering in the 2dF Galaxy Redshift Survey*, *Nature (London)* **410** (Mar., 2001) 169–173, [[astro-ph/0103143](#)].
- [12] E. Hawkins, S. Maddox, S. Cole, O. Lahav, D. S. Madgwick, P. Norberg, J. A. Peacock, I. K. Baldry, C. M. Baugh, J. Bland-Hawthorn, T. Bridges, R. Cannon, M. Colless, C. Collins, W. Couch, G. Dalton, R. De Propris, S. P. Driver, G. Efstathiou, R. S. Ellis, C. S. Frenk, K. Glazebrook, C. Jackson, B. Jones, I. Lewis, S. Lumsden, W. Percival, B. A. Peterson, W. Sutherland, and K. Taylor, *The 2dF Galaxy Redshift Survey: correlation functions, peculiar velocities and the matter density of the Universe*, *Mon. Not. R. Astron. Soc.* **346** (Nov., 2003) 78–96, [[astro-ph/0212375](#)].
- [13] L. Guzzo, M. Pierleoni, B. Meneux, E. Branchini, O. Le Fèvre, C. Marinoni, B. Garilli, J. Blaizot, G. De Lucia, A. Pollo, H. J. McCracken, D. Bottini, V. Le Brun, D. Maccagni, J. P. Picat, R. Scaramella, M. Scodreggio, L. Tresse, G. Vettolani, A. Zanichelli, C. Adami, S. Arnouts, S. Bardelli, M. Bolzonella, A. Bongiorno, A. Cappi, S. Charlot, P. Ciliegi, T. Contini, O. Cucciati, S. de la Torre, K. Dolag, S. Foucaud, P. Franzetti, I. Gavignaud, O. Ilbert, A. Iovino, F. Lamareille, B. Marano, A. Mazure, P. Memeo, R. Merighi, L. Moscardini, S. Paltani, R. Pellò, E. Perez-Montero, L. Pozzetti, M. Radovich, D. Vergani, G. Zamorani, and E. Zucca, *A test of the nature of cosmic acceleration using galaxy redshift distortions*, *Nature (London)* **451** (Jan., 2008) 541–544, [[arXiv:0802.1944](#)].

- [14] W. J. Percival and M. White, *Testing cosmological structure formation using redshift-space distortions*, *Mon. Not. R. Astron. Soc.* **393** (Feb., 2009) 297–308, [[arXiv:0808.0003](#)].
- [15] F. Beutler, C. Blake, M. Colless, D. H. Jones, L. Staveley-Smith, G. B. Poole, L. Campbell, Q. Parker, W. Saunders, and F. Watson, *The 6dF Galaxy Survey: $z \sim 0$ measurements of the growth rate and σ_8* , *Mon. Not. R. Astron. Soc.* **423** (July, 2012) 3430–3444, [[arXiv:1204.4725](#)].
- [16] B. A. Reid, L. Samushia, M. White, W. J. Percival, M. Manera, N. Padmanabhan, A. J. Ross, A. G. Sánchez, S. Bailey, D. Bizyaev, A. S. Bolton, H. Brewington, J. Brinkmann, J. R. Brownstein, A. J. Cuesta, D. J. Eisenstein, J. E. Gunn, K. Honscheid, E. Malanushenko, V. Malanushenko, C. Maraston, C. K. McBride, D. Muna, R. C. Nichol, D. Oravetz, K. Pan, R. de Putter, N. A. Roe, N. P. Ross, D. J. Schlegel, D. P. Schneider, H.-J. Seo, A. Shelden, E. S. Sheldon, A. Simmons, R. A. Skibba, S. Snedden, M. E. C. Swanson, D. Thomas, J. Tinker, R. Tojeiro, L. Verde, D. A. Wake, B. A. Weaver, D. H. Weinberg, I. Zehavi, and G.-B. Zhao, *The clustering of galaxies in the SDSS-III Baryon Oscillation Spectroscopic Survey: measurements of the growth of structure and expansion rate at $z = 0.57$ from anisotropic clustering*, *Mon. Not. R. Astron. Soc.* **426** (Nov., 2012) 2719–2737, [[arXiv:1203.6641](#)].
- [17] L. Samushia, W. J. Percival, and A. Raccanelli, *Interpreting large-scale redshift-space distortion measurements*, *Mon. Not. R. Astron. Soc.* **420** (Mar., 2012) 2102–2119, [[arXiv:1102.1014](#)].
- [18] C. Blake, I. K. Baldry, J. Bland-Hawthorn, L. Christodoulou, M. Colless, C. Conselice, S. P. Driver, A. M. Hopkins, J. Liske, J. Loveday, P. Norberg, J. A. Peacock, G. B. Poole, and A. S. G. Robotham, *Galaxy And Mass Assembly (GAMA): improved cosmic growth measurements using multiple tracers of large-scale structure*, *Mon. Not. R. Astron. Soc.* **436** (Dec., 2013) 3089–3105, [[arXiv:1309.5556](#)].
- [19] S. de la Torre, L. Guzzo, J. A. Peacock, E. Branchini, A. Iovino, B. R. Granett, U. Abbas, C. Adami, S. Arnouts, J. Bel, M. Bolzonella, D. Bottini, A. Cappi, J. Coupon, O. Cucciati, I. Davidzon, G. De Lucia, A. Fritz, P. Franzetti, M. Fumana, B. Garilli, O. Ilbert, J. Krywult, V. Le Brun, O. Le Fèvre, D. Maccagni, K. Małek, F. Marulli, H. J. McCracken, L. Moscardini, L. Paioro, W. J. Percival, M. Polletta, A. Pollo, H. Schlegel, M. Scodreggio, L. A. M. Tasca, R. Tojeiro, D. Vergani, A. Zanichelli, A. Burden, C. Di Porto, A. Marchetti, C. Marinoni, Y. Mellier, P. Monaco, R. C. Nichol, S. Phleps, M. Wolk, and G. Zamorani, *The VIMOS Public Extragalactic Redshift Survey (VIPERS) . Galaxy clustering and redshift-space distortions at $z \sim 0.8$ in the first data release*, *Astron. Astrophys.* **557** (Sept., 2013) A54, [[arXiv:1303.2622](#)].
- [20] N. Dalal, O. Doré, D. Huterer, and A. Shirokov, *Imprints of primordial non-Gaussianities on large-scale structure: Scale-dependent bias and abundance of virialized objects*, *Phys. Rev. D* **77** (June, 2008) 123514–+, [[arXiv:0710.4560](#)].
- [21] D. J. Eisenstein and W. Hu, *Baryonic Features in the Matter Transfer Function*, *Astrophys. J.* **496** (Mar., 1998) 605–614, [[astro-ph/9709112](#)].
- [22] W. Hu, D. J. Eisenstein, and M. Tegmark, *Weighing neutrinos with galaxy surveys*, *Phys. Rev. Lett.* **80** (Jun, 1998) 5255–5258.
- [23] N. Kaiser, *Clustering in real space and in redshift space*, *Monthly Notices of the Royal Astronomical Society (ISSN 0035-8711)* **227** (July, 1987) 1–21.
- [24] K. B. Fisher, *On the Validity of the Streaming Model for the Redshift-Space Correlation Function in the Linear Regime*, *Astrophys. J.* **448** (Aug., 1995) 494, [[astro-ph/9412081](#)].

- [25] A. N. Taylor and A. J. S. Hamilton, *Non-linear cosmological power spectra in real and redshift space*, *Mon. Not. R. Astron. Soc.* **282** (Oct., 1996) 767–778, [[astro-ph/9604020](#)].
- [26] R. K. Sheth, L. Hui, A. Diaferio, and R. Scoccimarro, *Linear and non-linear contributions to pairwise peculiar velocities*, *Mon. Not. R. Astron. Soc.* **325** (Aug., 2001) 1288–1302, [[astro-ph/0009167](#)].
- [27] R. Scoccimarro, *Redshift-space distortions, pairwise velocities, and nonlinearities*, *Phys. Rev. D* **70** (Oct., 2004) 083007, [[astro-ph/0407214](#)].
- [28] T. Matsubara, *Nonlinear perturbation theory with halo bias and redshift-space distortions via the Lagrangian picture*, *Phys. Rev. D* **78** (Oct., 2008) 083519, [[arXiv:0807.1733](#)].
- [29] C. M. Hirata, *Tidal alignments as a contaminant of redshift space distortions*, *Mon. Not. R. Astron. Soc.* **399** (Oct., 2009) 1074–1087, [[arXiv:0903.4929](#)].
- [30] P. McDonald, *Gravitational redshift and other redshift-space distortions of the imaginary part of the power spectrum*, *JCAP* **11** (Nov., 2009) 026, [[arXiv:0907.5220](#)].
- [31] A. Taruya, T. Nishimichi, and S. Saito, *Baryon acoustic oscillations in 2D: Modeling redshift-space power spectrum from perturbation theory*, *Phys. Rev. D* **82** (Sept., 2010) 063522, [[arXiv:1006.0699](#)].
- [32] V. Desjacques and R. K. Sheth, *Redshift space correlations and scale-dependent stochastic biasing of density peaks*, *Phys. Rev. D* **81** (Jan., 2010) 023526, [[arXiv:0909.4544](#)].
- [33] Z. Zheng, R. Cen, H. Trac, and J. Miralda-Escudé, *Radiative Transfer Modeling of Ly α Emitters. II. New Effects on Galaxy Clustering*, *Astrophys. J.* **726** (Jan., 2011) 38, [[arXiv:1003.4990](#)].
- [34] U. Seljak and P. McDonald, *Distribution function approach to redshift space distortions*, *JCAP* **11** (Nov., 2011) 039, [[arXiv:1109.1888](#)].
- [35] P. Zhang, J. Pan, and Y. Zheng, *Peculiar velocity decomposition, redshift space distortion, and velocity reconstruction in redshift surveys: The methodology*, *Phys. Rev. D* **87** (Mar., 2013) 063526, [[arXiv:1207.2722](#)].
- [36] N. McCullagh and A. S. Szalay, *Nonlinear Behavior of Baryon Acoustic Oscillations in Redshift Space from the Zel'dovich Approximation*, *Astrophys. J.* **798** (Jan., 2015) 137, [[arXiv:1411.1249](#)].
- [37] J. M. Bardeen, J. R. Bond, N. Kaiser, and A. S. Szalay, *The statistics of peaks of Gaussian random fields*, *Astrophys. J.* **304** (May, 1986) 15–61.
- [38] V. Desjacques, *Baryon acoustic signature in the clustering of density maxima*, *Phys. Rev. D* **78** (Nov., 2008) 103503–+, [[arXiv:0806.0007](#)].
- [39] M. Mirbabayi, F. Schmidt, and M. Zaldarriaga, *Biased tracers and time evolution*, *JCAP* **7** (July, 2015) 030, [[arXiv:1412.5169](#)].
- [40] W. D. Goldberger and I. Z. Rothstein, *Effective field theory of gravity for extended objects*, *Phys. Rev. D* **73** (May, 2006) 104029, [[hep-th/0409156](#)].
- [41] D. Baumann, A. Nicolis, L. Senatore, and M. Zaldarriaga, *Cosmological non-linearities as an effective fluid*, *JCAP* **7** (July, 2012) 051, [[arXiv:1004.2488](#)].

- [42] J. J. M. Carrasco, M. P. Hertzberg, and L. Senatore, *The effective field theory of cosmological large scale structures*, *Journal of High Energy Physics* **9** (Sept., 2012) 82, [[arXiv:1206.2926](#)].
- [43] M. P. Hertzberg, *Effective field theory of dark matter and structure formation: Semianalytical results*, *Physical Review D* **89** (Feb., 2014) 043521.
- [44] L. Senatore, *Bias in the effective field theory of large scale structures*, *JCAP* **11** (Nov., 2015) 007, [[arXiv:1406.7843](#)].
- [45] R. A. Porto, *The effective field theorist’s approach to gravitational dynamics*, *Phys. Rep.* **633** (May, 2016) 1–104, [[arXiv:1601.04914](#)].
- [46] J. N. Fry and E. Gaztanaga, *Biasing and hierarchical statistics in large-scale structure*, *Astrophys. J.* **413** (Aug., 1993) 447–452, [[astro-ph/9](#)].
- [47] P. Catelan, F. Lucchin, S. Matarrese, and C. Porciani, *The bias field of dark matter haloes*, *Mon. Not. R. Astron. Soc.* **297** (July, 1998) 692–712, [[astro-ph/9](#)].
- [48] R. K. Sheth and G. Tormen, *Large-scale bias and the peak background split*, *Mon. Not. R. Astron. Soc.* **308** (Sept., 1999) 119–126, [[astro-ph/9](#)].
- [49] P. McDonald, *Clustering of dark matter tracers: Renormalizing the bias parameters*, *Phys. Rev. D* **74** (Nov., 2006) 103512, [[astro-ph/0](#)].
- [50] P. McDonald and A. Roy, *Clustering of dark matter tracers: generalizing bias for the coming era of precision LSS*, *JCAP* **8** (Aug., 2009) 20, [[arXiv:0902.0991](#)].
- [51] K. C. Chan, R. Scoccimarro, and R. K. Sheth, *Gravity and large-scale nonlocal bias*, *Phys. Rev. D* **85** (Apr., 2012) 083509, [[arXiv:1201.3614](#)].
- [52] L. Verde, A. F. Heavens, S. Matarrese, and L. Moscardini, *Large-scale bias in the Universe - II. Redshift-space bispectrum*, *Mon. Not. R. Astron. Soc.* **300** (Nov., 1998) 747–756, [[astro-ph/9806028](#)].
- [53] R. Scoccimarro, H. M. P. Couchman, and J. A. Frieman, *The Bispectrum as a Signature of Gravitational Instability in Redshift Space*, *Astrophys. J.* **517** (June, 1999) 531–540, [[astro-ph/9808305](#)].
- [54] R. E. Smith, R. K. Sheth, and R. Scoccimarro, *Analytic model for the bispectrum of galaxies in redshift space*, *Phys. Rev. D* **78** (July, 2008) 023523, [[arXiv:0712.0017](#)].
- [55] F. A. Marín, R. H. Wechsler, J. A. Frieman, and R. C. Nichol, *Modeling the Galaxy Three-Point Correlation Function*, *Astrophys. J.* **672** (Jan., 2008) 849–860, [[arXiv:0704.0255](#)].
- [56] Z. Slepian and D. J. Eisenstein, *Modelling the large-scale redshift-space 3-point correlation function of galaxies*, *Mon. Not. R. Astron. Soc.* **469** (Aug., 2017) 2059–2076, [[arXiv:1607.03109](#)].
- [57] L. Verde, A. F. Heavens, W. J. Percival, S. Matarrese, C. M. Baugh, et al., *The 2dF Galaxy Redshift Survey: The Bias of galaxies and the density of the Universe*, *Mon. Not. Roy. Astron. Soc.* **335** (2002) 432, [[astro-ph/0112161](#)].
- [58] H. Gil-Marín, W. J. Percival, L. Verde, J. R. Brownstein, C.-H. Chuang, F.-S. Kitaura, S. A. Rodríguez-Torres, and M. D. Olmstead, *The clustering of galaxies in the SDSS-III Baryon Oscillation Spectroscopic Survey: RSD measurement from the power spectrum and bispectrum of*

- the DR12 BOSS galaxies*, *Mon. Not. R. Astron. Soc.* **465** (Feb., 2017) 1757–1788, [[arXiv:1606.00439](#)].
- [59] N. S. Sugiyama, S. Saito, F. Beutler, and H.-J. Seo, *A complete FFT-based decomposition formalism for the redshift-space bispectrum*, *ArXiv e-prints* (Mar., 2018) [[arXiv:1803.02132](#)].
- [60] B. Greig, E. Komatsu, and J. S. B. Wyithe, *Cosmology from clustering of Ly α galaxies: breaking non-gravitational Ly α radiative transfer degeneracies using the bispectrum*, *Mon. Not. R. Astron. Soc.* **431** (May, 2013) 1777–1794, [[arXiv:1212.0977](#)].
- [61] V. Desjacques, D. Jeong, and F. Schmidt, *Large-Scale Galaxy Bias*, [[arXiv:1611.09787](#)].
- [62] Planck Collaboration, *Planck 2015 results. I. Overview of products and scientific results*, *Astron. Astrophys.* **594** (Sept., 2016) A1, [[arXiv:1502.01582](#)].
- [63] Planck Collaboration, *Planck 2015 results. XIII. Cosmological parameters*, *Astron. Astrophys.* **594** (Sept., 2016) A13, [[arXiv:1502.01589](#)].
- [64] J. Yoo, A. L. Fitzpatrick, and M. Zaldarriaga, *New perspective on galaxy clustering as a cosmological probe: General relativistic effects*, *Phys. Rev. D* **80** (Oct., 2009) 083514–+, [[arXiv:0907.0707](#)].
- [65] A. Challinor and A. Lewis, *Linear power spectrum of observed source number counts*, *Phys. Rev. D* **84** (Aug., 2011) 043516, [[arXiv:1105.5292](#)].
- [66] T. Baldauf, U. Seljak, L. Senatore, and M. Zaldarriaga, *Galaxy bias and non-linear structure formation in general relativity*, *JCAP* **10** (Oct., 2011) 031, [[arXiv:1106.5507](#)].
- [67] C. Bonvin and R. Durrer, *What galaxy surveys really measure*, *Phys. Rev. D* **84** (Sept., 2011) 063505, [[arXiv:1105.5280](#)].
- [68] D. Jeong, F. Schmidt, and C. M. Hirata, *Large-scale clustering of galaxies in general relativity*, *Phys. Rev. D* **85** (Jan., 2012) 023504, [[arXiv:1107.5427](#)].
- [69] J. S. B. Wyithe and M. Dijkstra, *Non-gravitational contributions to the clustering of Ly α selected galaxies: implications for cosmological surveys*, *Mon. Not. R. Astron. Soc.* **415** (Aug., 2011) 3929–3950, [[arXiv:1104.0712](#)].
- [70] C. Behrens, C. Byrohl, S. Saito, and J. C. Niemeyer, *The impact of Lyman- α radiative transfer on large-scale clustering in the Illustris simulation*, *ArXiv e-prints* (Oct., 2017) [[arXiv:1710.06171](#)].
- [71] E. Krause and C. M. Hirata, *Tidal alignments as a contaminant of the galaxy bispectrum*, *Mon. Not. R. Astron. Soc.* **410** (Feb., 2011) 2730–2740, [[arXiv:1004.3611](#)].
- [72] D. Martens, C. M. Hirata, A. J. Ross, and X. Fang, *A radial measurement of the galaxy tidal alignment magnitude with BOSS data*, *Mon. Not. R. Astron. Soc.* **478** (July, 2018) 711–732, [[arXiv:1802.07708](#)].
- [73] E. Pajer, F. Schmidt, and M. Zaldarriaga, *The Observed squeezed limit of cosmological three-point functions*, *Phys. Rev. D* **88** (Oct., 2013) 083502, [[arXiv:1305.0824](#)].
- [74] V. Assassi, D. Baumann, D. Green, and M. Zaldarriaga, *Renormalized halo bias*, *JCAP* **8** (Aug., 2014) 56, [[arXiv:1402.5916](#)].

- [75] R. Angulo, M. Fasiello, L. Senatore, and Z. Vlah, *On the statistics of biased tracers in the Effective Field Theory of Large Scale Structures*, *JCAP* **9** (Sept., 2015) 029, [[arXiv:1503.08826](#)].
- [76] “Supplementary MATHEMATICA notebook.”
https://github.com/djeong98/pkgs_supplement.
- [77] J. E. McEwen, X. Fang, C. M. Hirata, and J. A. Blazek, *FAST-PT: a novel algorithm to calculate convolution integrals in cosmological perturbation theory*, *JCAP* **9** (Sept., 2016) 015, [[arXiv:1603.04826](#)].
- [78] M. Schmittfull and Z. Vlah, *Reducing the two-loop large-scale structure power spectrum to low-dimensional, radial integrals*, *Phys. Rev. D* **94** (Nov., 2016) 103530, [[arXiv:1609.00349](#)].
- [79] L. Senatore and M. Zaldarriaga, *The IR-resummed Effective Field Theory of Large Scale Structures*, *JCAP* **2** (Feb., 2015) 013, [[arXiv:1404.5954](#)].
- [80] T. Baldauf, M. Mirbabayi, M. Simonović, and M. Zaldarriaga, *Equivalence principle and the baryon acoustic peak*, *Phys. Rev. D* **92** (Aug., 2015) 043514, [[arXiv:1504.04366](#)].
- [81] D. Blas, M. Garny, M. M. Ivanov, and S. Sibiryakov, *Time-sliced perturbation theory II: baryon acoustic oscillations and infrared resummation*, *JCAP* **7** (July, 2016) 028, [[arXiv:1605.02149](#)].
- [82] A. Perko, L. Senatore, E. Jennings, and R. H. Wechsler, *Biased Tracers in Redshift Space in the EFT of Large-Scale Structure*, *ArXiv e-prints* (Oct., 2016) [[arXiv:1610.09321](#)].
- [83] L. Senatore and G. Trevisan, *On the IR-resummation in the EFTofLSS*, *JCAP* **5** (May, 2018) 019, [[arXiv:1710.02178](#)].
- [84] L. Senatore and M. Zaldarriaga, *Redshift Space Distortions in the Effective Field Theory of Large Scale Structures*, *arXiv.org* (Sept., 2014) 1225, [[arXiv:1409.1225](#)].
- [85] M. Lewandowski, L. Senatore, F. Prada, C. Zhao, and C.-H. Chuang, *EFT of large scale structures in redshift space*, *Phys. Rev.* **D97** (2018), no. 6 063526, [[arXiv:1512.06831](#)].
- [86] L. Fonseca de la Bella, D. Regan, D. Seery, and S. Hotchkiss, *The matter power spectrum in redshift space using effective field theory*, *JCAP* **11** (Nov., 2017) 039, [[arXiv:1704.05309](#)].
- [87] Z. Ding, H.-J. Seo, Z. Vlah, Y. Feng, M. Schmittfull, and F. Beutler, *Theoretical Systematics of Future Baryon Acoustic Oscillation Surveys*, *ArXiv e-prints* (Aug., 2017) [[arXiv:1708.01297](#)].
- [88] M. M. Ivanov and S. Sibiryakov, *Infrared Resummation for Biased Tracers in Redshift Space*, *ArXiv e-prints* (Apr., 2018) [[arXiv:1804.05080](#)].
- [89] P. J. E. Peebles, *The large-scale structure of the universe*. Princeton University Press, 1980.
- [90] Y. Ohta, I. Kayo, and A. Taruya, *Cosmological Density Distribution Function from the Ellipsoidal Collapse Model in Real Space*, *Astrophys. J.* **608** (June, 2004) 647–662, [[astro-ph/0402618](#)].
- [91] L. Fonseca de la Bella, D. Regan, D. Seery, and D. Parkinson, *Impact of bias and redshift-space modelling for the halo power spectrum: Testing the effective field theory of large-scale structure*, *ArXiv e-prints* (May, 2018) [[arXiv:1805.12394](#)].
- [92] T. Fujita, V. Mauerhofer, L. Senatore, Z. Vlah, and R. Angulo, *Very Massive Tracers and Higher Derivative Biases*, *ArXiv e-prints* (Sept., 2016) [[arXiv:1609.00717](#)].

- [93] D. Tseliakhovich and C. Hirata, *Relative velocity of dark matter and baryonic fluids and the formation of the first structures*, *Phys. Rev. D* **82** (Oct., 2010) 083520, [[arXiv:1005.2416](#)].
- [94] M. Lewandowski, A. Perko, and L. Senatore, *Analytic prediction of baryonic effects from the EFT of large scale structures*, *JCAP* **5** (May, 2015) 019, [[arXiv:1412.5049](#)].
- [95] F. Schmidt, *Effect of relative velocity and density perturbations between baryons and dark matter on the clustering of galaxies*, *Phys. Rev.* **D94** (2016), no. 6 063508, [[arXiv:1602.09059](#)].
- [96] F. Schmidt and F. Beutler, *Imprints of reionization in galaxy clustering*, *Phys. Rev. D* **96** (Oct., 2017) 083533, [[arXiv:1705.07843](#)].
- [97] F. Schmidt, *Large-scale velocities and primordial non-Gaussianity*, *Phys. Rev. D* **82** (Sept., 2010) 063001, [[arXiv:1005.4063](#)].
- [98] F. Bernardeau, S. Colombi, E. Gaztañaga, and R. Scoccimarro, *Large-scale structure of the Universe and cosmological perturbation theory*, *Phys. Rep.* **367** (Sept., 2002) 1–248, [[astro-ph/0](#)].